Progress in Oceanography 195 (2021) 102563

Contents lists available at ScienceDirect

Progress in Oceanography

journal homepage: www.elsevier.com/locate/pocean

Seasonal-to-decadal scale variability in primary production and particulate matter export at Station ALOHA

David M. Karl [a,*,1], Ricardo M. Letelier [b,1], Robert R. Bidigare [c], Karin M. Björkman [a], Matthew J. Church [d], John E. Dore [e], Angelicque E. White [a]

[a] Daniel K. Inouye Center for Microbial Oceanography: Research and Education, University of Hawaii at Manoa, Honolulu, HI 96822, USA
[b] College of Earth, Ocean and Atmospheric Sciences, Oregon State University, Corvallis, OR 97331, USA
[c] Hawaii Institute of Marine Biology, Kaneohe, HI 96744, USA
[d] Flathead Lake Biological Station, University of Montana, Polson, MT 59860, USA
[e] Department of Land Resources and Environmental Sciences, Montana State University, Bozeman, MT 59717, USA

ARTICLE INFO

Keywords:
Primary production
Biological carbon pump
Station ALOHA
Phytoplankton
Nutrient cycling
Biogeochemistry
North Pacific Subtropical Gyre

ABSTRACT

Station ALOHA (A Long-term Oligotrophic Habitat Assessment) was established in the North Pacific Subtropical Gyre (22°45′N, 158°W) as an oligotrophic ocean benchmark to improve our understanding of processes that govern the fluxes of carbon (C) into and from the surface ocean. At approximately monthly intervals, measurements of the primary production of particulate C (PC) using the ^{14}C method, and the export of PC and particulate nitrogen (PN) using surface-tethered sediment traps deployed at 150 m have been made along with a host of complementary physical, biological, and biogeochemical measurements. Euphotic zone depth-integrated (0–200 m) primary production ranged from 220.2 (standard deviation, SD, 10.8) mg C m^{-2} d^{-1} in Feb 2018 to 1136.5 (SD = 17.1) mg C m^{-2} d^{-1} in Jun 2000, with a 30-yr (1989–2018) mean of 536.8 (SD = 135.0) mg C m^{-2} d^{-1} (n = 271). Although the monthly primary production climatology was fairly well constrained, we observed substantial sub-decadal variability and a significant 0–125 m depth-integrated increasing trend of 4.0 ($p < 0.01$; 95% confidence interval, CI, 2.1–5.9) (mg C m^{-2} d^{-1}) yr^{-1} since 1989, displaying a large relative increase of 37% (CI = 18–55%) in the lower portion (75–125 m) of the euphotic zone. Chlorophyll (Chl) *a* and suspended PC and PN concentrations also displayed significant ($p < 0.01$) increases in the 75–125 m region of the euphotic zone. PC export at 150 m exhibited both short-term (monthly) and longer-scale variability with a 30-yr mean of 27.9 (SD = 9.7, n = 265) mg C m^{-2} d^{-1}. PC and PN export exhibited extended, multi-year periods of significantly lower or higher values compared to the 30-yr mean. These multi-year periods of anomalously low and high particle export, in the absence of contemporaneous variations in primary production, probably reflect periodic changes in remineralization efficiencies. The PC export ratio (e-ratio; PC export at 150 m ÷ 0–150 m depth-integrated ^{14}C-based primary production) was low, with a 30-yr mean of 0.054 (SD = 0.021, n = 248), and exhibited a significant ($p < 0.01$) long-term decreasing trend over the 30-yr observation period. The 30-yr long-term increases in primary production (~37%), Chl *a*, and suspended PC and PN concentrations (~17%, 8%, and 8%, respectively) in the 75–125 m portion of the water column are hypothesized to result from an enhanced supply of nutrients to the lower portion of the water column over the past three decades.

1. Introduction

The Joint Global Ocean Flux Study (JGOFS) program was established in 1986 to reduce uncertainties in oceanic carbon (C) cycle processes in order to obtain a better understanding of the atmosphere-to-ocean balance of carbon dioxide (CO_2) and its sensitivities to natural and human-induced climate change (Brewer et al., 1986). To achieve these goals, JGOFS scientists established several strategically located ocean time-series stations to document and interpret seasonal-to-interannual variability in primary production, new production (the portion of primary production that is supported by allochthonous sources of nutrients), and particle export from the surface ocean (Karl et al., 2003). Characterizing

* Corresponding author.
E-mail address: dkarl@hawaii.edu (D.M. Karl).
[1] Contributed equally to this effort.

https://doi.org/10.1016/j.pocean.2021.102563
Received 23 November 2020; Received in revised form 17 March 2021; Accepted 28 March 2021
Available online 2 April 2021

the magnitude and variance in the rates of primary production and particle export at different temporal scales is central to our understanding of the biological C pump (BCP), a set of inextricably linked processes that ultimately determines the net air-to-sea flux of CO_2 and the capacity for long-term (>100 yrs) sequestration of C into the deep sea (Volk and Hoffert, 1985).

Since October 1988, scientists in the Hawaii Ocean Time-series (HOT) program have employed a relatively consistent, approximately monthly sampling strategy for a number of discrete physical, chemical, and biological ship-based measurements and in situ experiments to constrain C cycle rates and processes. By employing standard protocols over periods of several decades, HOT observations enable long-term assessment of trends in the magnitude and variance of these rates, and serve as a test for predictions of contemporary models of the BCP in the oligotrophic North Pacific Subtropical Gyre (NPSG).

When the HOT program began in Oct 1988, we had only a rudimentary knowledge of the factors controlling primary production and particle export processes in oligotrophic ocean regions. For example, a novel and abundant photosynthetic microorganism, *Prochlorococcus*, had just been discovered in the North Atlantic (Chisholm et al., 1988), but there was no information on its abundance, distribution, or contribution to total primary production in the NPSG. In addition, the reliability of the traditional radiocarbon (^{14}C) method for field measurements of primary production (Steemann Nielsen, 1951; 1952) had been called into question on grounds of metal contamination and other incubation artifacts (Fitzwater et al., 1982; Williams and Robertson, 1989). Large inconsistencies began to emerge between rates obtained from short-term (~1 day) ^{14}C-based experiments and longer term (months to years) geochemical mass balances that both excited and incited the scientific community (Jenkins and Goldman, 1985; Platt and Harrison, 1986; Platt et al., 1989; Hayward, 1991). Furthermore, high sensitivity methods for accurate determinations of vanishingly low nutrient concentrations in oligotrophic waters were starting to emerge; methods for the determination of nanomolar concentrations of nitrate had just been field-tested (Garside, 1982) and, in the case of phosphate, had not yet been developed (Karl and Tien, 1992). Quantitative studies of the ecological role of dinitrogen (N_2) fixation as a source of new nitrogen in the NPSG were just beginning (Mague et al., 1974; Gundersen et al., 1976). With regard to particle export, only a few sediment trap experiments had ever been conducted in the NPSG, and the "open ocean composite" (the so-called Martin curve), an empirical description of sediment trap-derived PC export versus water depth, had just been published (Martin et al., 1987). Our knowledge of the rates, controls, and efficiencies of the BCP, a term not yet in the oceanographer's lexicon, was incomplete and inadequate for most modeling purposes.

This paper presents time-series data for several key ocean C cycle processes that have been collected at Station ALOHA during the past 30 years (1989–2018). We summarize and interpret these data, including several unexpected trends, and present new hypotheses as a research prospectus for the future.

2. Materials and methods

2.1. Field sampling strategies

All field experiments were conducted at Station ALOHA (22°45′N, 158°W), an oligotrophic, open ocean site in the eastern portion of the NPSG (Karl and Lukas, 1996). The data presented in this paper were collected on 306 cruises between January 1989 and December 2018, on approximately monthly intervals (Supplementary Figs. 1 and 2, and Supplementary Table 1). During each cruise (except as noted below), a single, ~12-hr (dawn-to-dusk), primary production incubation and a single sediment trap deployment of variable duration were performed (Karl et al., 1996; Supplementary Table 1). As detailed below, in situ primary production protocols were first employed in July 1989 (the eighth cruise in the series; HOT 8; see Supplementary Table 1 for cruise dates, data summaries, and other relevant information). Due to inclement weather or mechanical problems, the in situ primary production array was unsuccessful on 28 cruises (HOT cruise numbers 9, 20, 21, 24, 42, 43, 48, 59, 88, 100, 121, 123, 133, 138, 161, 168, 192, 207, 218, 219, 238, 240, 276, 278, 288, 299, 302, and 308), or was deployed but lost at sea on HOT 183 and HOT 282; this reduces the number of individual in situ primary production experiments to 271. While the temporal coverage during the 30-yr period was not biased to any particular month (Supplementary Fig. 1), there were 170 days of the year with no observations and 136 days with only a single primary production experiment (Supplementary Fig. 2). The deployment of the sediment trap array was unsuccessful on 37 cruises (HOT cruise numbers 12, 21, 25, 42, 43, 48, 59, 61, 84, 87, 88, 129, 133, 138, 144, 161, 177, 190, 192, 207, 218, 219, 227, 234, 235, 237, 238, 276, 278, 283, 288, 290, 299–301, 303, and 308), or was deployed but lost at sea on 5 cruises (HOT cruise numbers 151, 204, 279, 280, and 293) reducing the number of individual sediment trap experiments to 265. By comparison to primary production, we had much greater coverage in PC export with a mean of three observations per day and only 25 days of the year without a single observation (Supplementary Fig. 2). Consequently, the contemporaneous export ratio (e-ratio = PC export at 150 m ÷ 0–150 m depth-integrated ^{14}C-based primary production) is reported for 248 expeditions. Numerous complementary hydrographical, chemical, and biological measurements were also obtained (Karl and Lukas, 1996). A portion of the ancillary data is presented herein, and most other data are publicly available (*http://hahana.soest.hawaii.edu/hot/hot-dogs/*). Detailed HOT program methods are also available online (*http://hahana.soest.hawaii.edu/hot/methods/results.html*).

2.2. Primary production

Measurements of inorganic C assimilation were performed using the ^{14}C method following trace metal-clean procedures (Fitzwater et al., 1982; Letelier et al., 1996). The exact protocol was modified slightly (see below) during the 30-yr observation period. Initially (HOT 3–96), water samples were collected from 8 depths (5, 25, 45, 75, 100, 125, 150, and 175 m) approximately 3–4 hr before dawn using 30-l Teflon®-coated Go-Flo® bottles (General Oceanics), a Kevlar® line, a metal-free sheave, Teflon® messengers, and a stainless steel bottom weight. These water samples were used for measurements of photosynthetic pigments and for ^{14}C-based primary production. After seawater collection, triplicate 150 ml samples from each depth were withdrawn into dark polyethylene bottles for the fluorometric determination of chlorophyll *a* (Chl *a*; Letelier et al., 1996). In addition, six subsamples from each depth were withdrawn under dim light into 500 ml polycarbonate bottles, inoculated with $NaH^{14}CO_3$ (final radioactivity ~3.0–3.7 MBq l^{-1}), and placed in the dark until just prior to sunrise when the timed incubation period began. Triplicate light and triplicate dark bottle treatments were incubated for the entire daylight period (dawn to dusk), which ranged from <12 hr to >14 hr (see Supplementary Table 1). Initially (HOT 3–17), the samples were incubated in an on-deck, simulated in situ NORDA/USM system that reproduced both in situ photosynthetically available radiation (PAR; 350–700 nm) and temperature (Lohrenz et al., 1992). For nine cruises (HOT 8 and 10–17), we compared the deck incubation protocol to an in situ method using a free-drifting array. A detailed comparison of the two methods revealed that the deck incubations were compromised, especially for samples ≥45 m, presumably due to poor reproduction of the light field (Letelier et al., 1996). For this reason, we abandoned the use of the deck incubation system beginning on HOT 18, and have consistently employed only the in situ array since that time. We have elected not to include the on-deck ^{14}C-primary production data in the present analysis as the differences between in situ and on-deck incubations are viewed as irreconcilable.

Until HOT 96, we routinely conducted the dedicated Go-Flo® hydrocast, but we frequently encountered problems with bottle mis-trips and, more importantly, lacked vital continuous data on temperature,

salinity, pressure, dissolved oxygen, and Chl *a* fluorescence that are routinely collected when using a standard CTD-rosette water sampling system. Therefore, for the period from HOT 97–118, we sampled from both the Go-Flo® bottles and from rosette-mounted 12-l PVC bottles equipped with Teflon®-coated springs and Viton® o-rings. Comparisons of the two data sets showed that primary production measured using the two methods was not significantly different. So, since HOT 119 we have exclusively used the CTD-rosette sampling system and the in situ array protocol to measure primary production. For the period of sampling method overlap (HOT 97–118), and with the exception of the rosette sampling suspected to be contaminated on HOT-102, when full euphotic zone depth profiles derived from both sampling methods are available, we used only the CTD-rosette water cast in the current statistical analyses.

Beginning with HOT 118, we streamlined the relatively labor-intensive in situ primary production procedure by eliminating the triplicate dark bottles for all depths, and eliminating the two deepest light bottle depths (150 and 175 m). Instead of continuing to measure light bottle ^{14}C-uptake at these two deepest depths, we used the initial 12-yr monthly climatology to model seasonal changes in photosynthesis for the deepest portion of the euphotic zone, assuming that ^{14}C assimilation at 200 m was equal to zero. The mean monthly 125–200 m depth-integrated primary production based on the 12-yr observation period ranged from a minimum of 6.7 mg C m^{-2} d^{-1} in Nov to a maximum of 21.6 mg C m^{-2} d^{-1} in May (Supplementary Fig. 3), values equivalent to 1.45% and 3.45%, respectively, of the corresponding 0–200 m depth-integrated values. Deviations from the monthly climatologies were random over the 12-yr (1989–2000) observation period and had a mean of 0.17 (standard deviation, SD, = 9.42) mg C m^{-2} d^{-1} (n = 102; Supplementary Fig. 3). This mean deviation value is much smaller than the typical measurement error in the triplicate light bottles at all depths in the upper 125 m (~10% of mean value). Consequently, for HOT 118–307, total euphotic zone (0–200 m) depth-integrated primary production was calculated as the sum of the measured in situ 0–125 m ~12-hr light bottle ^{14}C assimilation plus the Station ALOHA climatological mean value for that month based on the in situ 125–200 m integral measured during the first 12-yr period of the HOT program. A similar approach was used to estimate the 0–150 m depth-integrated primary production for comparison to PC export measured at 150 m (Supplementary Fig. 4).

Following the in situ incubation, a subsample (250 μl) was removed from each bottle to measure total radioactivity in the sample. In this procedure, 500 μl of β-phenylethylamine was used as an inorganic C trapping agent, and either Aquasol-2 (Perkin Elmer, Inc.; HOT 8–177) or Ultima Gold LLT (Perkin Elmer, Inc.; HOT 178–307) was used as the liquid scintillation cocktail. The ^{14}C activities of the samples were counted (2% SD cut-off or 10 min maximum) using a liquid scintillation counter (LSC; four different Packard Instruments Co. or Perkin Elmer LSCs were used during the 30-yr period), and sample quench was assessed using the transformed Spectral Index of External standard (t-SIE) to calculate disintegrations per minute (dpm).

Larger subsamples (100–500 ml) were filtered onto 25-mm diameter glass fiber filters (Whatman GF/F) and each filter was placed directly into a glass vial for measurement of ^{14}C incorporation into particulate matter. The vials were stored for 2–3 days at −20 °C until processed at our shore-based laboratories. The samples were thawed, acidified by direct addition of 1 ml hydrochloric acid (HCl; 2 M) to each vial, and vented for 24 h prior to the addition of Aquasol-2/Ultima Gold LLT, as above, in preparation for liquid scintillation counting. Samples were counted at least twice during a 30-d period to track changes in ^{14}C activity over time (Karl et al., 1998); the 30-d dpm values were used for subsequent calculation of primary production. Dissolved inorganic carbon (DIC) was measured on each cruise using CO_2 coulometry (Winn et al., 1994) to determine the specific ^{14}C radioactivity (Bq mol^{-1} DIC) at each depth. This specific radioactivity value along with a ^{12}C-to-^{14}C isotope discrimination factor of 1.06 was used to calculate primary production.

On a separate hydrocast, we also collected larger volume water samples (4–10 l) from each of the primary production depths for the analysis of pigments via the high-performance liquid chromatography (HPLC) method of Bidigare et al. (1989) for HOT 1–50 and Bidigare et al. (2005) for HOT 51–308. These chlorophyll and carotenoid concentrations were used to estimate the contributions to total Chl *a* by the major algal groups in the lower portion of the euphotic zone (Letelier et al., 1993). Measurements of solar radiative flux at the sea surface were made using a LI-COR quantum sensor and data logger (models LI-192SA and LI-1000, respectively) on most HOT cruises (see Supplementary Table 1). The sensor was positioned approximately 4 m above the working deck to minimize the influence of shadows from the ship's superstructure. The quantum sensor was a cosine collector and measured photosynthetically available radiation (PAR). Irradiance was averaged over 10-min intervals and logged throughout each day at sea. Underwater light measurements, available for the period Feb 1998 to Dec 2018, were made using a profiling reflectance radiometer (Biospherical Instruments PRR 600 for HOT 90–214 and a Satlantic HyperPro for HOT 215–308). Daily integrated photon fluxes at depths corresponding to primary production incubations were calculated by combining the daily integrated surface PAR and the instantaneous profiling reflectance measurements (Letelier et al., 2017) on the day of the array deployment. These underwater light data were used to calculate C assimilation per Chl *a* per mol quanta at a given depth.

2.3. Particle export

A surface-tethered sediment trap array, based on the particle interceptor trap (PIT) design (Knauer et al., 1979), was deployed on most HOT cruises (see Section 2.1) to collect sinking particulate matter. The array was tracked using an Argos, and later Iridium, satellite transmitter. At each depth, 12 individual polycarbonate collector tubes, each fitted with a baffle and attached to a polyvinylchloride (PVC) cross-frame, were deployed. Initially (HOT 3–63), traps were positioned at 150, 300, and 500 m. The shallowest depth was selected to correspond to the region beneath the permanent deep chlorophyll maximum (DCM) layer near the photosynthetic compensation irradiance for photosynthesis (i.e., 0.054 mol quanta m^{-2} d^{-1}; Laws et al., 2014). An initial analysis of the flux attrition versus depth has been published elsewhere (Karl et al., 1996); only the 150-m data are presented herein. The trap array was routinely deployed within the 11-km radius circle that we define as Station ALOHA (Karl and Lukas, 1996), but the individual experiments varied considerably in their drift vectors which were most often to the west at speeds of ~4–11 km d^{-1} (Letelier et al., 2019; see Supplementary Table 1).

Prior to deployment, all PITs were acid-washed, distilled water rinsed, and filled with a high density seawater brine (60 g NaCl l^{-1} in surface seawater) containing 1% (vol:vol) formalin as a preservative (Knauer et al., 1979). The PIT solution was passed through a cartridge filter (0.5 μm) prior to filling the collector tubes and subsamples of the filtered PIT solution were processed as time-zero blanks. Post-recovery processing of sinking particulate matter was identical to the methods described by Karl et al. (1996). Very early in the HOT program (HOT 3–7), the contents of all 12 PITs from a given depth were combined, homogenized, and subsampled for the various analyses. Since HOT 8, the individual PITs have been processed separately to gain additional information on field variability. Typically, six replicate PITs were processed for the measurements of particulate C (PC) and nitrogen (PN) on the same filter, while the remaining traps were used for determinations of particulate phosphorus (PP), particulate inorganic C (PIC; i.e., calcium carbonate), particulate biogenic silica (opal), total mass, and other parameters. Herein we present only the PC and PN data sets which are the most complete of all sediment trap measurements (see below). Additional sediment trap data are publicly available at *http://hahana.soest.hawaii.edu/hot/hot-dogs/*.

Samples for PC and PN analyses were first screened through a 335-μm Nitex® mesh to remove large zooplankton (i.e., swimmers; Karl et al., 1996) then filtered onto pre-combusted (450 °C, 4 hr) 25-mm

diameter Whatman GF/F filters placed onto combusted (as above) tin foil contained in polystyrene Petri® dishes, and stored frozen (-20 °C) for shore-based analysis. After drying at 60 °C, each filter and matched foil were rolled together and pressed into a pellet for elemental analysis. From HOT 3–5, samples were analyzed using a Hewlett-Packard model 185B CHN analyzer (Sharp, 1974) but, after cross-comparison, a new Perkin-Elmer model 2400 CN analyzer was employed from HOT 7–55. Beginning with HOT 54 (through HOT 128), PC and PN samples were analyzed using a Europa ANCA-NT CN analyzer, and since HOT 130 samples have been analyzed using a Carlo-Erba NA 2500 elemental analyzer coupled via a Finnigan ConFlo-II to a Finnigan Delta-S mass spectrometer. The primary standard for all HOT program samples, acetanilide (C_8H_9NO; molecular weight = 135.16; C:N molar ratio = 8.0), was also analyzed as a check standard in each sample run. For samples analyzed between 2005 and 2018, the mean C:N molar ratio of the check standard was 8.03 (SD = 0.25, n = 222). We also routinely analyzed an in-house secondary standard prepared from dried, pulverized >335 μm zooplankton collected at Station ALOHA. The main purpose of the secondary standard is to make sure that the combustion/reduction is as complete with a complex field-collected sample as it is with the pure chemical standard. For samples analyzed between 2005 and 2018, the mean C:N molar ratio of the secondary standard was 4.82 (SD = 0.16, n = 237). As reported herein, our high-temperature combustion (~1000 °C) PC analysis includes both organic and inorganic (i.e., calcium carbonate) phases. Although we do not have a complete time series for particulate inorganic C (PIC), we do have measurements of sediment trap collected particles from 150 m for the period Mar 2001 through Oct 2016 (129 cruises; Supplementary Fig. 5), using methods described previously (Grabowski et al., 2019). PIC export averaged 1.85 (SD = 1.62; n = 129) mg C m^{-2} d^{-1}, a value that equated to 10.4% (SD = 4.6%) of the total PC export during the 19-yr observation period. Because we do not have a complete 30-yr time series for PIC, and hence POC (where POC = PC-PIC), our analyses herein are based upon the more complete PC data set. We also collected water samples from each of the primary production depths for the measurement of suspended PC and PN. A volume (4 l) was pre-screened through a 202-μm Nitex® screen and filtered onto a combusted 25-mm diameter glass fiber filter and analyzed using the method of Grabowski et al. (2019).

2.4. Statistical methodology

Depth integrations were performed using the trapezoidal rule:

$$\int_a^b f(x)dz \approx \sum_{z=1}^{N} \frac{f(x_{z-1}) + f(x_z)}{2} \Delta z \quad (1)$$

where x corresponds to the parameter being integrated over the depth Z. When integrating to the surface, the upper interval was considered to be homogeneously mixed if no surface sample had been collected. In addition, when integrating to 200 m depth, primary productivity and Chl *a* values at the 200 m depth horizon were assumed to be nil. Seasons are defined as: winter (Dec-Feb), spring (Mar-May), summer (Jun-Aug), and fall (Sep-Nov).

The total variance over the integration depth was calculated through error propagation as:

$$Var_{Total} = Z_{Surf}^2 * Var(x_{Surf})/n_{Surf} \quad (2)$$

$$+ (Z_2 - Z_{Surf})^2 * \left(Var(x_2)/n_2 + Var\left(x_{Surf}\right)/n_{Surf}\right)/2^2$$

$$+ \cdots$$

$$+ (Z_{final-1} - Z_{Sfinal})^2 * \left(Var\left(x_{2final-1}\right)/n_{final-1} + Var\left(x_{final}\right)/n_{final}\right)/2^2$$

where Z corresponds to depth, Var is the sample variance, and n corresponds to the sample size. The number of significant figures reported reflects the uncertainty of each value based on the sampling replication and the precision of the measurement.

Long-term, time-series trends were estimated by calculating the linear regression (model I) of residuals following the removal of the climatological seasonal cycles. These seasonal cycles were derived by fitting a fundamental frequency equivalent to the annual cycle, plus a first harmonic, to a generalized linear model (Keeling et al., 2004). In addition, the interannual variability was calculated based on the annual means of the residuals once both the seasonal cycle and long-term linear trend had been removed from the time-series. Finally, the contribution to the total time-series variance by the long-term trend, as well as by the seasonal and interannual variability, were estimated as the difference between the total variance and the variance of the residuals once the seasonal, long-term, and interannual components had been removed sequentially.

3. Results

3.1. Seasonal and interannual environmental variability

During the 30-yr observation period at Station ALOHA, there were both predictable and unexpected variations in the physical structure of the upper water column (Fig. 1). For example, the late winter and early fall exhibit the least and most stratified periods of the year, respectively, with extremes in sea surface temperature (SST) and water column stratification as evidenced by the depth of the surface mixed layer (Fig. 1). In addition to these predictable seasonal climatologies, we also observed significant interannual and subdecadal variability with several periods of unusually warm, less dense surface ocean conditions especially in 1995–1996, 2003–2005, and 2014–2018 (Fig. 1). These periods exhibited the shallowest surface mixed layers with values that were typically <40 m using the density criterion of de Boyer Montégut et al. (2004). Furthermore, during 2014–2018, there were unusually long periods of relatively shallow mixed layers with mean depths of 18.5 m from May-Sep 2014, 28.7 m from Apr – Sep 2015, 29.2 m from May-Aug 2016, and 30.0 m from Mar-Aug 2017, compared to the 30-yr spring, summer, fall, and winter mean values of 37.0 m (SD = 18.5 m, n = 78), 35.6 m (SD = 10.3 m, n = 76), 48.3 m (SD = 17.1 m, n = 73), and 62.1 m (SD = 26.1 m, n = 74), respectively. Deep winter mixing (mixed layer depths >100 m) was observed only in Dec 1997, Jan 2003, Jan 2008, Jan and Dec 2011, Jan 2015, and Dec and Feb 2017 (Fig. 1).

3.2. Nutrient and chlorophyll variability

The 30-yr climatologies of Chl *a* and major nutrients (nitrate plus nitrate [N + N] hereafter nitrate, soluble reactive phosphorus [SRP] hereafter phosphate, and silicate) are typical of historical data from the NPSG (Hayward et al., 1983; Letelier et al., 1993; Winn et al., 1995; Karl et al., 2001b; Figs. 2 and 3). The 0–300 m depth profiles of the major nutrients show consistently depleted surface waters (0–100 m) with deeper transitions to more nutrient-rich waters (Fig. 2). The top of the nutricline is near the photosynthetic compensation irradiance, the depth where net primary production is equal to zero over a 24-hr period. The photosynthetic compensation irradiance at Station ALOHA was estimated to be 0.054 mol quanta m^{-2} d^{-1} (95% confidence interval, CI, 0.016–0.178 mol quanta m^{-2} d^{-1}), corresponding to median and geometric mean compensation depths of 159 and 155 m, respectively (Laws et al., 2014). However, these 0–300 m nutrient contours (Fig. 2 a-c) mask significant seasonal and subdecadal deviations in nitrate and phosphate, especially in the upper mixed layer of the water column that are revealed through the application of high sensitivity analyses (Karl and Tien, 1997; Karl et al. 2001b; Letelier et al., 2019; Fig. 4). These high frequency nutrient variations, discussed in subsequent sections, are manifestations of both physical and microbiological processes that independently impact primary production and export. Furthermore, inventories of dissolved organic nitrogen and phosphorus (DON and

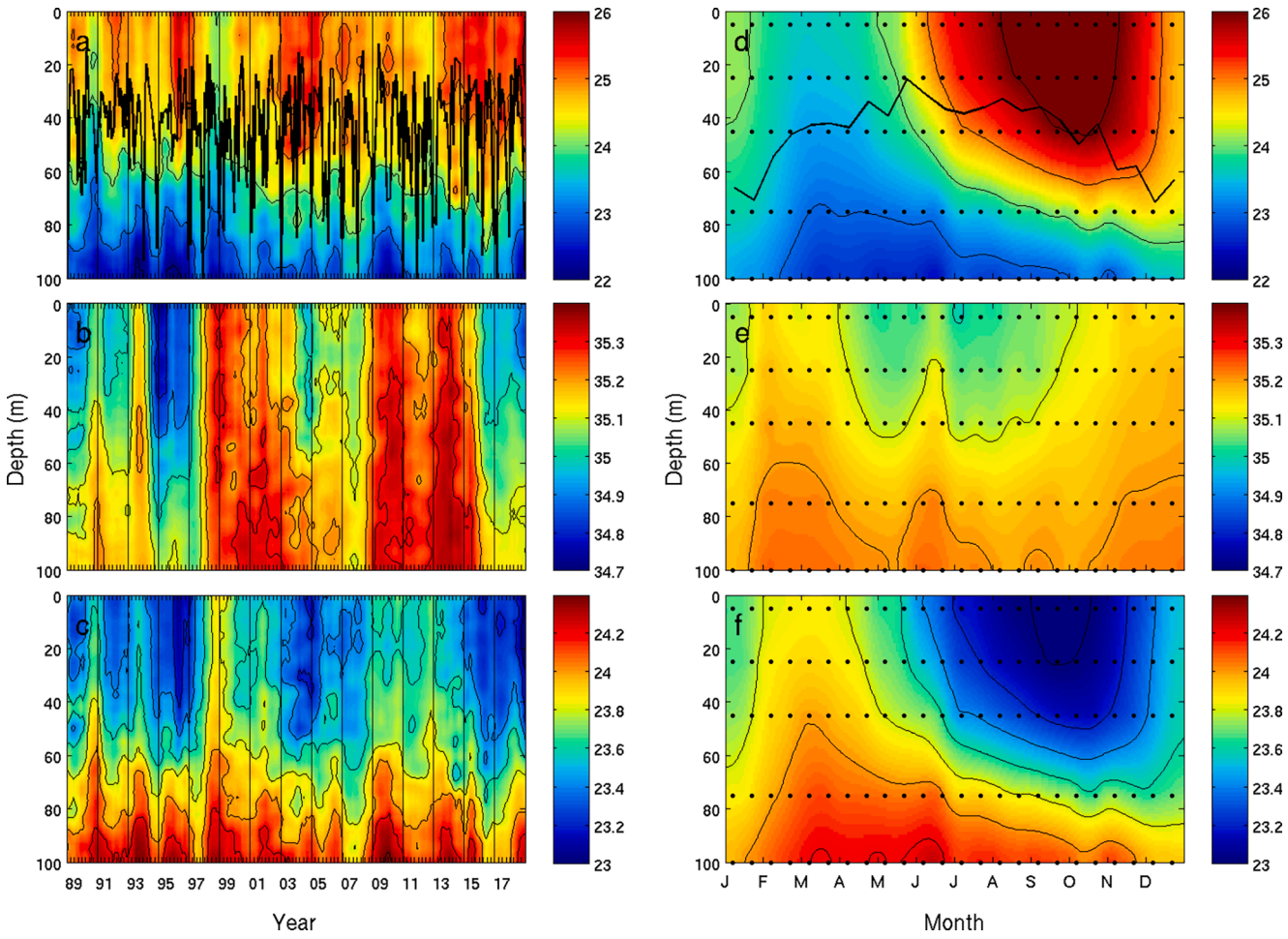

Fig. 1. Time-series (1989–2018), ship-based observations of (a) temperature (°C), (b) salinity, (c) potential density (sigma θ = [density (kg m^{-3}) – 1.000] × 1000) in the upper 0–100 m of the water column at Station ALOHA, and (d,e,f) monthly climatologies of the same properties of the water column for the 30-yr observation period. The solid black lines shown in a and c are the depths of upper mixed layer based on the density criterion of de Boyer Montégut et al. (2004). Warmer, less dense surface (0–50 m) waters were especially evident in the periods 1995–1996, 2003–2005, and 2014–2018.

DOP, respectively) exceed the inorganic pools, in the case of DON by 2–3 orders of magnitude (Karl et al., 2001b; Karl and Church, 2017), and should also be considered along with essential inorganic and organic trace nutrients, especially iron and vitamin B_{12} (Karl, 2002), which are not routinely measured, when trying to elucidate the controls of microbial activity at Station ALOHA.

Chl *a* concentrations were low in near-surface waters (0–30 m) with maxima in winter and minima in summer (Figs. 2 and 3, and Table 1). This predictable seasonal pattern at Station ALOHA is a manifestation of phytoplankton photoadaptation, which leads to a higher Chl *a* concentration per cell in winter (Winn et al., 1995). A conspicuous DCM was observed on every HOT cruise, but the magnitude, shape, and depth of occurrence varied on seasonal and subdecadal scales (Fig. 3 and Table 1). The 30-yr annual climatology displayed two maxima in Chl *a* concentration in the core of the DCM, one in the spring and the other in late summer-to-early winter (Fig. 3). The spring increase in Chl *a* tracks an increase in phytoplankton biomass as indicated by increasing particulate ATP concentrations and ^{14}C-based primary production (Winn et al., 1995; see below). The seasonal deepening of the DCM by ~30 m is a result of downward isolume displacement due to changes in surface PAR (Letelier et al., 2004). Finally, high frequency (~31 h) vertical oscillations of isopycnals near the base of the euphotic zone result in short-term vertical displacements of the DCM (Letelier et al., 1993; Karl et al., 2002). The 30-yr mean daily amplitude of DCM displacement is 38.8 (SD = 15.7 m, n = 281), but can be as large as 80 m. These vertical movements impact the light field, leading to either an enhancement or a depression of primary production depending upon the position of the DCM at local noon (Karl et al., 2002). And, because the period of the vertical oscillation at the latitude of Station ALOHA is 31 h, the timing of maximum upward excursion advances by 7 h from one day to the next, resulting in an approximately 4-d oscillation in the optimal light field for photosynthesis (Karl and Church, 2017). Since the water samples for each HOT primary production experiment were collected and subsequently incubated in situ at fixed depths, we do not capture these daily vertical displacement dynamics which could impact primary production and export, especially in the lower, light-limited portion of the euphotic zone.

3.3. ^{14}C-based primary production

3.3.1. Euphotic zone depth-integrated rates

Oceanographers often present data on euphotic zone depth-integrated primary production as a measure of total photosynthetic solar energy capture and an upper constraint on organic matter synthesis. Daily ^{14}C-based primary production in the euphotic zone at Station ALOHA during the 30-yr observation period ranged from 220.2 (SD = 10.8) mg C m^{-2} d^{-1} in Feb 2018 to 1136.5 (SD = 17.1) mg C m^{-2} d^{-1} in Jun 2000, with a 30-yr mean of 536.8 (SD = 135.0) mg C m^{-2} d^{-1} (n = 271; Fig. 5). For the 0–125 m region of the euphotic zone, the 30-yr ^{14}C-based primary production mean was 523.8 (SD = 132.7) mg C m^{-2} d^{-1}, or ~98% of the estimated 0–200 m depth-integrated value.

Euphotic zone depth-integrated primary production followed a

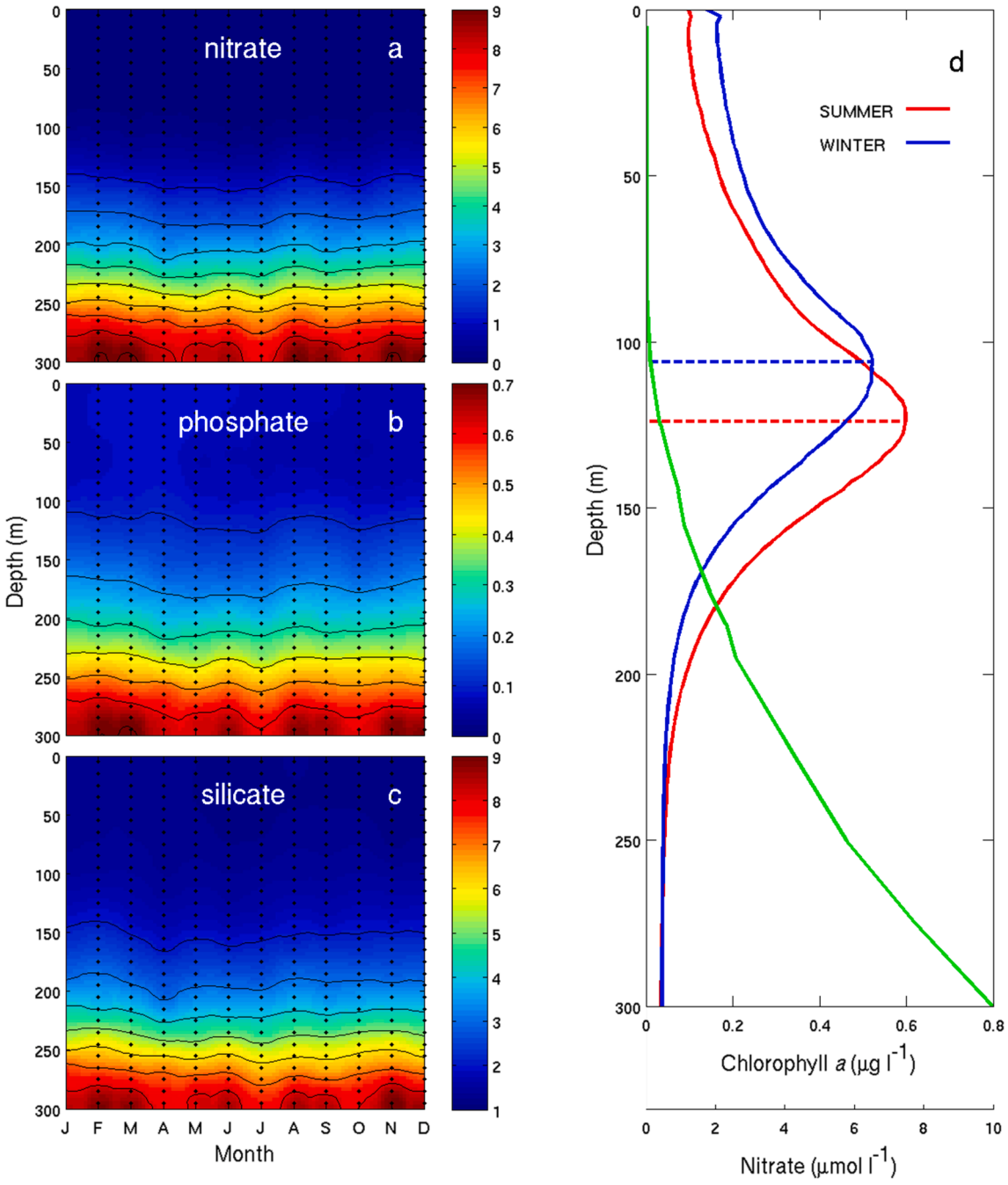

Fig. 2. Monthly climatologies of macronutrients (a) nitrate, (b) phosphate, (c) silicate; all in µmol l^{-1} in the upper 0–300 m of the water column at Station ALOHA. (d) Vertical profiles of Chl *a* (µg l^{-1}) for contrasting summer (red) and winter (blue) conditions and nitrate (µmol l^{-1}, green) in the upper 0–300 m of the water column at Station ALOHA. While the lower concentration of surface ocean Chl *a* in summer is a consequence of photoacclimation, the concomitant increase in the DCM magnitude reflects DCM seasonal changes in phytoplankton biomass.

predictable seasonal pattern with positive deviations from the mean during mid-Apr through mid-Sep and negative deviations during mid-Sep through Feb (Fig. 6). Maximum monthly excursions from the 30-yr mean value were approximately ± 100 mg C m^{-2} d^{-1}, although more extreme deviations were also observed on selected cruises (Figs. 5 and 6). Seven cruises (HOT 63, 116, 117, 159, 214, 253, and 295), all in the May-Aug time period, reported ^{14}C-based primary production values that were >2 SD above the 30-yr mean (Fig. 5). Four cruises (HOT 50, 82, 260, and 300), all in the Oct-Apr time period, reported values that were >2 SD below the 30-yr mean (Fig. 5). Because we rarely conducted more than one in situ primary production experiment on a given cruise, we do not know how representative these primary production estimates were either for the 2–3 d collection period of the contemporaneous sediment trap deployments, or for the much longer inter-cruise period (30–40 d). Day-to-day variations in PAR on a given cruise (Fig. 7 and Supplementary Table 1) could lead to significant, short-term variations in primary production. Recent studies conducted near Station ALOHA have reported considerable day-to-day variations in ^{14}C-based primary production (Wilson et al., 2015; Ferrón et al., 2015; see Section 4.7).

3.3.2. *Vertical and temporal variability in primary production*

Primary production at Station ALOHA exhibited both periodic variations with water depth and season, aperiodic variations on multiple time and space (depth) scales, and a sustained long-term increasing

Table 1
Chl *a* and primary production over the 30-yr observation period at Station ALOHA.

Depth	Chlorophyll *a* (mg m^{-3})[a,b]			Primary Production (mg C m^{-3} d^{-1})			
(m)	Annual	Winter[c]	Summer[c]	Annual	Winter (W)	Summer (S)	W/S (%)
5	0.088 ± 0.032 (n = 272)	0.106 ± 0.028 (n = 64)	0.075 ± 0.029 (n = 70)	6.78 ± 2.24 (n = 275)	6.06 ± 1.41 (n = 64)	7.51 ± 3.09 (n = 70)	80.7
25	0.090 ± 0.039 (n = 265)	0.108 ± 0.030 (n = 62)	0.080 ± 0.054 (n = 70)	6.66 ± 2.23 (n = 268)	5.72 ± 1.42 (n = 62)	7.63 ± 3.15 (n = 70)	75.0
45	0.101 ± 0.033 (n = 276)	0.117 ± 0.030 (n = 61)	0.090 ± 0.029 (n = 70)	5.49 ± 1.62 (n = 269)	4.44 ± 1.34 (n = 61)	6.23 ± 1.71 (n = 70)	71.3
75	0.158 ± 0.050 (n = 267)	0.158 ± 0.045 (n = 63)	0.149 ± 0.039 (n = 70)	3.36 ± 1.25 (n = 270)	2.51 ± 1.06 (n = 63)	3.95 ± 1.23 (n = 70)	63.5
100	0.210 ± 0.055 (n = 267)	0.197 ± 0.049 (n = 62)	0.211 ± 0.047 (n = 70)	2.03 ± 1.11 (n = 269)	1.30 ± 0.64 (n = 62)	2.58 ± 1.08 (n = 70)	50.4
125	0.164 ± 0.062 (n = 266)	0.145 ± 0.064 (n = 62)	0.171 ± 0.052 (n = 70)	0.71 ± 0.46 (n = 269)	0.46 ± 0.28 (n = 62)	0.89 ± 0.42 (n = 70)	51.7

[a] All values shown are mean ± 1 standard deviation.
[b] Chlorophyll *a* values are based on fluorometric analysis from primary production cast.
[c] Winter = Dec-Feb; Summer = Jun-Aug.

trend. Primary production was always greatest in the surface mixed layer, and decreased with increasing water depth (Fig. 8 and Table 1). Although several years stand out as having euphotic zone depth-integrated summertime production rates that were >2 SD above the 30-yr mean (1995, 2000, 2004, 2009, 2013, and 2017), only 1995 and 2000 showed evidence of elevated near-surface rate increases (0–25 m; Fig. 8) that would be typical of a "classical" phytoplankton bloom (Dore et al., 2008). The elevated euphotic zone depth-integrated rates in the other four years (2004, 2009, 2013, and 2014) resulted from increased production much deeper in the water column (Fig. 8).

While mean values of primary production were consistently higher in the upper portion of the water column, they varied seasonally at all depths with highest rates observed during the summer period and lowest rates in winter (Figs. 8 and 9; Table 1). Beneath the mixed layer, rates systematically decreased to values that were ~10% of the surface rates at 125 m (Figs. 8 and 9; Table 1). This vertical structure in primary production is controlled by phytoplankton biomass and growth rate, which are set by a balance between light and nutrient availability. The summer-to-winter transition in primary production is a manifestation of variations in solar irradiance (solar intensity and day length; Letelier et al., 2017). However, mean wintertime primary production at 5 m remained at ~80% of the mean summer rate (Fig. 9 and Table 1) despite the much larger difference in mean surface irradiance between seasons. A higher Chl *a* concentration per cell in winter (Fig. 2 and Table 1) enhances light harvesting and sustains the relatively high rates of near-surface photosynthesis throughout the year. In addition, light saturation of photosynthesis in these shallow layers uncouples the photosynthetic rate from solar intensity. In contrast, at greater depths (e.g., 100–125 m), the difference in primary production between summer and winter was approximately a factor of two (Fig. 9 and Table 1), much closer to the differences in daily integrated photon flux at those depths between seasons (Letelier et al., 2017), and significantly greater than the seasonal increase in Chl *a* (~20%) at 125 m.

Perhaps the most surprising result of the primary production time-series at Station ALOHA was a significant ($p < 0.01$), 3-decades-long increasing trend in the measured 0–125 m depth-integrated ^{14}C-based primary production (Fig. 10 and Table 2). Since 1989, 0–125 m depth-integrated primary production at Station ALOHA increased at an average rate of 4.0 (95% CI = 2.1–5.9) (mg C m^{-2} d^{-1}) yr^{-1}(Table 2). This sustained rate of 0.76% yr^{-1} over the 30-yr observation period equates to a total increase of 23% (95% CI = 12–34%) for the 0–125 m depth-integrated primary production. The observed increase in primary production is not uniform throughout the water column. Whereas the trend for the surface (0–25 m) mixed layer was not significantly different from zero, all depths >25 m, and especially in the 75–125 m region of the water column that includes the DCM, the increases in primary production were all significant (Fig. 10 and Table 2). For example, the long term trend for the 75–125 m depth interval was 1.2 (95% CI = 0.6–1.8) (mg C m^{-2} d^{-1}) yr^{-1}, representing a relative change of between 18 and 55% since Jan 1989. The long-term increasing trend in primary production is much greater for summer than for winter periods (Figs. 8 and 10, and Table 2) which is primarily the result of an increase in the seasonal amplitude of C-fixation in this light-limited portion of the water column (Letelier et al., 2004).

Similar long term trends were also observed for fluorometrically determined Chl *a* concentrations measured from the primary production cast and for suspended PC and PN concentrations during the period 1989–2018 (Table 2). For Chl *a* in the 75–125 m portion of the water column, the long term trend was significant ($p < 0.01$) with an observed increase of 0.054 (95% CI = 0.029–0.079) mg Chl *a* m^{-2} yr^{-1}, which is equivalent to a relative increase of 9.2–25.6% (Table 2) since Jan 1989. Since Jan 1989, PC and PN concentrations in the 75–125 m region of the euphotic zone have increased at 0.24 mmol C m^{-2} yr^{-1} and 0.04 mmol N m^{-2} yr^{-1} which were both significant ($p < 0.05$), whereas the suspended particulate matter molar C:N ratio (30-yr mean and SD = 6.37 ± 0.91) did not change significantly (Table 2). As for Chl *a* and primary production, there were no significant changes in suspended PC, PN, or C:N ratio in the upper portion of the water column (Table 2).

3.4. Particulate matter export

PC export over the 30-yr observation period ranged approximately 6-fold from 10 to 60 mg C m^{-2} d^{-1}, with a mean of 27.9 (SD = 9.7) mg C m^{-2} d^{-1} (n = 265; Fig. 11). The PC export time series displayed enigmatic sub-decadal variability with extended periods of relatively low flux during 1991–1996, 2010–2011, and 2013–2014 (Fig. 11). PC export also exhibited seasonal variability with maxima in the May-Aug period and minima in the Sep-Jan period (Fig. 11). The 30-yr means for PC export in summer and winter periods were 33.5 (SD = 9.8, n = 67) mg C m^{-2} d^{-1} and 23.8 (SD = 9.4, n = 62) mg C m^{-2} d^{-1}, respectively. A distinct PC export maximum in Aug was followed by an abrupt shift in Sep from values that were well above the 30-yr mean to values that were well below the mean (Fig. 11). This "end of summer" transition in particle export has also been observed for PC export to abyssal depths at Station ALOHA (Karl et al., 2012).

PN export over the 30-yr observation period ranged approximately 10-fold from 1 to 10 mg N m^{-2} d^{-1}, with a mean of 4.2 (SD = 1.5) mg N m^{-2} d^{-1} (n = 265; Fig. 12). The seasonal and subdecadal patterns, described above for PC export, were nearly identical to the patterns observed for PN export (Fig. 12). Neither PC nor PN export displayed a significant long-term trend (Table 2). The mean PC:PN molar ratio of exported particles was 7.99 (SD = 1.23, n = 260; Fig. 13), with

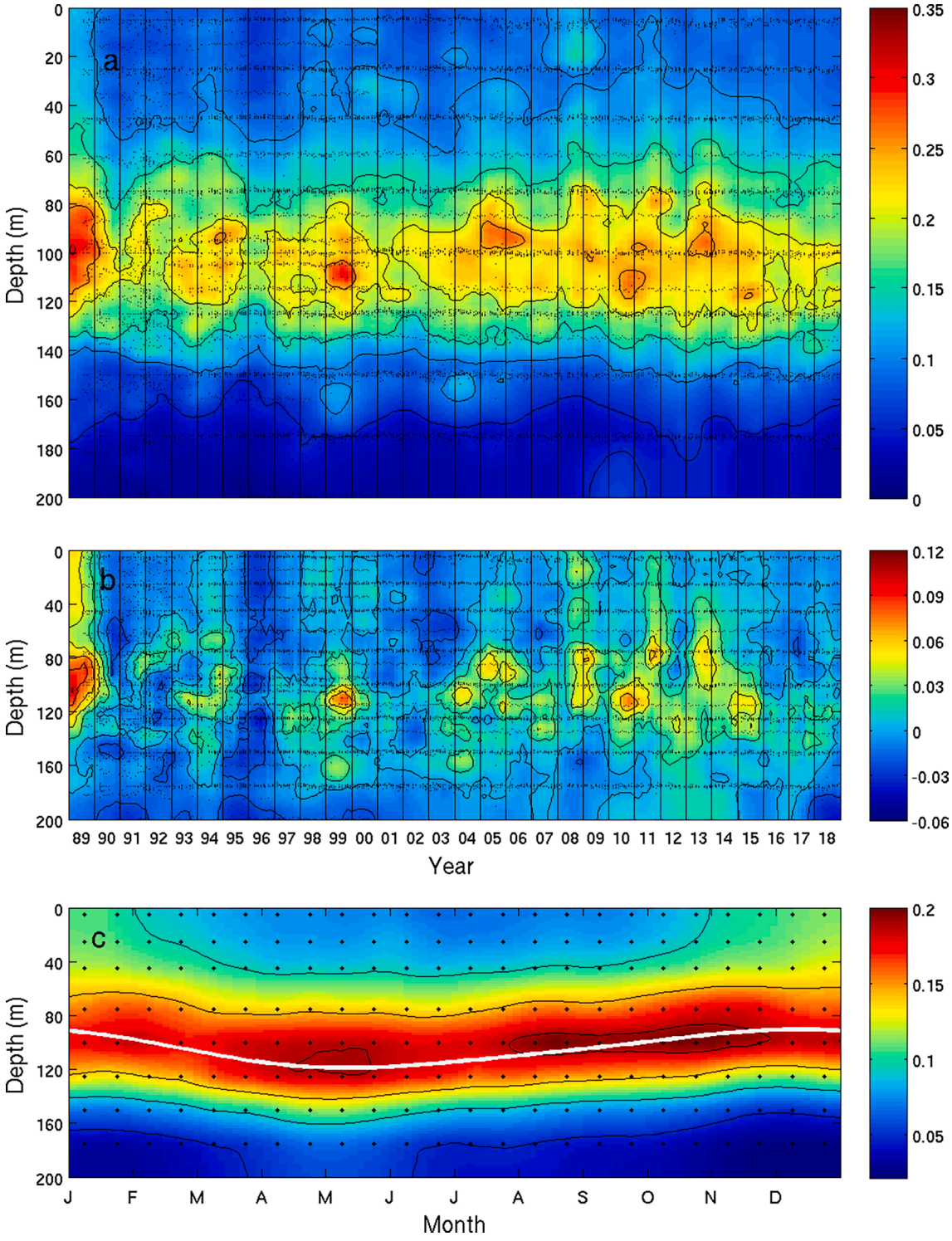

Fig. 3. (a) Time-series (1989–2018), ship-based measurements of fluorometric Chl *a* concentrations (μg l^{-1}) in the upper 0–200 m of the water column at Station ALOHA. (b) Time-series (1989–2018) of Chl *a* (positive/negative) deviations (μg l^{-1}) based on the measured value for each depth and cruise minus the 30-yr monthly climatologies shown in (c). Note the intensification of near-surface ocean Chl *a* concentration in winter, and the intensification and deepening of the deep Chl *a* maximum beginning in late spring, and permanent presence of the deep Chl *a* maximum centered at ~100 m. The white line in (c) depicts the depth of the 0.415 mol quanta m^{-2} d^{-1} isolume.

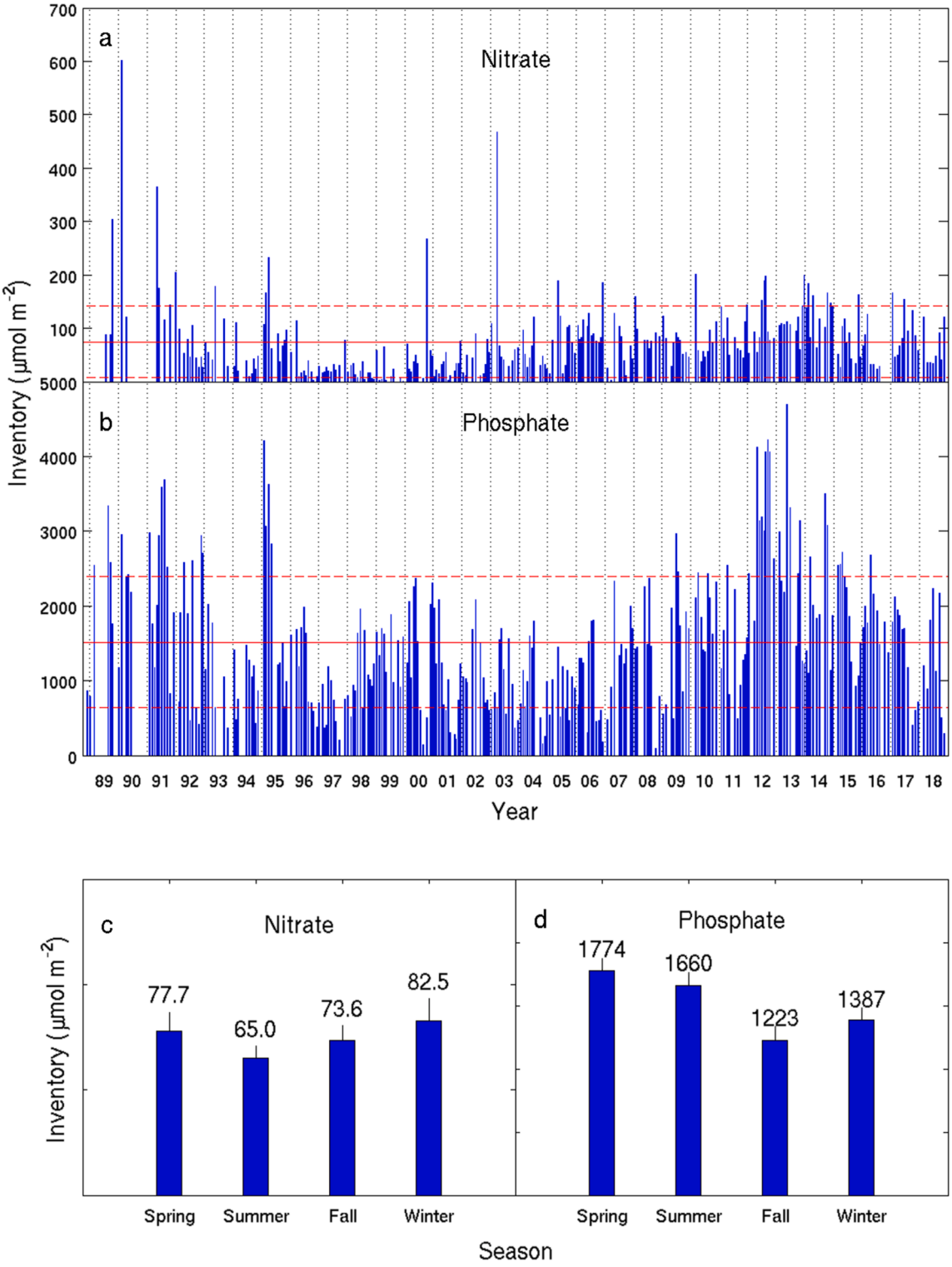

Fig. 4. Time-series (1989–2018) representation of high-sensitivity measurements of 0–25 m depth-integrated (a) nitrate and (b) phosphate inventories, both as µmol m^{-2} for the water column at Station ALOHA. The horizontal solid and dashed lines are the 30-yr mean ± 1 standard deviation. (c and d) Mean and standard deviation values of seasonal nitrate and phosphate for the 0–25 m portion of the water column during the 30-yr observation period.

negligible seasonal variability (e.g., mean spring, summer, fall, winter PC:PN ratios were 7.76, 8.09, 7.98, and 8.12, respectively). The molar PC:PN ratio in exported particles displayed a weak, but significant ($p < 0.01$, decreasing long term trend of −0.027 per year (Table 2).

The e-ratios ranged from 0.020 to 0.149 with a 30-yr mean of 0.054 (SD = 0.021, n = 248; Fig. 14). Because ^{14}C-based primary production can underestimate gross primary production (GPP) by up to a factor of two or more (Quay et al., 2010; also see Section 4.2), the sediment-trap derived e-ratios measured at Station ALOHA are indicative of a sustained, remineralization-intensive system. The relatively large range of e-ratios measured on individual cruises was greatly reduced when the data are presented on a monthly basis (Figs. 14 and 15). Both primary production and PC export were, on average, highest in summer and lowest in winter, so the e-ratios did not vary systematically with season.

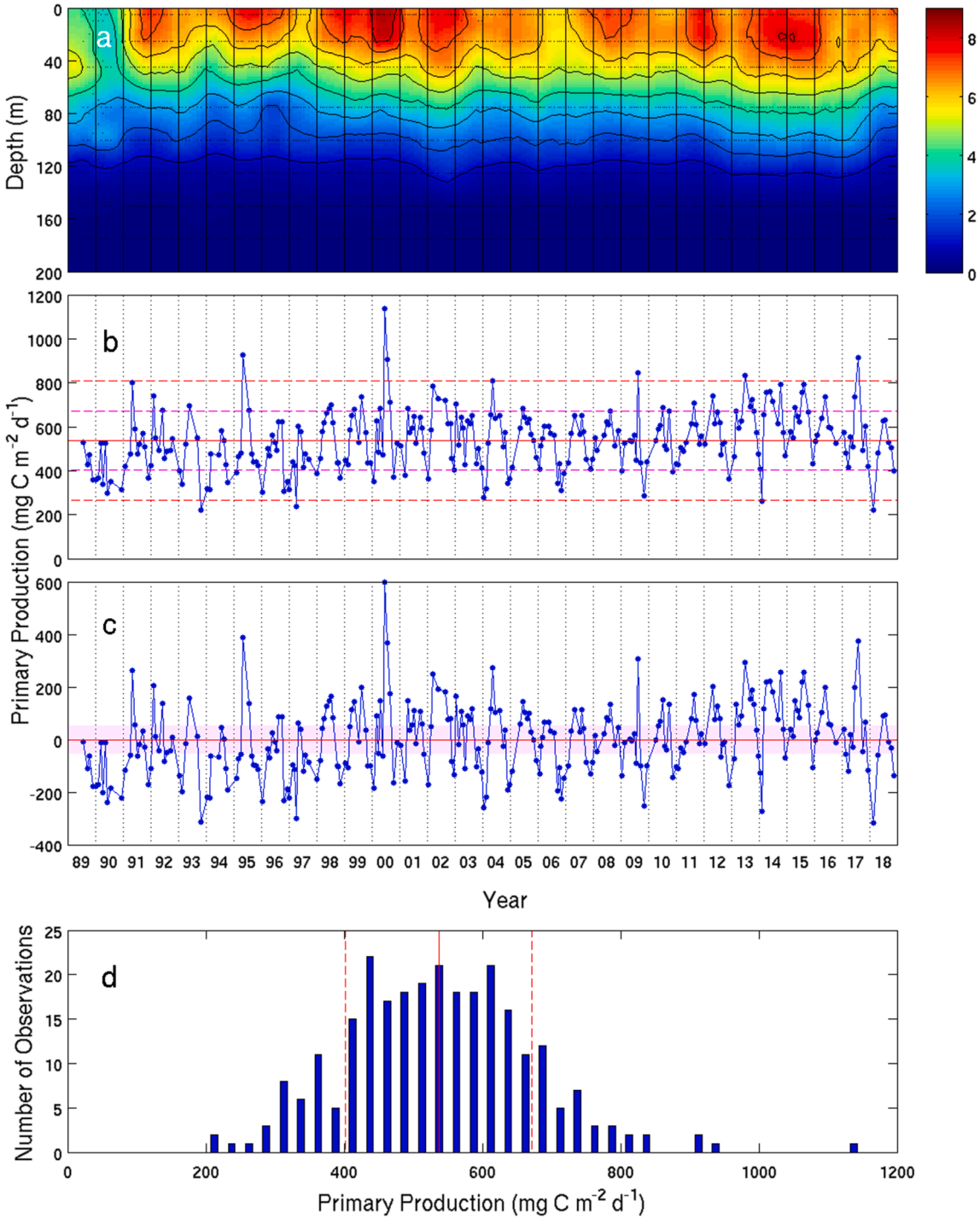

Fig. 5. (a) Time-series (1989–2018) representation of ^{14}C-based primary production (mg C m^{-3} d^{-1}) for the upper 0–200 m of the water column at Station ALOHA. (b) Euphotic zone (0–200 m) depth-integrated primary production time-series (1989–201) showing the mean value 536.8 (mg C m^{-2} d^{-1}; solid line) plus one and two standard deviations (±135.0 and ± 270.0 mg C m^{-2} d^{-1}) as reference points. (c) Primary production for each cruise presented as the difference from the monthly 30-yr mean value. The horizontal line is the zero reference point and the shaded region shows ± 1 standard deviation. (d) Frequency distribution of the 271 observations showing the mean value ± 1 standard deviation as solid and dashed vertical lines.

Indeed, the highest monthly e-ratio was in Feb and the lowest was in Sep, although the differences were not large (Fig. 14). However, when the e-ratio was expressed on an annual basis, there was greater variability with higher than average e-ratios in 1989, 1990, and 1997, and a lower than average e-ratio in 2013 (Figs. 14 and 15). If these four outliers are removed, the 30-yr average drops slightly to 0.052. The minimum in 1990 for annual primary production corresponded to the second highest annual PC export for the entire 30-yr observation period (Fig. 15). Conversely, the 30-yr primary production maximum in 2013 resulted in the lowest annual PC export for the entire observation period (Fig. 15). Furthermore, the increasing trend in annual primary production discussed above, is not reflected in the annual PC export, so the e-ratio shows a significant ($p < 0.01$) decreasing trend of -8.0×10^{-4} yr^{-1} over the 30-yr observation period (Fig. 15 and Table 2). This is equivalent to a long term decrease of 43.9% over the 30-yr observation period (Table 2).

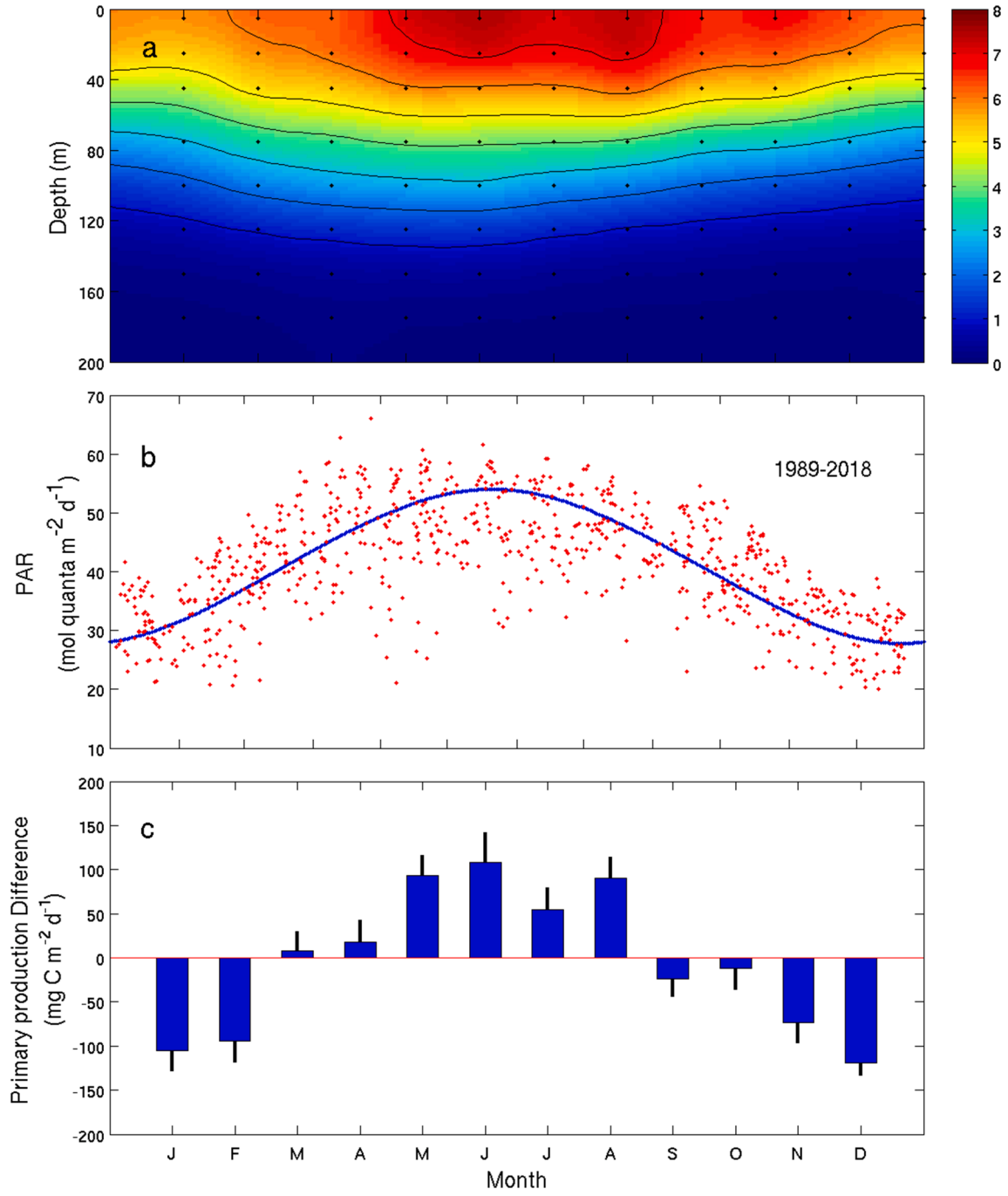

Fig. 6. (a) Monthly climatology of ^{14}C-based primary production (mg C m^{-3} d^{-1}) for the 30-yr observation period (1989–2018). (b) Measured photosynthetically available radiance (PAR; mol quanta m^{-2} d^{-1}) at Station ALOHA for each cruise. The solid blue line is the clear sky radiance at 22°45′N latitude. (c) Monthly climatologies for the 30-yr ^{14}C-based 0–200 m depth-integrated primary production data set presented as difference from the 30-yr mean value (536.8 mg C m^{-2} d^{-1}).

4. Discussion

4.1. Environmental setting and seascape variability

The physical characteristics of the upper water column, including the vertical profiles of temperature, salinity, and density, are key determinants for establishing stratification, mixed layer dynamics, and the turbulent exchange of mass between the lower portion of the euphotic zone and upper portion of the mesopelagic zone. Together with seasonal changes in solar radiation (Letelier et al., 2004; see below), these physical features regulate primary production and particle export. In a pioneering assessment of global primary production, Longhurst et al. (1995) reported a mean value of 160 mg C m^{-2} d^{-1} (59 g C m^{-2} yr^{-1}) for the NPSG, one of 12 secondary biogeochemical provinces of the trade winds domain. Their analysis was based on monthly mean near-surface satellite-based Chl concentrations for the period 1979–1986, the application of a primary production-solar irradiance model, and local incident radiation to compute euphotic zone depth-integrated primary production. These values were consistent with historical (pre-1982) ^{14}C-based estimates of ~250 (summer) and ~200 (winter) mg C m^{-2} d^{-1} for the Climax study area (28°N, 155°W; Hayward, 1987). However, Venrick et al. (1987) reported that the total Chl *a* in the euphotic zone

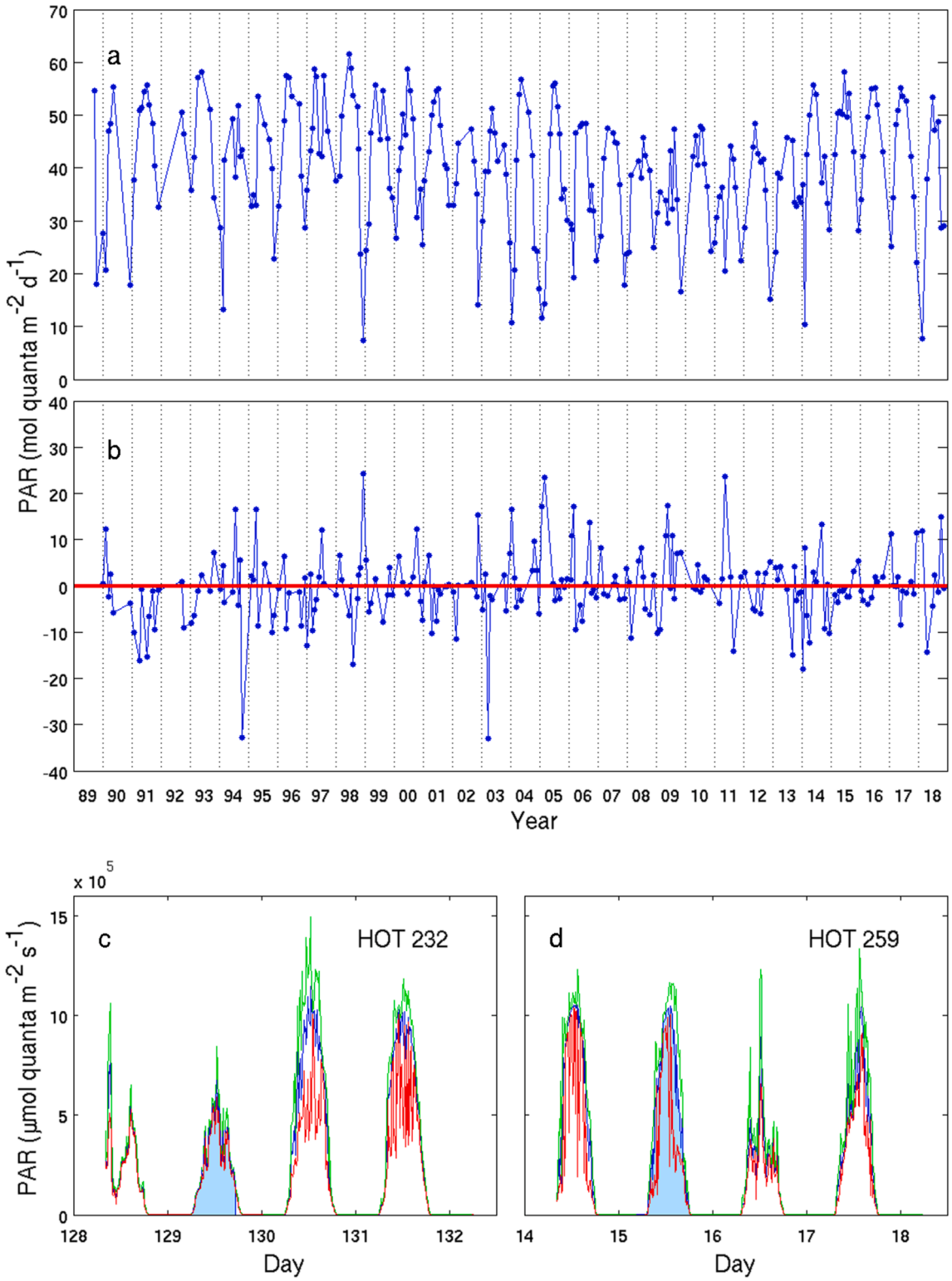

Fig. 7. (a) Time-series (1989–2018) representation of surface photosynthetically available radiation (PAR) in units of mol quanta m^{-2} d^{-1} measured on the day that primary production was conducted for each cruise. (b) The signed difference in daily integrated PAR, as above, measured on the day following the primary production experiment. (c and d) PAR time-series for two representative HOT program cruises (H 232 and H 259) showing 10-min averages (blue) as well as maximum (green) and minimum (red) values during each 10-min bin. The PAR for the day when primary production was measured (shaded portion) was either much lower or much higher, respectively, than the subsequent day. Integrated photon fluxes for the primary production and following day were: HOT 232 = 21.1 and 44.7 mol quanta m^{-2} d^{-1} and HOT 259 = 36.9 and 18.8 mol quanta m^{-2} d^{-1}.

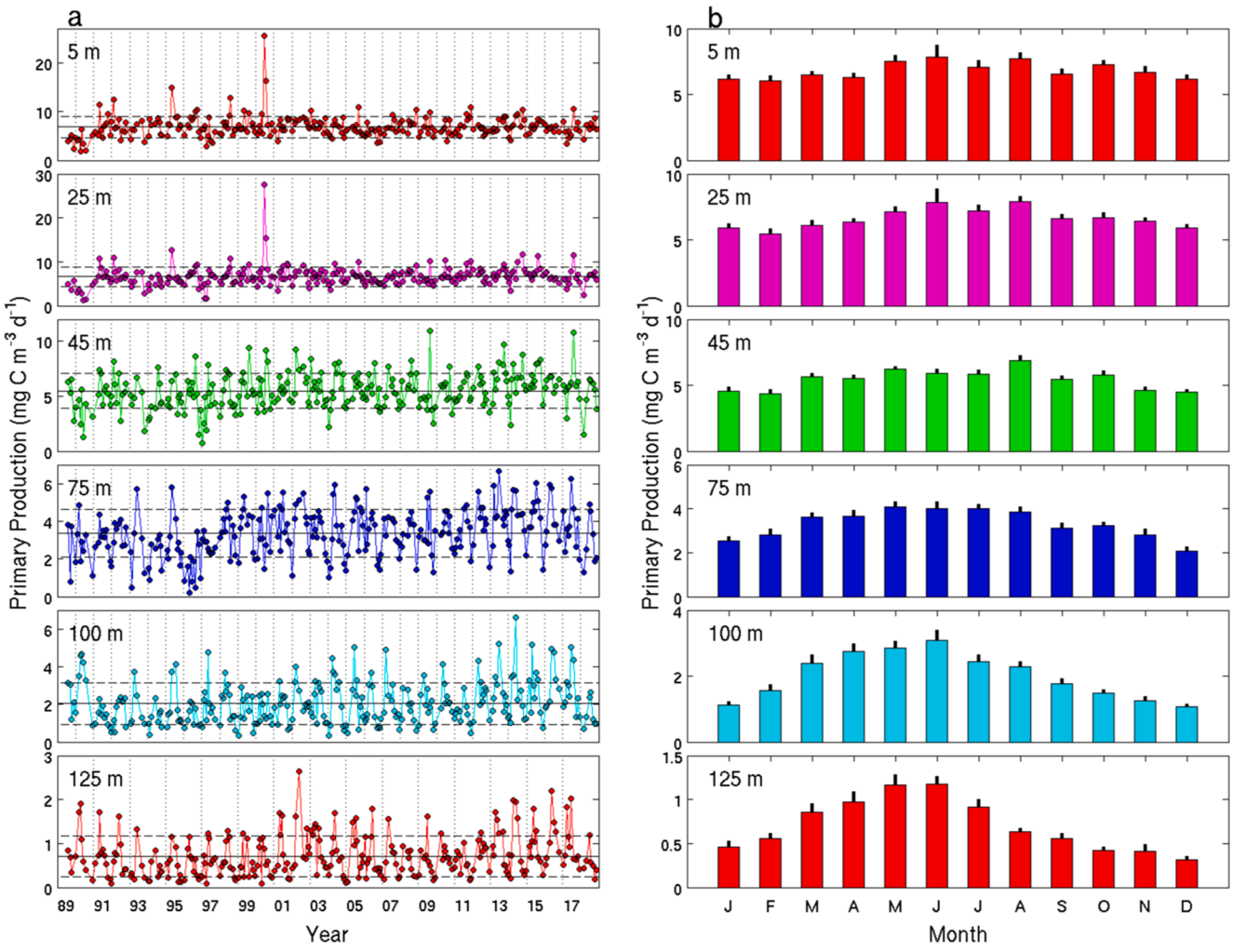

Fig. 8. (a) Time-series (1989–2018) representation of ^{14}C-based primary production (mg C m^{-3} d^{-1}) at the six reference depths at Station ALOHA. The solid and dashed horizontal lines are the mean values ± 1 standard deviation for the 30-yr data set (also see Table 2). (b) Monthly climatologies (1989–2018) of ^{14}C-based primary production (mg C m^{-3} d^{-1}) at the six reference depths at Station ALOHA showing the mean and standard deviation at each depth.

during summer in the Climax study area had nearly doubled since 1968, although their sampling resolution was insufficient to determine the temporal dynamics of this change. Their ^{14}C-based primary production time series was also of insufficient length and temporal frequency to detect any significant change. Nevertheless, Chl *a* values since 1980 were significantly greater than those prior to 1974 (Venrick et al., 1987). Furthermore, the change in total Chl *a* was primarily due to an increased thickness of the 95–120 m DCM whereas the increase of Chl *a* in the surface waters (0–5 m) was negligible (Venrick et al., 1987). They hypothesized that environmental fluctuations, in particular atmospheric forcing via changes in winter storm tracks and sea-level pressure, had altered the carrying capacity of the NPSG epipelagic ecosystem. The long-term increase in Chl *a* could have resulted from a decreased flux of nutrients out of the euphotic zone, or an increased nutrient delivery from allochthonous sources (Venrick et al., 1987). Unfortunately, the approximately 20-year-long Climax time series was terminated just as the Chl *a* trend was reported.

Station ALOHA was established in Oct 1988 with funding from the U. S. National Science Foundation under the auspices of the JGOFS and World Ocean Circulation Experiment (WOCE) programs. The initial research objective was to design, establish, and maintain a deep-water hydrostation as a NPSG benchmark for observing and interpreting physical and biogeochemical variability, and to improve our understanding of the ocean C cycle, especially controls on the BCP (Karl and Lukas, 1996). In this regard, the report by Venrick et al. (1987), linking climate variability to ecosystem structure and function, represented a general unifying hypothesis for the HOT program mission.

The present study reports the time-series data sets for primary production and particle export, two key components of the BCP, from 1989 to 2018 based on over 1000 days of field observations at Station ALOHA (Supplementary Figs. 1 and 2, and Supplementary Table 1). Several previous studies presented and interpreted abbreviated portions of the 30-yr time series of primary production or export (Winn et al., 1995; Karl et al., 1996; Letelier et al., 1996; Emerson et al., 1997; Karl et al., 1998; Scharek et al., 1999; Benitez-Nelson et al., 2001; Karl et al., 2001a; Ondrusek et al., 2001; Neuer et al., 2002; Karl et al., 2003; Corno et al., 2005; Brix et al., 2006; Corno et al., 2008; Dore et al., 2008; Dave and Lozier, 2010; Quay et al., 2010; Saba et al., 2010; Chavez et al., 2011; Karl et al., 2012; Luo et al., 2012; Church et al., 2013; White et al., 2015; Laws et al., 2016; Rii et al., 2016; Letelier et al., 2017; White et al., 2017). In several of these abbreviated analyses, there was evidence for "sustained" subdecadal trends some of which we now know were only transient features based on the analysis of the much longer, 30-yr data set.

Kavanaugh et al. (2018) provided a comprehensive analysis of the three decades of Eulerian observations at Station ALOHA in the context of the larger dynamic environmental heterogeneity of the NPSG as determined by long-term satellite observations and a biogeochemical element cycling model embedded into the Community Earth System Model (CESM-BEC; Moore et al., 2013). This study built on a prior analysis of habitat variability in the North Pacific, which identified

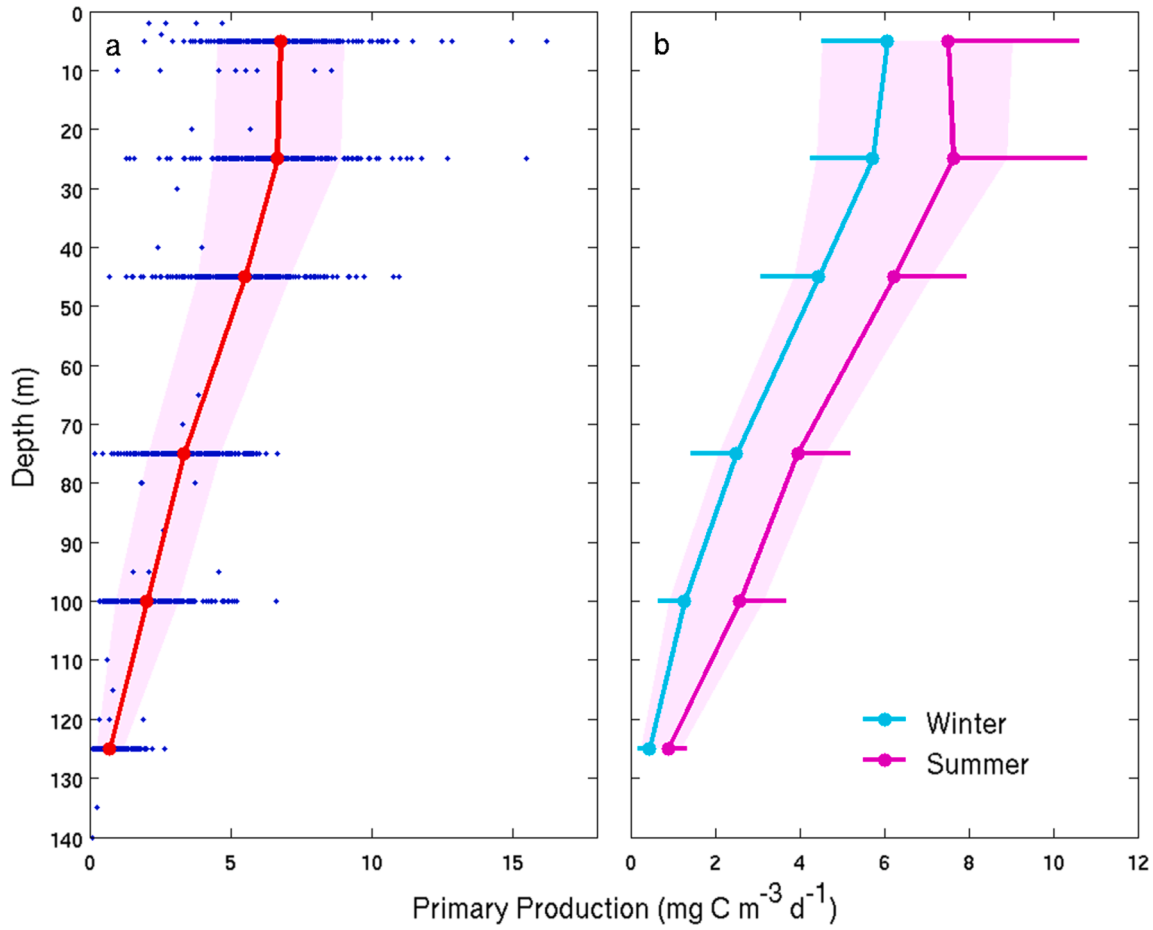

Fig. 9. (a) Vertical profiles of ^{14}C-based primary production for the 6 reference depths at Station ALOHA showing all observations for the period 1989–2018. The shaded region defines ± 1 standard deviation of the mean values. (b) Summer versus winter ^{14}C-based primary production measurements during the 30-hr observation period. Shown are mean values + 1 (summer) or −1 (winter) standard deviations of the respective seasonal mean values. The shaded region defines the ± 1 standard deviation range for the full data set, as shown on left.

several geographically distinct seascapes with Station ALOHA positioned within the subtropical region (Kavanaugh et al., 2014). In the initial study, the authors showed that the aerial extent of the subtropical seascape as well as the distance from Station ALOHA to the boundary of the oligotrophic region have both varied considerably over the past three decades suggesting changes in gyre circulation strength. The environmental forcing associated with the North Pacific Gyre Oscillation (NPGO), the Multivariate El Niño-Southern Oscillation Index (MEI), and the Pacific Decadal Oscillation (PDO), all had predictable effects on conditions at Station ALOHA. Changes in the magnitudes, durations, and synchronies of these independent climate indices were important considerations. For example, from the start of the HOT program in 1988 through 1998, PDO and MEI were out of phase but moved into phase during the 1997–1998 El Niño and remained in phase at least through 2017 (Kavanaugh et al., 2018). In contrast, NPGO was anticorrelated with the other two indices, but led PDO and MEI by 5 and 8 months, respectively (Kavanaugh et al., 2018). These complex climate oscillations are superimposed on any secular trends that might occur at Station ALOHA. However, like all complex processes in nature, no single index or even set of climate indices is sufficient to fully characterize climate variability (Bond et al., 2003).

During the 30-yr Station ALOHA observation period, there have been two very strong (1997–98 and 2015–16) and one strong (1991–92) El Niño events, five strong (1988–89, 1998–99, 1999–00, 2007–08, and 2010–11) La Niña events, and numerous moderate events of both phases based on sea surface temperature anomalies for the Niño 3.4 region (i.e., 5°N-5°S, 120°-170°W; *https://ggweather.com/enso/oni.htm*). It was previously hypothesized that El Niño/La Niña oscillations might impact ecosystem dynamics at Station ALOHA by modulating ocean stratification/mixing, nutrient fluxes to the upper euphotic zone, and the selection for (El Niño) or against (La Niña) *Trichodesmium*, a common dinitrogen (N_2)-fixing cyanobacterium in the NPSG (Karl et al., 1995), all with implications for the BCP. However, this analysis was based on a single, strong El Niño event (1991–92), and since that time there have been two very strong El Niño periods (1997–98 and 2015–16) and five strong La Niña that can be used as field tests of the stratification-nutrient-N_2 fixation hypothesis. From the data presented herein, neither of these very strong El Niño events led to unusually stratified, nutrient-enriched, or productive periods at Station ALOHA (Figs. 1 and 5). This supports previous work at Station ALOHA that also failed to detect El Niño-Southern Oscillation (ENSO)-like frequency variability in any of the core HOT program parameters for the period 1989–2013 (Dore et al., 2014). Furthermore, several new groups of unicellular N_2-fixing cyanobacteria have been discovered in the NPSG since the HOT program began (Zehr et al., 1998; 2001; 2008), so the previous conceptual model based solely on *Trichodesmium* (Karl et al., 1995; Letelier and Karl, 1996) may not be adequate to predict N_2-fixation based ecosystem responses at Station ALOHA.

Corno et al. (2007) analyzed the Station ALOHA time series from 1989 to 2004, which included the very strong 1997–98 El Niño. They reported an approximately 50% increase in euphotic zone depth-integrated primary production over the 15-yr observation period that was punctuated by abrupt changes in both MEI and PDO climate indices. The temporal alignments and strengths of these independent measures of North Pacific Ocean climate variability led to complex environmental

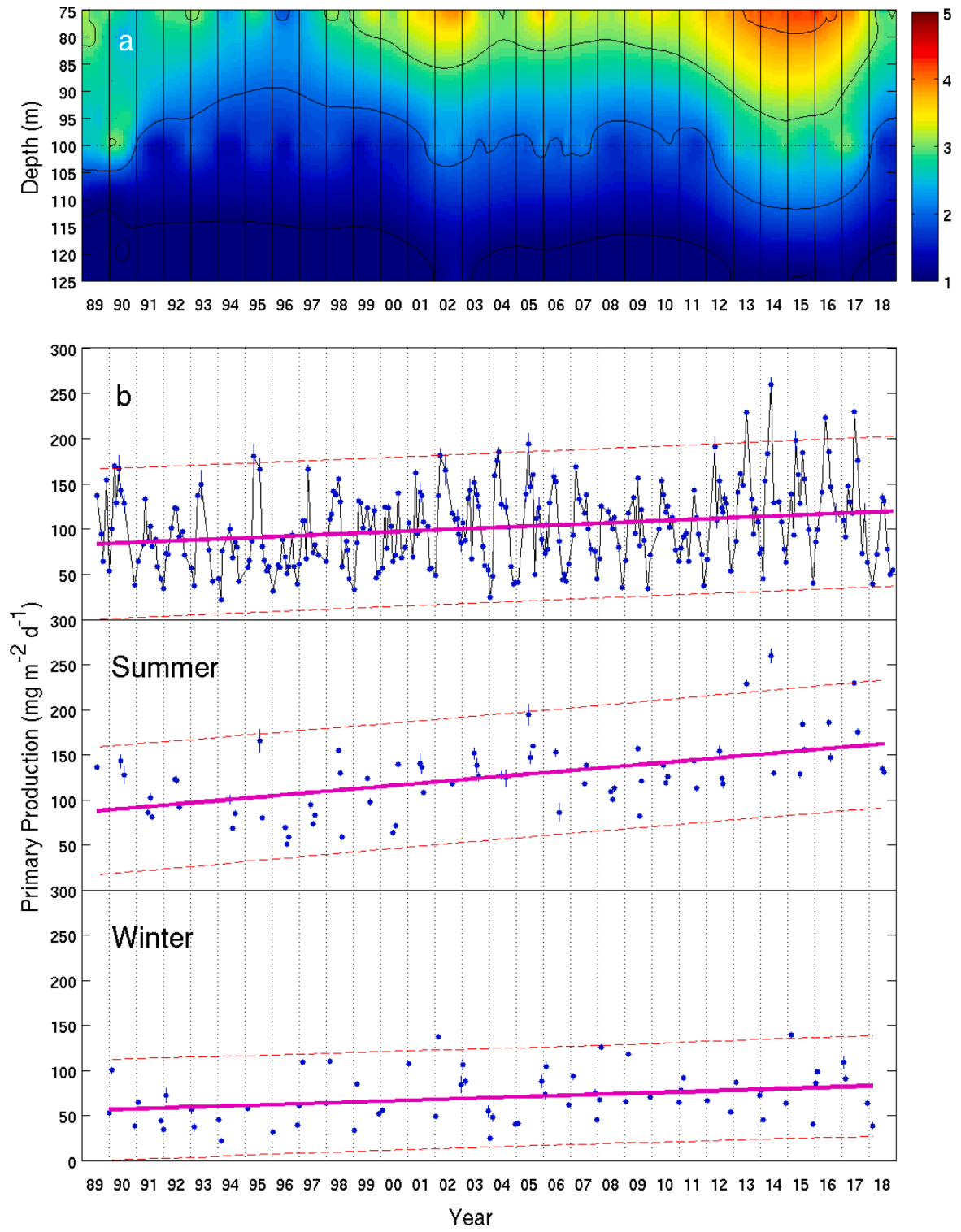

Fig. 10. (a) Contour plot of ^{14}C-based primary production (mg C m^{-3} d^{-1}) for the lower portion (75–125 m) of the euphotic zone. (b) Time-series (1989–2018) representation of the 75–125 m depth-integrated ^{14}C-based primary production showing the increasing trend (±95% confidence interval) for the full data set as well as for summer and winter seasons (also see Table 3 for statistical analysis).

interactions depending primarily upon whether the indices were in or out of phase (Corno et al., 2007). The strongest influences appeared to be on upper ocean stratification and nutrient delivery, with attendant consequences for primary production and export (Corno et al., 2007). However, despite the predicted mechanistic relationship between surface ocean stratification and primary production in oligotrophic ecosystems, analysis of local stratification at Station ALOHA for the period 1988–2008 found no consistent correlation to primary production at any depths within the euphotic zone (Dave and Lozier, 2010).

A comprehensive analysis of the impact of climate variations on ecosystem structure and dynamics was obtained by combining Station ALOHA observations with a coupled physical-biogeochemical model (Bidigare et al., 2009). The model components included a Regional Ocean Modeling System (ROMS) configured for the North Pacific Ocean

Table 2
Long-term (1989–2018) trends for depth-integrated primary production, Chl *a*, suspended particulate C and N, mesozooplankton biomass, PC export at 150 m depth, and export ratio. Italic = p < 0.05, Italic-bold = p < 0.01.

Parameter	Depth or Interval	Mean (SD)	Long-term Trend (95% CI)	Long-term % Change (95% CI)	P-value
Primary Production		(mg C m^{-2} d^{-1})	(mg m^{-2} d^{-1}) $year^{-1}$		
	0–45 m	*289.2 (85.8)*	*1.5 (1.2)*	*15.9 (12.9)*	*1.46 10^{-2}*
	0–125 m	***523.8 (132.7)***	***4.0 (1.9)***	***23.0 (10.7)***	***3.01 10^{-5}***
	75–125 m	***101.7 (43.0)***	***1.2 (0.6)***	***36.6 (18.3)***	***7.22 10^{-5}***
(summer)	75–125 m	***125.1 (40.5)***	***2.6 (1.0)***	***61.3 (24.5)***	***2.56 10^{-6}***
(winter)	75–125 m	*69.9 (28.0)*	*0.9 (0.8)*	*40.7 (34.5)*	*1.57 10^{-2}*
Chlorophyll *a*		(mg m^{-2})	(mg m^{-2}) $year^{-1}$		
	0–45 m	4.12 (1.49)	0.012 (0.022)	8.8 (15.7)	2.73 10^{-1}
	0–125 m	***17.28 (3.49)***	***0.069 (0.049)***	***11.9 (8.5)***	***6.75 10^{-3}***
	75–125 m	***9.26 (1.88)***	***0.054 (0.025)***	***17.4 (8.2)***	***7.15 10^{-5}***
Particulate Carbon		(mmol m^{-2})	(mmol m^{-2}) $year^{-1}$		
	0–45 m	101.1 (17.8)	0.18 (0.26)	5.4 (7.6)	1.31 10^{-1}
	0–125 m	*255.5 (37.0)*	*0.58 (0.51)*	*6.9 (6.0)*	*2.17 10^{-2}*
	75–125 m	*88.7 (14.7)*	*0.24 (0.20)*	*8.0 (6.9)*	*2.27 10^{-2}*
Particulate Nitrogen		(mmol m^{-2})	(mmol m^{-2}) $year^{-1}$		
	0–45 m	14.5 (2.5)	0.02 (0.04)	4.9 (7.3)	1.91 10^{-1}
	0–125 m	38.3 (5.9)	0.07 (0.08)	5.6 (6.2)	3.42 10^{-1}
	75–125 m	*14.1 (2.5)*	*0.04 (0.03)*	*8.5 (7.4)*	*2.28 10^{-2}*
Particulate C:N		(mol mol^{-1})	(mol mol^{-1}) $year^{-1}$		
	0–45 m	7.03 (1.01)	−0.006 (0.014)	−2.6 (6.1)	4.10 10^{-1}
	0–125 m	6.74 (0.93)	−0.005 (0.013)	−2.4 (5.8)	4.16 10^{-1}
	75–125 m	6.37 (0.91)	−0.010 (0.013)	−4.9 (6.2)	1.19 10^{-1}
Mesozooplankton biomass[a]		(g m^{-2})	(g m^{-2}) $year^{-1}$		
Day	0–160 m	***0.78 (0.32)***	***0.9 × 1 10^{-2} (0.57 × 10^{-2})***	***29.2 (18.3)***	***1.89 10^{-3}***
Night	0–160 m	***1.17 (0.40)***	***1.04 × 10^{-2} (0.72 × 10^{-2})***	***22.4 (15.3)***	***4.31 10^{-3}***
Migrant	0–160 m	0.39 (0.25)	0.14 × 10^{-2} (0.46 × 10^{-2})	8.7 (29.5)	5.08 10^{-1}
Particulate Export		(mg m^{-2} d^{-1})	(mg m^{-2} d^{-1}) $year^{-1}$		
Carbon	150 m	27.9 (9.8)	−0.11 (0.15)	−12.1 (16.2)	1.42 10^{-1}
Nitrogen	150 m	4.2 (1.5)	0.01 (0.02)	−4.6 (16.3)	5.73 10^{-1}
C:N Flux		(mol mol^{-1})	(mol mol^{-1}) $year^{-1}$		
	150 m	***7.99 (1.23)***	***−0.027 (0.019)***	***−10.2 (7.1)***	***4.58 10^{-3}***
Export ratio[b]		(mg mg^{-1})	(mg mg^{-1}) $year^{-1}$		
	150 m	***0.054 (0.021)***	***−8.0 × 10^{-4} (3.1 × 10^{-4})***	***−43.9 (16.5)***	***3.02 10^{-5}***

[a] Mesozooplankton sampling period starts in 1994.
[b] particulate C export at 150 m ÷ 0–150 m integrated primary production.

and the Carbon, $Si(OH)_4$, Nitrogen Ecosystem (CoSINE) model of Chai et al. (2002). Variations in observed and modeled parameters at Station ALOHA for the period 1990–2004 were analyzed in relation to phases of ENSO, PDO, and the North Pacific Index (NPI; *http://www.beringclimate.noaa.gov*). As with the previous analysis by Corno et al. (2007), the very strong El Niño (1997–98), which was in phase with PDO and coincident with a shift in NPI from positive to negative values, was the dominant feature explaining the variability observed in their analysis (Bidigare et al., 2009). It was hypothesized that after 1998, changes in salinity, reduced stratification of the upper euphotic zone, and increased wind mixing resulted in a two-fold increase in the modeled nitrate flux into the euphotic zone. This increased availability of new nitrogen resulted in a 45% increase in the abundance of larger (3–4 μm) eukaryotic algae, including diatoms, prymnesiophytes, and pelagophytes (as determined by pigment biomarkers), as well as an equally large increase in mesozooplankton biomass which maintained the modeled phytoplankton at relatively constant levels through grazing and enhanced the export of PN via fecal pellet formation (Bidigare et al., 2009).

In addition, it has recently been hypothesized that climate variability drives oscillations of phosphorus and iron limitation at Station ALOHA. Interannual variations in the transport and deposition of iron-rich Asian dust across the North Pacific Ocean led to oscillating periods of iron limitation and sufficiency due to basin-scale changes in atmospheric pressure, as reflected by the PDO index (Letelier et al., 2019). Iron addition to the nitrogen-starved waters of the NPSG stimulates N_2 fixation, leading eventually to phosphorus limitation of primary production and export. At Station ALOHA, the threshold concentration for the onset of phosphorus limitation was estimated to be 50–60 nM, a value that is very close to the observed long-term mean value reported for near-surface waters (Fig. 4). Using output from the Community Atmospheric Model, version 4 (CAM4), embedded within the Community Earth System Model (CESM; Albani et al., 2014) for the period 1980–2014, Letelier et al. (2019) demonstrated a positive correlation between PDO and iron deposition at Station ALOHA. These climate variations, in turn, led to observed decreases in euphotic zone phosphate concentration as diazotrophs were relieved of iron limitation (Letelier et al., 2019). Under negative PDO phases, there was a reduction in iron deposition and a general weakening of water column stratification, eventually resulting in iron limitation and the accumulation of phosphate due to net in situ regeneration and enhanced advective supply. These complex, climate-driven interactions between phosphorus and iron supplies may have fundamental consequences for primary production, as well as the strength and efficiency of the BCP at Station ALOHA.

Finally, one of the key climate-sensitive environmental variables that might exert a control on primary production and export is the mixed layer depth, and especially the mixing rate within this near-surface isopycnal layer. Surface ocean mixed layer depth is an important variable for primary production because it regulates both solar photon flux and nutrient supply, the two main controls on primary production. Enhanced ocean stratification generally leads to a condition of higher light and lower nutrient concentrations in surface waters, with the possible exception of nutrients like iron, which can be delivered via dry and wet atmospheric deposition. Conversely, deeper surface mixed layers lead to a decrease in average photon flux available for photosynthesis (depending on rate of

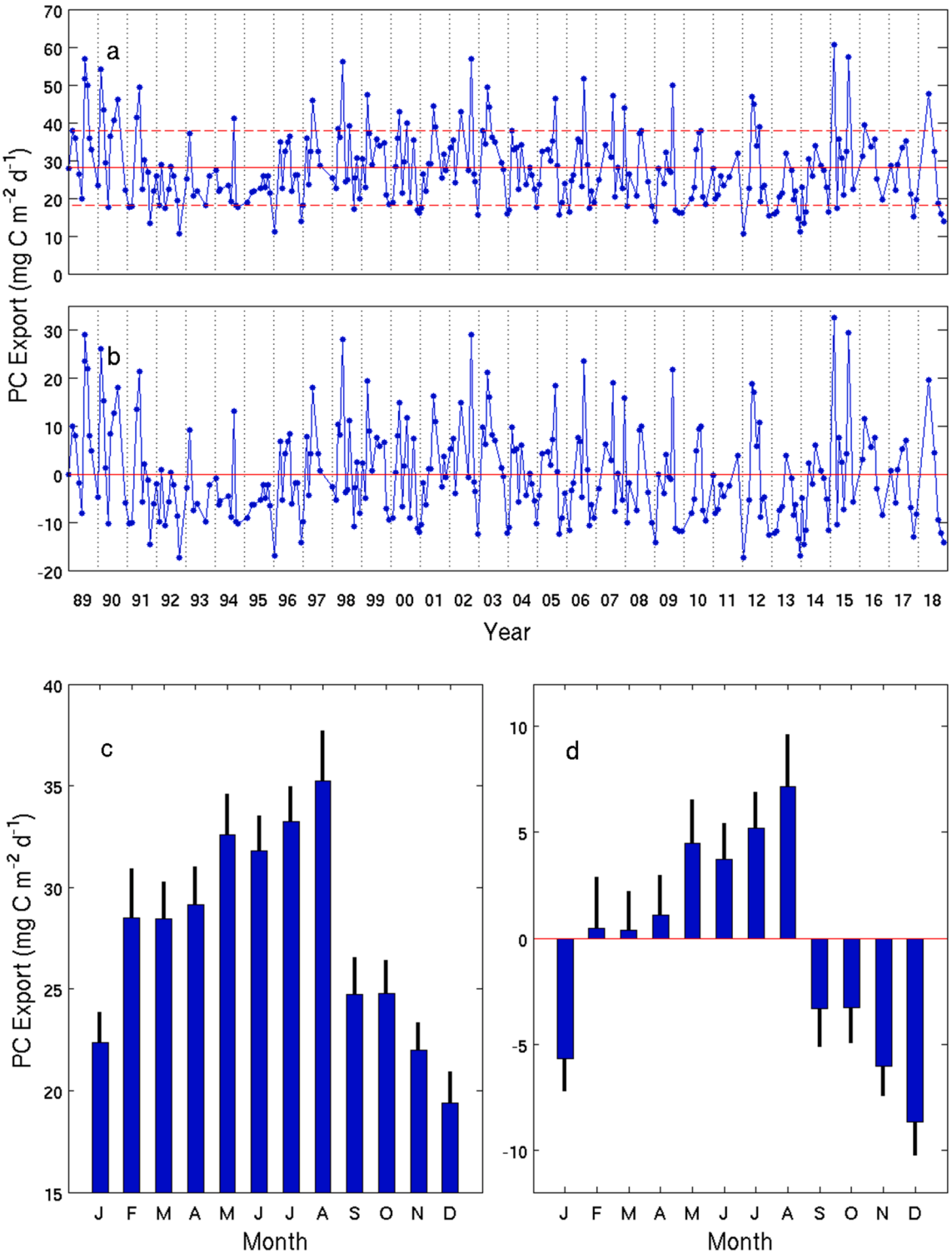

Fig. 11. (a) Time-series (1989–2018) representation of particulate carbon (PC) export (mg C m^{-2} d^{-1}) at the 150 m reference depth at Station ALOHA. The solid and dashed horizontal lines show the mean (27.9 mg C m^{-2} d^{-1}) ± 1 standard deviation (9.7 mg C m^{-2} d^{-1}) for the 30-yr observation period. (b) Signed difference between each measurement and the monthly climatology. (c and d) Plots showing the monthly PC export climatology and the signed difference between the 30-yr mean value and the monthly means.

mixing; Bidigare et al., 2014). Exceptionally deep mixed layers can erode the top of the nutricline and rapidly transport nutrients to the surface, while exchanging heat and mass between the upper and lower regions of the euphotic zone. However, none of the observed deep mixing events reached the 150 m reference depth where particle export was measured. Numerous criteria have been used to determine the surface ocean mixed layer depth. These are based either on temperature or density threshold criteria, with values typically measured from either the ocean's surface (0 m) or a reference depth of 10 m. Application of the most commonly used criteria, namely 0.125 σ_θ and 0.5 °C from 0 m (Levitus, 1982), or 0.2 °C (Kara et al., 2000) and 0.03 σ_θ from 10 m (de Boyer Montégut et al., 2004) at Station ALOHA leads to four different climatologies for mixed layer depth, both for any given cruise, as well as for monthly and annual climatologies (Supplementary Fig. 6). The temperature-based methods,

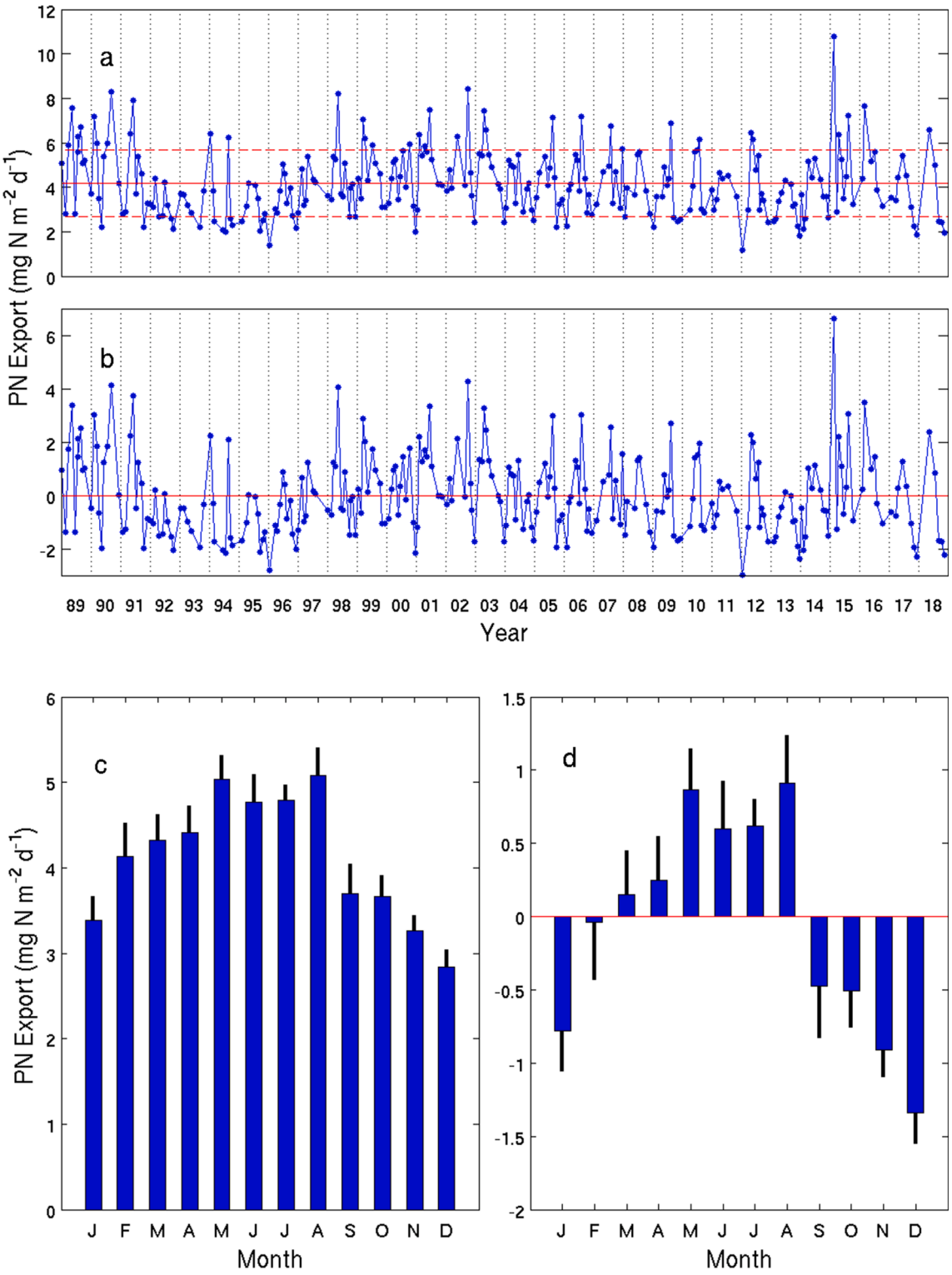

Fig. 12. (a-d) Time-series (1989–2018) representation of particulate nitrogen (PN) export (mg N m^{-2} d^{-1}) for the 150 m reference depth at Station ALOHA presented as for PC export in Fig. 11. The 30-yr mean and standard deviation of PN export are 4.2 ± 1.5 mg N m^{-2} d^{-1}, respectively.

on average, imply deeper mixed layers than the density-based methods. For example, the mean summer and winter mixed layer depths based on the 0.5 °C from 0 m criterion are 49.7 m (SD = 10.8 m, n = 76) and 94.8 m (SD = 24.9 m, n = 74), respectively, compared to 35.6 m (SD = 10.3 m, n = 76) and 62.1 m (SD = 26.1 m, n = 74), respectively, for the 0.03 σ_θ from 10 m criterion. Temperature-based mixed layer depth estimation may not be valid for Station ALOHA due to the significant and unpredictable changes that are observed in sea surface salinity (Lukas 2001; Fig. 1). de Boyer Montégut et al. (2004) recommend the 0.03 kg m^{-3} density threshold as most representative of the layer that has been "actively mixed within the past day or few days." In principle, all physical and biogeochemical properties should be homogeneous within the mixed layer, but this is not always the case for processes that respond rapidly to solar irradiation (e.g., pigments). Of greatest relevance to controls of primary production and export processes may be the daily integrated light field that varies with the rate of turbulent mixing within the mixed

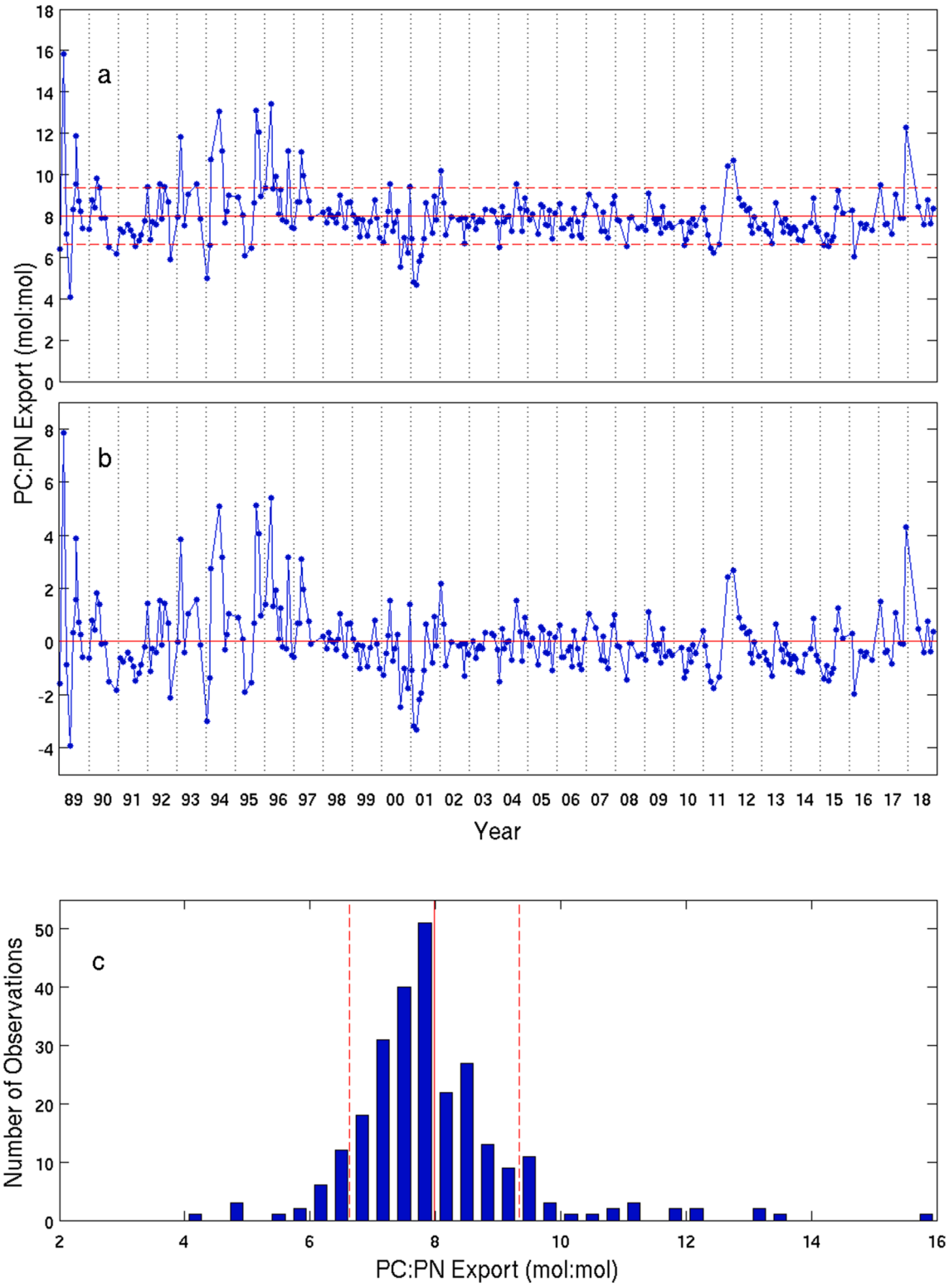

Fig. 13. (a) Time-series (1989–2018) representation of the molar carbon-to-nitrogen (PC:PN) ratios for particulate matter collected in sediment traps at the 150 m reference depth at Station ALOHA. The solid and dashed horizontal lines are the mean (7.99) ± 1 standard deviation (1.23) values for the 30-yr observation period. (b) Plot showing signed deviations from the monthly 30-yr mean values. (c) Frequency distribution of the 265 PC:PN ratios. The solid and dashed vertical lines show the mean ± 1 standard deviation.

layer region. Bidigare et al. (2014) explored upper ocean mixing at Station ALOHA by measuring the dynamics of the xanthophyll pigment cycle, namely the light-dependent de-epoxidation state kinetics, to estimate the turbulent transfer velocity (TTV) in the mixed layer. TTVs ranged from 0.3 to 0.5 cm s^{-1} on a cruise in summer 2012 (Bidigare et al., 2014). Large day-to-day variations (2-fold or larger) were observed in mixed layer depth (using the 0.03 kg m^{-3} from 10 m criterion). Their analysis indicated that the time scale of mixing within the mixed layer on that expedition was 2–4 hrs, which was consistent with the distribution of dissolved carbon monoxide that is produced primarily via photochemical

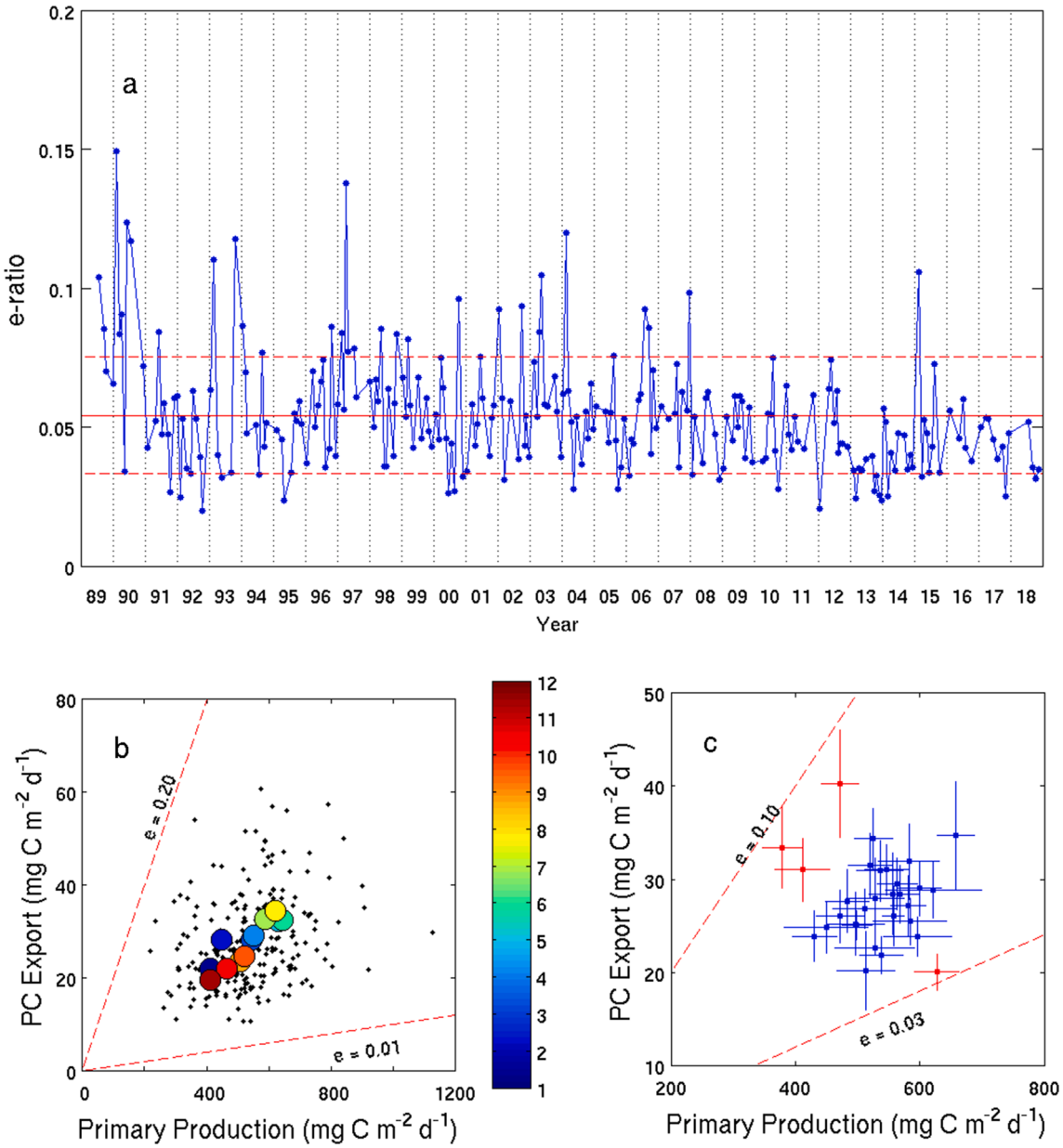

Fig. 14. (a) Time-series (1989–2018) representation of export (e) ratios (e = PC export at 150 m ÷ ^{14}C-based 0–150 m depth-integrated primary production) at Station ALOHA. The solid and dashed horizontal lines depict the mean (0.054) and ± 1 standard deviation (0.021) for the 248 measurements over the 30-yr observation period. (b) Depth-integrated (0–150 m) primary production (mg C m^{-2} d^{-1}) versus the 150 m PC export (mg C m^{-2} d^{-1}) at Station ALOHA. The small solid symbols are the data from individual cruises while the larger colored symbols (colored by month) are the monthly climatologies for the 30-yr observation period. The dashed red lines represent the boundaries for e-ratios = 0.01 and 0.20. (c) Primary production and PC export, as in b. Symbols are the 30 individual annual mean 0–150 m depth-integrated primary production and 150 m PC export values (shown with ± 1 standard deviations for the respective variable) along with boundaries for e-ratios = 0.03 and 0.10. The four years, shown in red, have anomalously high export compared to primary production (1989, 1990, and 1997) or anomalously low export (2013) compared to the full 30-year data set.

degradation of chromophoric dissolved organic matter in the tropical ocean (Bidigare et al., 2014). This elegant, but fairly labor-intensive analysis has not been repeated at Station ALOHA, so we have only fragmentary information on mixed layer mixing rates.

4.2. *Primary production at Station ALOHA: The mean state, seasonal climatology, and subdecadal scale variability*

In this present study, we report ^{14}C-assimilation into particulate matter after dawn–to-dusk in situ incubations. Notwithstanding the long tradition of debate surrounding terminology used to describe the conversion of light energy into chemical energy via the process of photosynthesis (e.g., Flynn, 1988; Williams, 1993; Williams, 2014), herein we refer to this measurement as primary production at Station ALOHA. In this section we discuss the mean state of euphotic zone depth-integrated primary production over the 30-yr observation period, as well as controls on the temporal and vertical variability of primary production. Section 4.3 discusses the controls and ecological consequences of the long-term increasing trend of primary production at Station ALOHA.

The three-decades-long primary production data set from Station ALOHA is the most extensive of its kind for any location in the NPSG. Compared to historical estimates of ^{14}C-based primary production obtained from the Climax time-series program (1965–1980; Hayward, 1991), the 30-yr mean value of 536.8 mg C m^{-2} d^{-1} measured at Station

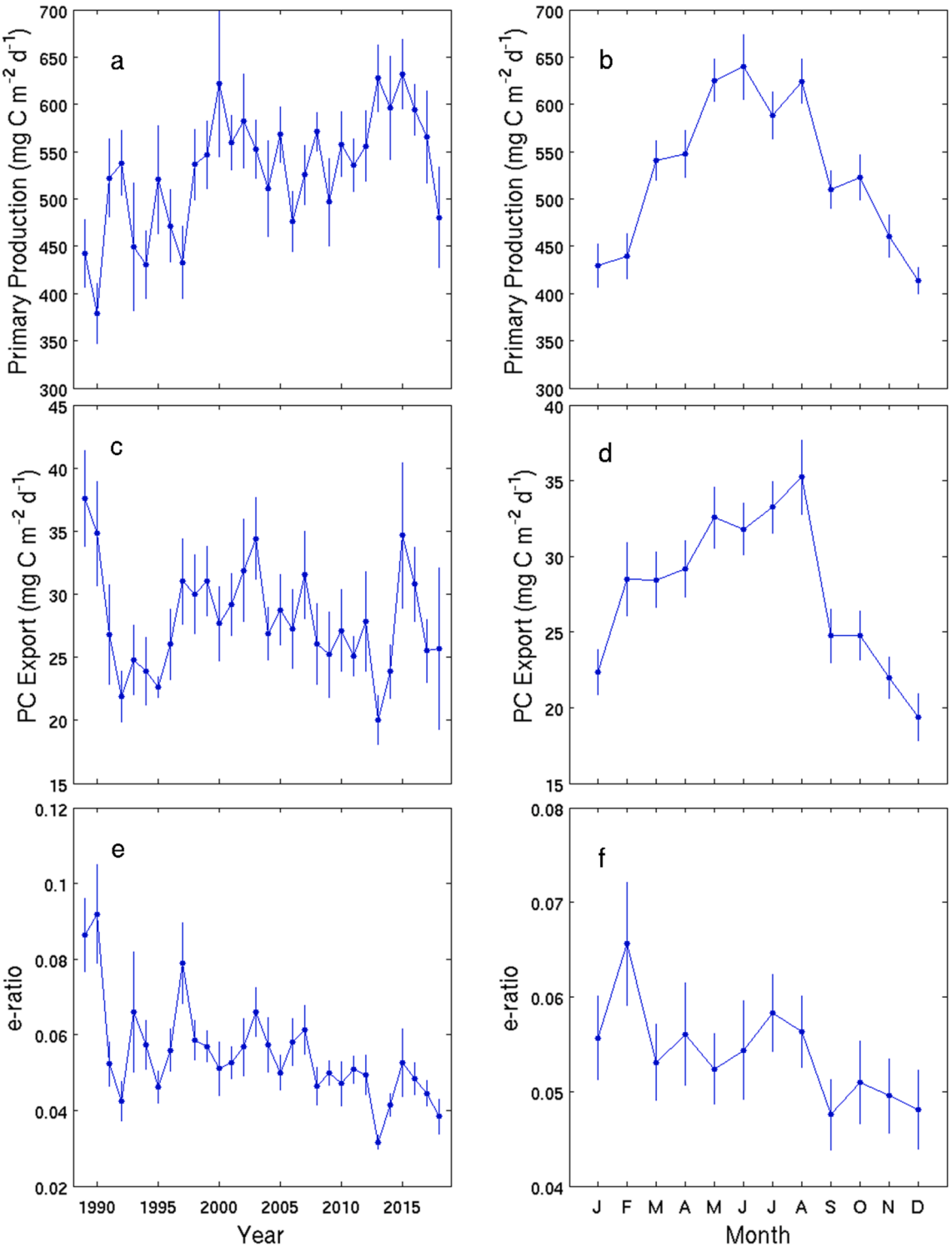

Fig. 15. (a and b) Time-series (1989–2018) representation of annual and monthly 0–150 m depth-integrated primary production (mg C m^{-2} d^{-1}) at Station ALOHA showing mean values ± 1 standard deviation. (c and d) Time-series (1989–2018) representation of annual and monthly 150 m PC export (mg C m^{-2} d^{-1}) at Station ALOHA showing mean values ± 1 standard deviation. (e and f) Time-series (1989–2018) representation of annual and monthly 150 m e-ratio at Station ALOHA.

ALOHA is approximately 2–3 times higher. Most of the pre-1980 ^{14}C-based primary production estimates near the Climax site were incubated on deck with neutral density light filters and circulating surface seawater. The incubation experiments typically lasted ~6 hr (noon-sunset), and primary production was reported as "half-day" ^{14}C assimilation (daily rates were assumed to be twice the "half day" rate; Hayward, 1987). Although methodological improvements may preclude direct comparisons, the higher values for ^{14}C-based primary production post-1980 coincide with higher concentrations of Chl *a* (Venrick et al., 1987), consistent with a higher phytoplankton biomass and productivity during the HOT program era at Station ALOHA compared to Climax (Karl et al., 2001a). The methods used for sampling and quantification of Chl *a* concentrations by fluorometry are similar to those used prior to the HOT-era, so the post-1980 change, indicative of increases in Chl *a* or of a shift in the phytoplankton community structure toward a Chl *b*-rich assemblage (Karl et al., 2001a), lends support to the hypothesis that

primary production in the NPSG has also increased.

Our ^{14}C-based primary production estimates at Station ALOHA can also be compared to in situ values obtained during the VERTEX program in Jul-Aug 1983 at 28°N, 155°W (401 mg C m^{-2} d^{-1}; Martin et al., 1987) and the PRPOOS program in Aug-Sep 1985 at 28°N, 155°W (456 mg C m^{-2} d^{-1}; Marra and Heinemann, 1987). Since 1989, the 0–125 m euphotic zone depth-integrated primary production at Station ALOHA has continued to increase at a rate of 4.0 (mg C m^{-2} d^{-1}) yr^{-1} (>0.7% yr^{-1}) with summertime rates now exceeding 600 mg C m^{-2} d^{-1} (Figs. 5 and 15, Table 2; also see Section 4.3). In an attempt to reconcile their relatively high primary production during the summer of 1985 in the absence of available fixed nitrogen, Marra and Heinemann (1987) hypothesized that either atmospheric deposition of nitrate or nitrogen fixation, or both, may have been systematically underestimated. While we observed significant temporal variations on scales from months to decades, it is undeniable that primary production in the NPSG has been on an increasing trend over the past three decades, and possibly longer. The sustained, 30-yr increasing trend in primary production reported here is primarily a result of elevated rates in the lower euphotic zone (75–125 m), rather than an increase in the light-saturated region (Table 2; also see Section 4.3).

The ^{14}C-based primary production estimates as presented in this study are less than gross primary production (GPP), but probably greater than net primary production (NPP; Marra, 2009; Pei and Laws, 2014) which is typically measured on a 24-hr daily basis. We also know that a portion of the recently fixed ^{14}C is excreted as ^{14}C-labeled dissolved organic carbon (^{14}C-DOC; Karl et al., 1998), some of which is remineralized by heterotrophic microorganisms back to $^{14}CO_2$ or converted into new biomass during the ~12-hr incubation period. In addition, protistan grazing on ^{14}C-labeled phytoplankton and indirectly labeled heterotrophic bacterial cells, viral lysis, phytoplankton respiration, death, and autolysis all contribute to losses of recently produced organic matter. For selected periods of time (Oct 1988 – Jul 1997, Oct 2004 – Oct 2007, and Apr 2010 – Oct 2012), both ^{14}C-POC and ^{14}C-DOC production at Station ALOHA were measured. It was determined that the type of filter used for the ^{14}C-POC analysis affected the apparent partitioning between POC and DOC, but there was clear evidence for significant ^{14}C-DOC production (Karl et al., 1998). A more recent investigation at Station ALOHA provided a comprehensive analysis of vertical and temporal trends in the dynamics of ^{14}C-POC and ^{14}C-DOC pools (Viviani et al., 2015). The most striking result was the variability observed in the ratio of ^{14}C-DOC to total ^{14}C production, indicating that the pathways controlling the distributions of recently fixed C are also temporally variable (Viviani et al., 2015). Since DOC and POC have fundamentally different fates in oligotrophic oceanic ecosystems, this apparent temporal decoupling of C and energy flow is likely to have a major impact on fundamental ecosystem processes such as the net metabolic balance (i.e., the difference between primary production and respiration) and C sequestration via the BCP.

Additional evidence to support our assumption that the measured 0–125 m euphotic zone depth-integrated ^{14}C-based primary production is less than GPP is based on comparisons to previously reported ^{18}O-H_2O-based estimates of GPP at Station ALOHA (Juranek and Quay, 2005, Quay et al., 2010). Generally, the $^{18}O_2$-based estimates exceeded the ^{14}C-based estimates, especially in the light-saturated portion of the water column (<25 m). However, the differences between the two estimates decreased with depth and became indistinguishable at ~100 m (Juranek and Quay, 2005; Quay et al., 2010). The ratio of NPP:GPP would be expected to vary as a function of light intensity, phytoplankton community structure, and growth/grazing rates, although we lack a comprehensive understanding at the present time.

Euphotic zone depth-integrated primary production at Station ALOHA varied on a broad range of temporal scales from days to decades, and only ~25% of the time was the measured value within ± 10% of the long-term mean value of 536.8 mg C m^{-2} d^{-1} (Fig. 5). Letelier et al. (1996) presented an authoritative summary of the seasonal and interannual variations in primary production at Station ALOHA for an initial period (1988–1992) of the HOT program. The much longer 30-yr ^{14}C-based primary production time series presented herein confirms some of the earlier results, but also presents novel unexpected trends and

Table 3
Contributions to the observed time-series (1989–2018) variance by the climatological seasonal cycle, interannual variability, and long-term linear trend. The sub-seasonal contribution is estimated as the residual variance once the seasonal, interannual, and long-term components have been subtracted from the total variance.

Parameter	Depth or Interval	% Variance			
		Seasonal	Interannual	Long-term trend	Sub-seasonal
Primary Production					
	0–45 m	11.2	22.8	2.2	63.8
	0–125 m	27.7	20.4	6.3	45.6
	75–125 m	40.3	19.5	5.7	34.5
Chlorophyll *a*					
	0–45 m	17.2	10.6	0.0	72.2
	0–125 m	8.8	19.3	2.3	69.4
	75–125 m	3.9	20.0	5.6	70.5
Particulate Carbon					
	0–45 m	27.4	10.8	0.8	61.0
	0–125 m	32.1	15.4	1.8	50.7
	75–125 m	17.5	16.8	1.8	63.9
Particulate Nitrogen					
	0–45 m	15.0	14.5	0.6	69.9
	0–125 m	18.2	16.8	1.0	64.0
	75–125 m	11.3	16.9	1.8	70.0
Mesozooplankton biomass[a]					
Day	0–160 m	26.2	22.2	4.0	47.6
Night	0–160 m	16.4	31.7	3.4	48.5
Migrant	0–160 m	1.5	19.1	0.2	79.4
Particulate Export					
Carbon	150 m	21.9	19.7	0.9	57.6
Nitrogen	150 m	21.5	20.9	0.9	57.7
Export ratio[b]					
	150 m	2.0	20.7	9.3	68.0

[a] Mesozooplankton sampling period starts in 1994.
[b] particulate C export at 150 m ÷ 0–150 m integrated primary production.

controls. For example, with only a 4-yr data set, Letelier et al. (1996) were not able to resolve a seasonal cycle in euphotic zone depth-integrated primary production. However, at depths >100 m a clear seasonal pattern (attributed to changes in surface irradiance) was observed with maximum primary production in late spring and early summer (Letelier et al., 1996). More recently, Karl et al. (2002), Saba et al. (2010), Chavez et al. (2011), and Church et al. (2013) have all reported a weak but significant seasonality in euphotic zone depth-integrated primary production at Station ALOHA. The 30-yr 0–125 m depth-integrated primary production confirms a seasonal cycle contributing to ~30% of the total observed variance (Table 3), with maximum values in summer (mean = 616.2, SD = 129.1 mg C m^{-2} d^{-1}, n = 68) and minimum values in winter (mean = 424.9, SD = 99.5 mg C m^{-2} d^{-1}, n = 64; Figs. 7, 9, and 15). However, the seasonal cycle in primary production is much more distinct at depths >75 m than in the much more productive upper portion of the water column (Fig. 8). The 30-yr mean winter:summer primary production ratios systematically decreased through the water column from a value of 0.81 at 5 m to a minimum of ~0.50 at depths ≥100 m (Fig. 9). This pattern of a relatively weak seasonal signal in the upper euphotic zone is indicative of an ecosystem that is chronically nutrient-limited and light-saturated compared to the lower portion of the water column which is light-limited. Furthermore, Letelier et al. (2004) have documented that the downward seasonal displacement of PAR isolumes in summer induces a deepening of the DCM from 105 m in winter to 121 m in summer with a concomitant increase in Chl *a* and the disappearance of 36 mmol m^{-3} of nitrate from the lower portion of the water column.

The seasonal variations in euphotic zone depth-integrated primary production are due, in large part, to predictable variations in PAR. While there are stochastic day-to-day variations in photon flux due to cloud cover and aerosol optical depth of the atmosphere relative to clear sky irradiance for a given day (Fig. 7 and Supplementary Table 1), the greatest changes in light are based on day length and solar power at 22°45′N, and these parameters can be predicted. Light appears to be a master variable at Station ALOHA, at least in the mean state, with average winter and summer primary production being approximately −100 mg C m^{-2} d^{-1} and +100 mg C m^{-2} d^{-1} of the 30-yr mean value (Fig. 6). However, the large interannual variations for a given season (e.g., summer of 1990 versus summer of 2000, or winter of 1992 versus winter of 2000; Fig. 5), which account for ~20% of the total variance (Table 3), and the irregular deviations in the monthly primary production climatologies (~45% of the total variance; Table 3), especially in mid-summer (Figs. 6 and 15), cannot be attributed to PAR alone. Additional controls on primary production, most likely variations in macronutrient, trace metal, or vitamin availability may be important regulators of primary production at Station ALOHA. These variables are not well constrained despite the enormous sampling and scientific efforts invested in the HOT program. For example, while macronutrient (nitrate and phosphate) concentrations are routinely measured each month, we do not measure nutrient fluxes, and the vanishingly low concentrations of nitrate (<10 nM) are probably as much a manifestation of rapid uptake as they are a result of low supply rates. The average nitrate and phosphate concentrations in the upper 0–25 m, where primary production is highest, are both time variable (e.g., the variations in nitrate and phosphate concentrations are in excess of an order of magnitude), but do not co-vary (Fig. 4). While near-surface nitrate concentrations are greatest in late winter and early spring, with occasional spikes due to deep water mixing, and at a minimum in summer, phosphate inventories are highest in spring and lowest in fall-winter (Fig. 4). There are also very large interannual variations in 0–25 m nitrate and phosphate inventories with generally higher values in the periods 1989–1991, distinct minima from 1996 to 2006, and increasing concentrations in the period 2012–2014 (Fig. 4). The latter increases in both nitrate and phosphate are especially enigmatic because they do not lead to higher primary production or higher Chl *a* concentrations, challenging our current paradigm of a macronutrient-controlled NPSG ecosystem.

In addition to nitrate and phosphate concentrations, we have a more limited data set on dissolved organic N and P (DON and DOP). DON and DOP concentrations are much larger than the corresponding nitrate and phosphate pools, in the case of DON by three orders of magnitude (mixed layer DON values ~5–6 μM; Karl et al., 2001b). Moreover, the mean molar DON:DOP ratio (26:1) of the organic pool is greater than the Redfield ratio of 16:1, whereas the mean molar nitrate:phosphate ratio is much lower than the Redfield ratio (~0.05). We presently have only limited information on the chemical composition and, hence, the bioavailability of these organic nutrient pools.

The well resolved climatology reveals two periods of elevated near-surface primary production. The first period begins in May and peaks in Jun (Figs. 6 and 8). This is essentially the Station ALOHA "spring bloom" and is a consequence of increasing solar irradiance. However, there is an early summer reduction in primary production, especially in the most productive (0–45 m) portion of the water column (Figs. 6 and 8). Because irradiance is still at an annual maximum, this "Jul lull" is most likely a consequence of fixed N limitation. Primary production increases again in Aug through Sep, even though surface irradiance begins to decrease. We refer to this feature as the "late summer bloom" at Station ALOHA. We further hypothesize that this enhancement in primary production relative to available light and depletion of nitrate is the result of a seasonal selection for N_2-fixing microorganisms (mostly cyanobacteria) that proliferate during stratified late summer periods when nitrate delivery via physical processes is at its seasonal minimum (Karl, 2002; Dore et al., 2008; Böttjer et al., 2017). N_2 fixation is an important process at Station ALOHA since it provides a source of new nitrogen to support primary production and export even when fixed N sources are otherwise limiting (Karl et al., 2002). Therefore, we interpret the higher than expected (based strictly on PAR) ^{14}C-based primary production in the HOT program climatology following the Jul lull (Fig. 7), as a manifestation of fixed N delivery via N_2 fixation. This enhanced, N_2 fixation-supported primary production was detected in the light-saturated region of the euphotic zone (0–45 m), below which ^{14}C-primary production tracked the expected summer to fall decreases in PAR (Fig. 8). From Sep through Mar, primary production is consistently at or below the long-term mean of 536.8 mg C m^{-2} d^{-1} (Fig. 6). We have also confirmed the observation, first reported by Letelier et al. (1996), of a clear seasonality of primary production at depths ≥75 m, contributing to ~40% of the total variance in the 75–125 m depth range (Fig. 8; see Section 4.3).

Previous studies of N_2 fixation at Station ALOHA have shown that N_2-fixing microorganisms are both diverse and seasonally variable in abundance. For example, cyanobacterial N_2 fixers are present as free-living unicellular (e.g., *Crocosphaera*) and filamentous morphologies (e.g., *Trichodesmium*), as well as in symbiotic associations with a variety of eukaryotic algae (e.g., *Richelia* and UCYN-A). While earlier studies at Station ALOHA focused primarily on *Trichodesmium* (Letelier and Karl, 1996; 1998) and to a lesser extent on endosymbiotic associations of *Richelia* with several diatom species, the discovery of abundant unicellular cyanobacterial species (Zehr et al., 1998; 2000; 2001) at Station ALOHA demanded a reassessment of the role of N_2 fixation in the NPSG (Karl et al., 2008; Zehr and Capone, 2020). The *nifH* gene expression patterns, measured by reverse-transcribed quantitative polymerase chain reaction (RT-QPCR) methods revealed complex, but highly ordered, diel patterns with greatest transcription activity during the daylight period (Church et al., 2005). These initial observations were confirmed during a recent, comprehensive study of the regulation of growth, activity, and gene transcription in natural populations of *Crocosphaera* near Station ALOHA (Wilson et al., 2017). While N_2 fixation at Station ALOHA occurs throughout the year, average rates are greatest in late summer-to-early fall (Böttjer et al., 2017). Furthermore, diatom-associated *Richelia* and *Calothrix* spp. abundances and *nifH* gene copies attributable to heterocystous cyanobacteria both peaked in summer (White et al., 2018). Excess ammonium and bioavailable dissolved organic N, both produced by N_2-fixing cyanobacteria, fuel primary production of phytoplankton that are unable to fix N_2, a phenomenon

referred to as an echo bloom (Devassy et al., 1979). However, sustained N_2 fixation-based new production requires a supply of both phosphorus and iron, which may ultimately set an upper limit on N_2-based new production and export at Station ALOHA.

Time-series measurements of euphotic zone N_2-fixation at Station ALOHA using the $^{15}N_2$ tracer technique are available for the periods Jul 2000 – Jun 2001 (Dore et al., 2002), Apr 2004 – Mar 2005 (Grabowski et al., 2008), and Nov 2004 – Sep 2007 (Church et al., 2009), and a comprehensive synthesis of the temporal variability of approximately monthly rates of N_2 fixation from Jun 2005 – Dec 2013 has recently appeared (Böttjer et al., 2017). During this same time period, several changes were made to the basic method of Montoya et al. (1996), including the procedure used to introduce and to dissolve the gaseous tracer ($^{15}N_2$) into the sample (Mohr et al., 2010; Großkopf et al., 2012). The error using the conventional $^{15}N_2$ bubble injection versus the improved dissolved $^{15}N_2$ gas injection was found to be variable; (e.g., 2–6 fold differences in N_2 fixation with bubble always being lower; Großkopf et al., 2012; Wilson et al., 2012). Based on a 4-cruise intercomparison of the two methods ($^{15}N_2$ bubble versus dissolved $^{15}N_2$) at Station ALOHA that included 2 cruises in summer and 1 each in fall and winter, Böttjer et al. (2017) reported a consistent, 2-fold difference in euphotic zone depth-integrated N_2 fixation and applied that correction factor to the approximately monthly data that had been collected from Jun 2005 – Aug 2012. Analysis of the 9-yr time series of "corrected" N_2 fixation (Böttjer et al., 2017) indicated that rates peaked in Sep (395 ± 159 μmol N m^{-2} d^{-1}) and remained high, but much more variable, in Oct (324 ± 318 μmol N m^{-2} d^{-1}). Mesoscale physical forcing, specifically the presence of anticyclonic eddies, may contribute to the heterogeneity that is observed in both diazotrophic cell biomass and rates of N_2 fixation at Station ALOHA (Church et al., 2009; Böttjer et al., 2017). Other technical issues have since arisen including potential contamination of commercial $^{15}N_2$ gas stocks with ^{15}N-labeled nitrate and ammonium (Dabundo et al., 2014), and the need to measure the ^{15}N atom percent enrichment of the sample and of particulate matter at the start of the incubation (White et al., 2020).

A previous study of the summertime drawdown in salinity-normalized dissolved inorganic carbon (n-DIC) at Station ALOHA in the nitrate-depleted mixed layer was attributed to N_2 fixation-supported export (Karl et al., 2003). This phenomenon was first reported at the Bermuda Atlantic Time-series Study (BATS) site in the North Atlantic (Michaels et al., 1994) and later shown to be a global phenomenon in tropical and subtropical environments (Lee et al., 2002). More recently, Ko et al. (2018) re-assessed the magnitude of the seasonal reduction of n-DIC in nitrate-depleted (<0.2 μmol kg^{-1}) waters using a much larger data base (6.5 million data points versus 16,000 observations in Lee et al., 2002), along with additional thermodynamic model refinements and corrections for recent estimates of atmospheric deposition of fixed N. When their model was applied to observations at Station ALOHA for the period 1989–2014, primary production that can be attributed to N_2 fixation was 0.9 ± 0.2 mol C m^{-2} over the 8-mo period of warming, or an average rate in the surface mixed layer of 45 mg C m^{-2} d^{-1}. By comparison, the measured ^{15}N-based N_2 fixation rates (converted to C using a C:N molar ratio of 7) for the period Jun 2005 to Dec 2013 equates to an average of 18.4 mg C m^{-2} d^{-1} (Ko et al., 2018). Differences between these two estimates could be due to the C:N ratio assumption, to an underestimation of N_2 fixation due to spatial and temporal variability, specifically the undersampling of aperiodic blooms, or underestimates of gross N_2 fixation using the ^{15}N-based method, as discussed by Wilson et al. (2012). However, even this lower bound on N_2-based new production of 18.4 mg C m^{-2} d^{-1} would account for 3–4% of the annual mean primary production and equates to >50% of the mean PC export, assuming steady-state conditions (see Section 4.5).

4.3. Primary production at Station ALOHA: Decadal scale trends

The analysis of the mean state and seasonal climatology of total euphotic zone depth-integrated primary production ignore depth-dependent dynamics of phytoplankton assemblages at Station ALOHA and their responses to physical forcing and longer term climate variability. An unexpected result from the 30-yr period of observation was the long-term, increasing trend in primary production, with relative changes greater than 30% in the lower portion of the water column surrounding the DCM (75–125 m) over these three decades (Fig. 10 and Tables 2, 4, and S2). Furthermore, the sustained increase in primary production is a result of a greater increase in summertime rates in the 75–125 m region of the water column than in winter: summer = 2.6 (95% CI = 1.6–3.6) (mg C m^{-2} d^{-1}) yr^{-1} ($p < 0.01$) compared to winter = 0.9 (95% CI = 0.1–1.7) (mg C m^{-2} d^{-1}) yr^{-1} ($p < 0.05$; Table 2).

In addition to the long-term trend in primary production, we also observed a sustained, increasing trend in Chl *a* concentrations in the 75–125 m region of the water column that accounts for approximately one-half of the increase in primary production, and a smaller (~8–8.5%), but still significant ($p < 0.05$), 30-yr increasing trend for the

Table 4
125 m Depth horizon mean (SD), long-term linear trend (95% Confidence Interval of trend) and estimated 30-year change in Chl *a*, C assimilation, photosynthetically available radiation (PAR), temperature, and salinity. Values for PAR and PAR derived parameters are based on data collected from February 1998 to Dec 2018. Italic = $p < 0.05$, Italic-bold = $p < 0.01$.

Parameter	Mean (SD)	Long-term Trend (95% CI)	Long-term Change (95%CI) (1989–2018)	P-value
Chl *a* (Fluor)	mg m^{-3}	mg m^{-3} $year^{-1}$	mg m^{-3}	
	0.164 (0.062)	***1.73 10^{-3} (8.03 10^{-4})***	***5.56 10^{-2} (2.41 10^{-2})***	***3.8 10^{-4}***
Chl *a* (HPLC)	mg m^{-3}	mg m^{-3} $year^{-1}$	mg m^{-3}	
	0.227 (0.077)	***1.5 10^{-3} (1.1 10^{-3})***	***4.40 10^{-2} (3.29 10^{-2})***	***9.3 10^{-3}***
Chl $a_{(Euk)}$: Chl $a_{(Total)}$	g g^{-1}	(g g^{-1}) $year^{-1}$	g g^{-1}	
	0.38 (0.06)	***-1.69×10^{-3} (0.87×10^{-3})***	***-0.05 (0.03)***	***1.5 10^{-4}***
Primary Production	mmol C m^{-3} d^{-1}	mmol m^{-3} $year^{-1}$	mmol C m^{-3} d^{-1}	
	6.31×10^{-2} (3.97×10^{-2})	***8.9×10^{-3} (4.7×10^{-3})***	***2.48×10^{-2} (1.41×10^{-2})***	***8.4 10^{-3}***
C_{assim} (Chl *a*)$^{-1}$	mmol (mg Chl *a* d)$^{-1}$	mmol (mg Chl *a* d^{-1}) $year^{-1}$	mmol (mg Chl *a* d)$^{-1}$	
	0.37 (0.20)	1.92×10^{-3} (4.87×10^{-3})	0.06 (0.15)	2.1 10^{-1}
PAR	mol quanta m^{-2} d^{-1}	(mol quanta m^{-2} d^{-1}) $year^{-1}$	mol quanta m^{-2} d^{-1}	
	0.19 (0.01)	6.1×10^{-4} (1.8×10^{-3})	0.02 (0.06)	5.2 10^{-1}
C_{assim} (Chl *a* * PAR)$^{-1}$	C m^2 (quanta mg Chl *a*)$^{-1}$	C m^2 (quanta mg Chl *a*)$^{-1}$ $year^{-1}$	C m^2 (quanta mg Chl *a*)$^{-1}$	
	2.40×10^{-3} (1.87×10^{-3})	-3.02×10^{-3} (3.3×10^{-2})	-0.1×10^{-3} (1.6×10^{-3})	7.9 10^{-1}
Quantum yield	mol C (mol quanta)$^{-1}$	mol C (mol quanta)$^{-1}$ $year^{-1}$	mol C (mol quanta)$^{-1}$	
	0.057 (0.037)	-1.04×10^{-4} (1.06×10^{-3})	-0.3×10^{-3}(3.2×10^{-3})	8.3 10^{-1}
Temperature	°C	°C $year^{-1}$	°C	
	21.9 (0.9)	*1.18×10^{-2} (2.11×10^{-2})*	*0.35 (0.63)*	*4.2 10^{-2}*
Salinity	‰	‰ $year^{-1}$	‰	
	35.21 (0.11)	***3.8×10^{-3} (3.9×10^{-6})***	***1.2×10^{-1} (1.2×10^{-4})***	***3.1 10^{-6}***

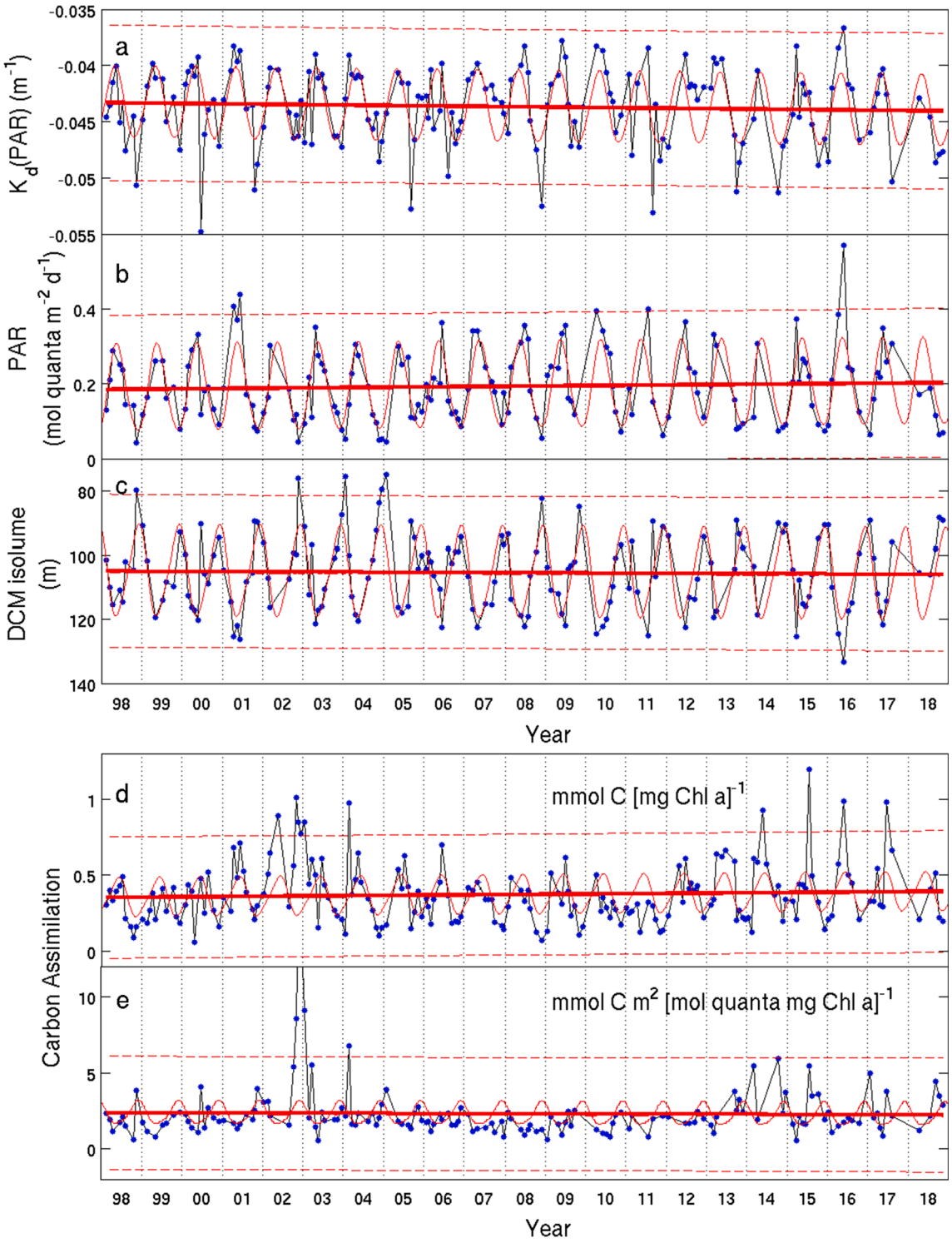

Fig. 16. Time-series (1998–2018) of light distribution in the lower euphotic zone and its effect on the variability of ^{14}C-based primary production: (a) Mean euphotic zone attenuation coefficient $k_{d(PAR)}$, (m^{-1}); (b) 125 m depth photon flux (mol quanta m^{-2} d^{-1}); (c) Depth of the 0.415 mol quanta m^{-2} d^{-1} isolume, corresponding to the seasonal vertical displacement of the Deep Chlorophyll Maximum (DCM) layer, (d) 125 m depth horizon ^{14}C-based primary production normalized per unit Chlorophyll *a* (mmol C mg^{-1} Chl *a* d^{-1}), (e) 125 m depth horizon ^{14}C-based primary production normalized per unit Chlorophyll *a* and photon flux (mmol C m^{-2} [mol quanta mg Chl *a*]$^{-1}$). Blue solid symbols are observations, red solid (thick) and dashed horizontal lines are the long-term linear regressions with 95% confidence intervals, and red solid (thin) lines are the seasonal components.

concentrations of suspended PC and PN (Tables 2 and 3). We explored evidence for five potential mechanisms, that are not mutually exclusive, to explain the increasing long-term trends in the lower euphotic zone at Station ALOHA: (1) a change in the phytoplankton assemblage, specifically a shift in the photosynthetic eukaryote:prokaryote ratio, with a selection for species with higher rates of photosynthesis per unit biomass (P^B) under ambient light conditions, (2) a change in the total photon flux to the lower portion of the euphotic zone or in the quantum yield of photosynthesis, (3), a systematic change in the intracellular ^{14}C allocation pattern of the phytoplankton community and resultant shift in the

apparent net:gross ratio of photosynthesis, (4) a change in mesozooplankton abundance leading to a top-down, trophic cascade-like response, and (5) an increased flux of new nutrients.

Is there evidence for a decadal-scale change in the phytoplankton assemblage at Station ALOHA? Based on research conducted in the Climax region north of Station ALOHA, Venrick (1982, 1990) reported that the vertical structure of large (>5 μm) eukaryote phytoplankton was characterized by distinct shallow (<100 m) and deep (>100 m) water assemblages, essentially nutrient-limited and light-limited regimes, respectively. The transition region between shallow and deep assemblages occurred over a relatively narrow depth interval of <20 m (Venrick, 1988). Between the period 1967–1985, when a doubling of the euphotic zone depth-integrated Chl *a* had been observed, there was only a small change in the rank order abundance of species, suggesting that these assemblages were stable over at least 1000 generations. The slow changes that did take place over this period were greater in the deep assemblage, particularly among diatoms (Venrick, 1990). Following the establishment of Station ALOHA, Venrick (1997) obtained samples in August 1994 for a comparison with her previous (1973–1985) observations from the Climax region located ~650 km to the northeast (28°N, 155°W). Of the 142 eukaryotic phytoplankton species found at Station ALOHA, all but 6 species had also been seen in the Climax region, and the characteristic 2-layered structure was also evident at Station ALOHA (Venrick, 1997). The mechanism(s) responsible for the persistence of rank order species abundances over both time and space in the NPSG, despite a doubling of the Chl *a* in the Climax region since the early 1970s, is not known.

Venrick's pioneering research on phytoplankton in the Climax region did not consider species in the size class <5 μm, which we now know are numerically dominant at Station ALOHA. *Prochlorococcus*, *Synechococcus*, and picoeukaryotic (<3 μm) phytoplankton are all present and, at times, represent significant components of the total Chl *a* concentration, especially within the DCM (Letelier et al., 1993; Venrick, 1993; Campbell et al., 1994; Li et al., 2013; Pasulka et al., 2013). Based on a 5-yr (1990–1994) study at Station ALOHA, Campbell et al. (1997) reported that *Prochlorococcus*, *Synechococcus*, picoeukaryotes, and 3–20 μm eukaryotic algae represented 60.6%, 2.6%, 20.2%, and 16.5% of the euphotic zone (0–200 m) depth-integrated algal biomass. Pasulka et al. (2013) reported similar results at Station ALOHA for the period Jun 2004 – Jan 2009, and found that *Prochlorococccus* varied from ~50% of total autotrophic biomass for the first half of the year, decreasing to 30–40% in late summer to early fall when larger phytoplankton became more abundant. *Synechococcus* was confirmed as a minor biomass component. Prymnesiophytes and other autotrophic flagellates were the dominant eukaryotes, with dinoflagellates and diatoms each contributing ~1% to total community biomass throughout the year (Pasulka et al., 2013).

Li et al. (2011) reported that the maximum biomass (Chl *a*)-normalized assimilation (P^B_m) and maximum quantum efficiency (α) derived from short-term photosynthesis vs. irradiance (P-E) incubation experiments were both significantly larger (~1.5–3 fold depending on sample depth) for the >2 μm size class of phytoplankton compared to picophytoplankton (0.2–2 μm). In their comprehensive analysis of euphotic zone (0–125 m) samples collected from Station ALOHA during a 5-yr period (2004–2009; a total of 88 individual P-E experiments), picophytoplankton accounted for 91 ± 2% of the Chl *a* but only 74 ± 7% of the ^{14}C-based primary production (Li et al., 2011). Consequently, variations in the eukaryote:prokaryote ratio of the phytoplankton assemblage could explain how ^{14}C-based primary production at Station ALOHA can be increasing at a rate greater than the increase in Chl *a* concentrations. The higher P^B_m for autotrophic eukaryotes is also consistent with their dominance under natural bloom conditions or following the addition of nutrients during shipboard perturbation experiments (McAndrew et al., 2007; Alexander et al., 2015; Mahaffey et al., 2012; Rii et al., 2018).

Letelier et al. (1993) developed and applied a pigment algorithm to examine temporal changes in phytoplankton community structure in the DCM at Station ALOHA over a 3-yr period (1989–1991). This approach employed the use of diagnostic pigments that are present in specific algal taxa to determine their relative contributions to total Chl *a* and, hence, the eukaryote:prokaryote ratio of the phytoplankton assemblage. We applied the Letelier et al. (1993) pigment algorithm to test for changes in the eukaryote:prokaryote ratio in the lower portion of the euphotic zone (125 m) since 1989 (Table 4). Using the HOT program HPLC data set, which is necessary for the pigment algorithm, we confirmed that HPLC-Chl *a* at 125 m also displayed a significant increase of 1.5 μg m^{-3} yr^{-1} (95% CI = 0.4–2.6 μg Chl *a* m^{-3} yr^{-1}; $p < 0.01$) over the 30-yr observation period, a result that is consistent with the fluorometrically-determined Chl *a* trend for the 75–125 m depth region (Table 4). The eukaryote Chl *a*:prokaryote Chl *a* ratios exhibited a small (13%), but significant ($p < 0.01$), decrease during the observation period (Table 4), rather than the expected increase if the long-term increasing trends in Chl *a* and primary production were the result of a change in eukaryotic phytoplankton with higher α and P^B compared to prokaryotic phytoplankton. Although the mean contribution of prokaryotes to total Chl *a* (62 ± 6%) displayed a small decrease in summer periods to values of ~52%, none of the specific phytoplankton pigment taxonomic markers displayed significant ($p < 0.05$), long-term increasing trends at 125 m. Therefore, it appears unlikely that the sustained, 30-yr increases in Chl *a* and primary production in the lower portion of the euphotic zone are caused by a systematic change in the phytoplankton assemblage.

Has the total photon flux to the lower portion (75–125 m) or the quantum yield of photosynthesis in that depth region at Station ALOHA changed since Jan 1989? Light availability, which could lead to changes in Chl *a* and primary production, is controlled by surface irradiance and the inherent optical properties (absorption and scattering) of the water column. We found no evidence for a systematic change in surface PAR, or for photon fluxes at 75, 100, or 125 m (Figs. 7 and 16, and Table 4). Consequently, changes in the underwater distributions of light cannot explain the observed long-term increasing trends in Chl *a*, suspended PC and PN, and primary production at Station ALOHA.

We next explored the possibility that changes in the quantum efficiency of photosynthesis (i.e., C assimilation per unit Chl *a* per photon absorbed) might be responsible for the enhancement of primary production, relative to Chl *a*, over the latter portion of our observation period (1998–2018). The use of a 21-yr rather than 30-yr observation period was necessitated due to absence of water column PAR data prior to 1998. Two different approaches were employed: (1) a normalization of C assimilation per Chl *a* per PAR at each depth horizon (75, 100, 125 m), using propagation of errors and averaged over the 75–125 m depth range, and (2) an estimate of Chl *a*-specific light absorption attributed to photosynthetic pigments as a function of PAR ($\alpha^*_{\phi\ (PSP)}$; see Letelier et al., 2017) for each depth horizon and averaged over 75–125 m. Neither of these independent analyses provides evidence for a systematic change in photon-normalized carbon assimilation at Station ALOHA over the 21-yr observation period (Fig. 16 and Table 4).

Is there evidence for a systematic change in the subcellular allocation of recently fixed ^{14}C over the 30-yr observation period at Station ALOHA? Research on the allocation of assimilated inorganic carbon by microalgae was fundamental to the discovery of the biochemical pathway of carbon in photosynthesis (Ruben and Kamen, 1940; Calvin and Benson, 1948). Decades later, it was suggested that the patterns of photosynthetic carbon allocation into unique biochemical pools (e.g., proteins, polysaccharides, lipids, and low molecular weight substrates) of natural phytoplankton assemblages might provide information on the physiological state of the community (Olive et al., 1969; Morris et al., 1974; Morris, 1981). Because lipids and polysaccharides can serve as intracellular stores of energy, the percentage of carbon allocated to these polymers varies with environmental conditions, including light, nutrient availability, and temperature. However, measurements of carbon allocation during the relatively short term (~12 hr), in situ incubations described herein are complicated by the differential turnover rates of the separate pools and non-uniform ^{14}C-specific radioactivities of precursor

and product pools (Li and Harrison, 1982), as well as potential variations in carbon allocation patterns among various individual species in the population (Rivkin, 1985). Nonetheless, photosynthetic carbon allocation can reveal temporal changes in the metabolic strategies of the phytoplankton community due to changing environmental conditions (Perin et al., 2002; Suárez and Marañón, 2003).

More recently, detailed laboratory-based experiments revealed complex patterns in carbon allocation over the cell cycle in a variety of eukaryotic phytoplankton (Halsey et al., 2011; 2013). The carbon allocation strategies for both chlorophytes (*Dunaliella tertiolecta*) and diatoms (*Thalassiosira weissflogii*) were shown to be growth rate-dependent, with a greater abundance of shorter half-life, newly formed carbon products at slower growth rates (Halsey et al., 2013). At higher growth rates, the majority of ^{14}C was initially fixed into polysaccharides and lipids whereas at slower growth rates, ^{14}C was initially incorporated into proteins (Halsey et al., 2011). The possibility of a variable pattern of ^{14}C allocation into different macromolecular pools with changes in nutrient availability, light, temperature, or other controls on growth rate, first observed in the green algae *Euglena gracilis* (Cook, 1963), could influence the interpretation of the field measurements of ^{14}C assimilation at Station ALOHA. Specifically, a shift in the balance between gross and net primary production (Milligan et al., 2015), or in the ^{14}C-DOC:^{14}C-POC production ratio, could occur without altering the total rate of photosynthesis. A significant change in growth rate for phytoplankton at Station ALOHA would likely be restricted to the lower portion of the euphotic zone since light-saturated phytoplankton growth rates previously reported for the NPSG are already high (1–2 d^{-1} based on a variety of methods; Laws, 2013). On the other hand, growth rate-dependent changes in carbon allocation without a change in total primary production might reconcile the apparent uncoupling that we report between ^{14}C-based 0–150 m depth-integrated primary production and PC export at 150 m. Because we did not measure the cellular allocation of ^{14}C, we lack direct evidence to support or refute the ^{14}C allocation hypothesis. This mechanism, if it is important in our field study, would imply a long-term trend of increasing growth rate in the lower euphotic zone of one or more species of the phytoplankton community over the past three decades since a change in carbon allocation is a consequence of environmental variability. Presumably, such a trend would be accompanied by observable changes in phytoplankton community structure or photophysiology; yet these are not apparent in our data, as discussed above.

Are the observed changes in Chl *a*, suspended PC and PN, and primary production a result of a top-down food web trophic cascade? Trophic cascades are complex food web interactions that can alter abundances and biomasses of organisms across more than one trophic level (Pace et al., 1999; Ripple et al., 2016). For example, in a hypothetical three trophic level food chain (primary producer, herbivore, and carnivore), removal of the top predator would allow the herbivore population to increase in abundance resulting in a decreased abundance and productivity of the primary producer population. Conversely, if third trophic level predators became more abundant, then herbivores would decrease and phytoplankton biomass would increase. In theory, the long-term increases in Chl *a*, suspended PC and PN, and primary production could be the result of an indirect top-down control caused by changes in the population dynamics of grazer and predator populations, including mesozooplankton. To evaluate whether our observations are consistent with an indirect trophic cascade at Station ALOHA, we need information on food web structure and dynamics of grazer and predator populations. Because the phytoplankton population ranges in size from 0.6 μm to >10 μm, the Station ALOHA food web supports a diverse assemblage of grazers from protists to herbivorous zooplankton. Although protistan grazers are not routinely measured at Station ALOHA, Pasulka et al. (2013) reported that the autotrophic-to-heterotrophic protist ratios (both for cell abundances and biomasses) in the upper 0–100 m of the water column (no deeper data were reported) were relatively stable over a 5-yr period (2004–2008).

A component of the HOT core program (M. R. Landry, principal investigator) routinely measures euphotic zone (0–160 m) depth-integrated mesozooplankton and reports displacement volumes, dry weights, C, and N for a range of size classes (0.2–0.5, 0.5–1, 1–5, and >5 mm; Al-Mutairi and Landry, 2001). For each HOT cruise, 3 daytime (1000–1400 hr) and 3 nighttime (2200–0200) oblique net tows are made to distinguish vertically migrating plankton (diel migrations to depths of 300–600 m) from those mesozooplankton that are permanently resident in the upper water column. Temporal trends of mesozooplankton at Station ALOHA of various durations have been reported (Al-Mutairi and Landry, 2001 [1994–1996]; Landry et al., 2001 [1994–1996]; Sheridan and Landry, 2004 [1994–2002]; Hannides et al., 2009 [1994–2006]; Pasulka et al., 2013 [2004–2008]). The longest published time series revealed significant increasing trends for both daytime and nighttime dry weight of mesozooplankton (and, hence, also for total migrant biomass) at rates of 60 mg dry weight m^{-2} yr^{-1} for nighttime collections and 45 mg dry weight m^{-2} yr^{-1} for daytime collections (Sheridan and Landry, 2004). We extended their analyses through 2018 using the publicly available mesozooplankton database (*http://hahana.soest.hawaii.edu/hot/hot-dogs/interface.html*), and confirmed that the initial increasing trend of daytime mesozooplankton has been sustained over the entire observation period 1994–2018 while the migrating component has remained relatively constant (Supplementary Fig. 7 and Table 2; note: no mesozooplankton data are available for Station ALOHA prior to 1994). Furthermore, based on an amino acid-specific stable nitrogen isotopic composition analysis of abundant herbivores and carnivores, Hannides et al. (2009) reported that their trophic positions have remained essentially constant over a 10-yr (1995–2005) period. We conclude that the increasing dry weight biomasses of mesozooplankton at trophic levels 2–3 observed at Station ALOHA since 1994 are linked to the increasing Chl *a*, suspended PC and PN, and primary production, and does not support a top-down trophic cascade that would require a decrease in carnivorous mesozooplankton. The observations from Station ALOHA are more consistent with a bottom-up, nutrient control of ecosystem productivity.

Finally, is there any evidence to support an enhanced delivery of growth-rate-limiting nutrients to the lower portion of the water column at Station ALOHA since 1989? An increasing allochthonous supply of new nutrients, by the combined processes of N_2 fixation, atmospheric deposition, turbulent mixing, and lateral advection, would lead to higher phytoplankton biomass and primary production, higher mesozooplankton biomass, and a possible accumulation of suspended PC and PN, until the rate-limiting nutrient is depleted. There does not appear to be any long-term change in the delivery of nutrients to the surface mixed-layer because neither Chl *a*, suspended PC and PN, nor ^{14}C-based primary production changed significantly over the 30-year observation period in that region of the water column (Table 2). Nevertheless, it is possible that the flux of nutrients to the lower portion of the euphotic zone has increased over the past few decades, as originally hypothesized by Venrick et al. (1987) to explain their observed doubling of Chl *a*. Based on field observations of nitrate concentrations over a 2-yr period using profiling floats deployed near Station ALOHA, Johnson et al. (2010) were able to obtain a high-resolution (5-d interval) mass balance in the upper 0–300 m of the water column. An unexpected result was the episodic, short-lived (<10 d; float cycle time of 5 d) entrainment of nitrate into the lower portion of the euphotic zone, a feature that was not evident at shallower depths (Johnson et al., 2010). The frequency of events where 1 μM nitrate could be detected above 110 m was 12 out of 127 profiling float cycles, or approximately monthly. Assuming that phytoplankton in the lower portion of the euphotic zone consumed all of the available nitrate, a lower bound on event-driven vertical transport would be 88 mmol N m^{-2} yr^{-1}, a value that was 80% of the observed PN export at 150 m (Johnson et al., 2010). The observation period (19 Dec 2008 – 22 Mar 2009) was too short to detect any temporal trend in the frequency of nitrate pulses.

A follow-on analysis used the Johnson et al. (2010) float data set as well as observations from three more recent float deployments in the NPSG, the WHOTS mooring time-series, HOT program cruise data

(1988–2010), satellite-derived dynamic topography of the sea surface from Archiving, Validation and Interpretation of Satellite Oceanographic data (AVISO), and the 32-layer vertical Hybrid Coordination Ocean Model (HYCOM) for ocean circulation around Hawaii (166°W to 150°W, and 16°N to 26°N) to diagnose nitrate transport into the euphotic zone (Ascani et al., 2013). Their analysis of the observations and model simulations discovered that the episodic injections were generally correlated with changes in the depth of isopycnal surfaces, associated with features of relatively small (<20 km) horizontal scale, and found throughout the water column (at least to the profiling depth of 1000 m). With these characteristics, the authors concluded that the most likely cause of the nitrate injection was rapid temporal change in the balanced mesoscale eddy field. Based on 45 separate virtual profiling float time series simulations, nitrate anomalies were most frequently associated with periods when the profiling float was sampling the sharp edge of a rapidly evolving eddy (Ascani et al., 2013). The ecological and biogeochemical consequences of these injections for primary production and export are not known. In all likelihood, nitrate is rapidly consumed, and a portion of the newly formed phytoplankton biomass is exported. Letelier et al. (2000) documented one such event at Station ALOHA in Mar-Apr 1997 during the passage of a large cyclonic eddy. Under these nutrient-amended conditions, diatoms and other large eukaryotic phytoplankton are selected for (McAndrew et al., 2007; Alexander et al., 2015) and this selection facilitates the export of silica which otherwise would accumulate in the euphotic zone over time by this pulsed nutrient delivery process. Indeed, the export of particulate Si (which has only been measured at Station ALOHA since 2001) is highly variable and punctuated with episodic high flux events that might result from pulsed nutrient delivery (Brzezinski et al., 2011). Furthermore, the molar Si:N ratio of the particulate matter exported from the euphotic zone is ~0.5 which is consistent with a major contribution (~50%) from diatoms, especially compared to their very low (~1%) contribution to the "background" phytoplankton assemblage.

To evaluate whether aperiodic transport of nitrate into the lower euphotic zone is responsible for the 30-yr trends in primary production in the 75–125 m depth interval, the frequency of mesoscale features and the total eddy kinetic energy near Station ALOHA would need to be known. Chen and Qiu (2010) reported mesoscale eddy activity during a 16-yr period (1992–2008) for two regions northeast of the Hawaiian islands. Their southernmost region ("box A," 21-30°N, 170-150°W) included Station ALOHA. Eddy kinetic energy displayed significant seasonal and interannual variability with highest values (>150 cm s^{-1}) in 1995 and 1998, and a continuous 3-yr minimum (<75 cm s^{-1}) for the period 2000–2002 (Chen and Qiu, 2010). Furthermore, they demonstrated a relationship between eddy kinetic energy and the PDO index with highest correlation when a 14-month lag behind PDO was employed (Chen and Qiu, 2010). More recently, Barone et al. (2019a) analyzed a 23-yr (1993–2015) record of satellite observations of sea surface height to assess linkages, if any, to the ecological and biogeochemical state of Station ALOHA. The measured sea level anomaly was corrected for the rate of sea level rise (1.5 mm yr^{-1}) and for a sinusoidal seasonal cycle (2.4 cm amplitude with maximum in summer) to produce a corrected sea level anomaly (SLA_{corr}) that was then compared to a number of biogeochemical observations in the 0–175 m of the water column at Station ALOHA. They also identified specific mesoscale eddies and determined a number of characteristics including origin, size, age, amplitude change, and horizontal displacement (Barone et al., 2019a). Between 1994 and 2015, Station ALOHA was within a tracked eddy for 31% of the time with 71 cyclones and 64 anticyclones having mean amplitudes of −6.5 (SD = 3.9) cm and +7.1 (SD = 3.9) cm, respectively. Large temporal variations ranging from months to years were also observed for SLA_{corr}, as previously reported by Chen and Qiu (2010) for eddy kinetic energy. However, based on this comprehensive sea level analysis, neither primary production in the upper or lower portions of the euphotic zone nor particulate matter export were significantly correlated with SLA_{corr} (Barone et al., 2019a).

Recently, it has been reported that the atmospheric deposition of anthropogenic fixed N from northeastern Asia has increased significantly over the past few decades (Duce et al., 2008; Kim et al., 2014). By analyzing excess fixed N, relative to phosphate, termed N* (N* = N-$R_{N:P}$ × P, where N and P are the measured concentrations of nitrate and phosphate and $R_{N:P}$ is the Redfield molar N:P ratio of 16:1), and chlorofluorocarbon-12 (CFC-12)-derived ventilation ages of specific water parcels, Kim et al. (2014) were able to quantify N deposition to the North Pacific Ocean over the past 40 years. An analysis of the temporal change of excess N at Station ALOHA revealed a rate of N increase in the lower euphotic zone (100–200 m) that was equivalent to a mean of 0.04 (SD = 0.02) μmol N kg^{-1} yr^{-1} during the period 1988–2011 (Kim et al., 2014). Presumably the deposition of pollutant N has increased since 2011, so the 0.04 μmol N kg^{-1} yr^{-1} estimate is likely to be a conservative one. Indeed, projections for the year 2030 suggest that atmospheric deposition of fixed N in mid-latitudes of the North Pacific Ocean will be 30% higher than they were in 2000 (Ciais et al., 2013). Assuming that all other growth-limiting nutrients are available, this allochthonous supply of fixed N is more than sufficient to support the significant increasing trend of euphotic zone (0–125 m) ^{14}C-based primary production at Station ALOHA since 1989. It is not known whether anthropogenic iron is also delivered via this same mechanism, but a recent expedition north of Station ALOHA along 158°W has observed the presence of anthropogenic lead and iron in the North Pacific Transition Zone at ~35°N latitude (Pinedo-Gonzalez et al., 2020). Without effective pollution abatement over the next decades to centuries, this allochthonous input of iron and nitrate would eventually lead to an increasing deficit of phosphate in the water column (Letelier et al., 2019), and reduced primary production and export despite the nitrate and iron subsidy to the lower portion of the euphotic zone.

Dave and Lozier (2010) reported that primary production and salinity in the lower euphotic zone at Station ALOHA were correlated. They hypothesized that this could be a direct North Pacific Gyre Oscillation (NPGO) effect on local hydrography due to variability in the transport of North Pacific Tropical Water (NPTW). The lower euphotic zone (75–125 m), where Chl *a*, suspended PC and PN, and primary production have all increased since Jan 1989, coincides with the core of the NPTW, a distinctive subsurface salinity maximum feature at Station ALOHA (potential density = 24.3–24.7 kg m^{-3}; 100–140 m; Lukas and Santiago-Mandujano, 2008; Supplementary Fig. 8). The NPTW originates in surface waters of a large region of the subtropical frontal zone from 150°E to 130°W between 20° to 30°N and subducts and flows first southward then westward through a complex series of transport pathways (Katsura et al., 2013; Nie et al., 2016). The dynamics of NPTW flow are correlated with PDO, especially since the major climate shift in the mid-1970s (Qu and Chen, 2009).

Letscher et al. (2016) coupled the Parallel Ocean Program 2 (POP2) ocean circulation model to the Biogeochemical Elemental Cycling (BEC) v1.2 model of the Community Earth System Model (CESM) to estimate the role of lateral transport processes in the supply of nutrients to the NPSG. Their results suggested that 14% of the nitrogen and 60% of the phosphorus required to support NCP at Station ALOHA are derived from lateral processes during the May to Oct period of enhanced water column stratification (Letscher et al. 2016). The nutrient delivery balance between vertical and horizontal processes would be expected to change in favor of horizontal processes with the enhanced upper water column stratification that is predicted from ocean warming.

In their report of an increasing trend for Chl *a* in the lower portion of the water column, Venrick et al. (1987) postulated that the change in standing stock of Chl *a* must have resulted from a reapportionment of nutrients, either a decrease in export from the euphotic zone or an increased input. Our hypothesis of an enhanced flux of anthropogenic, pollutant nutrients via the NPTW transport pathway is a formal mechanism for the delivery of excess nutrients. While the trend of increasing primary production at Station ALOHA is significant over the entire 30-yr observation period, it is punctuated by shorter periods of higher and

lower rates of change (Fig. 10) that might correspond to climate-forced changes in the atmospheric delivery of pollutants or in NPTW subduction dynamics. However, the sustained 30-yr trend is consistent with a semi-continuous allochthonous nutrient source (i.e., atmospheric deposition of pollutant nitrogen) rather than being the result of any specific climate index oscillation. Indeed, the increasing trend may be much longer than we report herein, and could be one and the same as the feature beginning in the late 1960s as reported by Venrick et al. (1987), and perhaps even earlier. This would help to reconcile why the Chl *a* and primary production trends in the NPSG previously attributed to the PDO polarity reversal (Mantua et al., 1997; Karl et al., 2001a) continued unabated well after that phase of the climate forcing ended. Nutrient delivery to the lower euphotic zone at Station ALOHA may be modulated by climate-ocean interactions, but we hypothesize that it is ultimately caused by the atmospheric delivery of pollutant nutrients and their contribution to preformed nutrients in NPTW subducted waters.

Summarizing this section on decadal scale trends, neither changes in the phytoplankton assemblage, changes in the quantum yield of photosynthesis, nor indirect effects of trophic level cascades can be invoked as primary mechanisms for the long-term eutrophication at Station ALOHA. The multi-decade increasing trends of Chl *a*, suspended PC and PN, and primary production, especially in the lower portion of the euphotic zone, as well as 0–160 m depth-integrated mesozooplankton biomass, are all consistent with our hypothesized increase in the horizontal supply of nutrients. We suggest that nutrient delivery via atmospheric deposition to the northwest of Station ALOHA and subduction along isopycnals via NPTW transport pathways are the most likely causes of the long-term biogeochemical patterns observed in the lower euphotic zone of Station ALOHA since 1989.

4.4. Carbon and nitrogen export: Controls on temporal variability

The ocean's BCP is an integral component of the global C cycle and is largely responsible for long-term sequestration of CO_2 into the meso- and abyssopelagic zones (Volk and Hoffert, 1985). The BCP is fueled by solar energy, through the process of photosynthesis in the euphotic zone. Most biogeochemical models predict that the strength and efficiency of the BCP are dependent upon the structure of the phytoplankton community with larger, ballasted cells (e.g., diatoms) supporting a more efficient BCP (Legendre and LeFèvre, 1989; Karl et al., 2003). However, picoplankton (Richardson and Jackson, 2007) and nanoplankton (Juranek et al., 2020) also contribute to C export. A recent study of PC export at Station ALOHA using size class-specific lipid and isotopic markers documented the role of submicron particles as a potentially important component of the BCP (Close et al., 2013). The authors hypothesized that continuous disaggregation and reaggregation of particles during the export process could transfer very small particles to great ocean depths. Evidence for mesopelagic repackaging based on the quantity and types of fecal pellets has also been reported (Karl and Knauer, 1984b), and a conceptual detritus-microbe model depicting interactions between sinking particles and pools of dissolved and suspended organic matter has been formulated (Karl and Knauer, 1984a). More recently, Briggs et al. (2020) assessed the role of particle fragmentation in the BCP by tracking changes in large and small mesopelagic particle concentrations using optical measurements on Biogeochemical Argo floats. Their results support the process of large particle fragmentation as a major loss term in the downward flux of particulate matter in the open ocean. Nevertheless, a small fraction of the particulate matter exported from the euphotic zone arrives at the seabed without any appreciable change in chemical composition (Karl et al., 2012), supporting the model for the role of large, fast-sinking particles as the dominant mechanism for matter and energy flux into the deep sea (McCave, 1975; Lal, 1977).

Grabowski et al. (2019) recently presented data on particulate matter energy export from the euphotic zone, and on changes in the C-specific energy contents of sediment trap-collected particles as they sink and age. Their results documented the presence of at least two major classes of particles: (1) fast-sinking, energy-replete organic matter that is ballasted by associations with opal and calcium carbonate and (2) slow sinking, energy-depleted organic matter that also contained black C (Grabowski et al., 2019). Sinking particulate matter collected at the 150 m reference depth in their study had a C-specific energy content of ~45 J mg^{-1}C, which was slightly less than the C-specific energy content of photosynthetically produced organic matter (~50–60 J mg^{-1}C). This slight difference in the C-specific energy content means that the remineralization-intensive euphotic zone at Station ALOHA exports C that is slightly more oxidized than the organic matter that is initially produced via photosynthesis. This also has bearing on the value of the respiratory quotient (RQ) that is used in models to inter-convert O and C currencies. During organic matter remineralization in the euphotic zone, a greater amount of oxygen per unit C will be required to completely oxidize the organic matter that is retained in the euphotic zone, leading to a condition that may be misinterpreted as being net heterotrophic even though no organic matter subsidy is required to sustain it. Regardless, oligotrophic oceanic ecosystems like Station ALOHA are clearly remineralization-intensive and exist very close to a net metabolic balance point, where GPP and R are nearly equal when integrated over several days (Ferrón et al., 2015; Barone et al., 2019b).

The present study was focused on gravitational settling of particulate matter at the base of the euphotic zone (150 m). Export at Station ALOHA varied considerably over the 30-yr observation period (Figs. 11 and 12). The mean values for PC and PN export were 27.9 (SD = 9.7, n = 265) mg C m^{-2} d^{-1} and 4.2 (SD = 1.5, n = 265) mg N m^{-2} d^{-1}, respectively, with a mean molar PC:PN ratio of 7.99 (SD = 1.23, n = 265; Fig. 13 and Table 2). For the period 2001–2016, we also measured PIC and were able to calculate particulate organic C (POC = PC-PIC):PN ratios. PIC export averaged 10.4% (SD = 4.6%, n = 127) of the contemporaneous PC export (Supplementary Fig. 5), and the "PIC corrected" molar POC:PN ratio for exported particles averaged 6.88 (SD = 0.78, n = 127). This value is nearly identical to the recently reported POC:PN ratio of 6.76 (SD = 0.05) where PIC = 8.3% of PC (Grabowski et al., 2019) for the export of organic matter at 150 m, and to the PC:PN molar ratio of suspended particulate matter at Station ALOHA (Hebel and Karl, 2001). Grabowski et al. (2019) also documented a depth-dependent increase in the PIC:PC ratio due to the differences in organic matter diagenesis versus calcium carbonate dissolution processes. However, it is important to point out that most carbonate mineral particles in seawater have organic coatings that render them partially protected from chemical interactions with surrounding seawater (Chave, 1965).

The PC and PN export time series (Figs. 11 and 12) displayed enigmatic subdecadal variability with extended periods (1992–1996 and 2009–2014) when the seasonally detrended mean annual fluxes were consistently below the long-term mean, and additional periods (1989–1990 and 1997–2003) when they remained consistently above it (test for randomness, $p = 7 \times 10^{-4}$). Although the 2002–03 periods of higher than average particle export coincided with years of higher than average 0–150 m depth-integrated primary production, the 1989–90 high export period had the lowest recorded 0–150 m depth-integrated primary production during the entire 30-yr observation period (Fig. 15). Likewise, the low PC flux observed in 2013 corresponded to the year when 0–150 m depth-integrated primary production was much higher than the 30-yr mean. These apparent decouplings of primary production and PC/PN export extending over a period of one or more years requires that we revise our current BCP paradigm, at least for oligotrophic regions like Station ALOHA (see Section 4.5).

The monthly climatologies for PC and PN export also show nearly identical patterns with lower than average fluxes from Sep through Jan, and higher than average fluxes during the spring and summer periods (Figs. 11 and 12). The PC and PN export peaks in Aug are followed by abrupt decreases in Sep to values that are lower than long-term means. A similar pattern is observed for the 0–150 m depth-integrated primary

production climatology (Figs. 6 and 15) and may be a consequence of phosphorus limitation and the termination of the late summer period of N_2 fixation-supported new production, as discussed above.

In addition to sinking particles, other export processes including seasonal and aperiodic advective mixing, downward diffusion of dissolved organic matter (DOM), and diel vertical migrations of mesozooplankton (Longhurst and Harrison, 1989) can also remove C and N from the euphotic zone. Other processes, including atmospheric deposition, the upward flux of buoyant particles and phytoplankton (Simoneit et al., 1986; Villareal et al., 1993), and lateral transport (see above) can import C and N into the euphotic zone. At Station ALOHA, surface mixing never exceeded the euphotic zone depth (Fig. 1), so the vertical advective pump is probably negligible. And, although inputs from local atmospheric deposition and buoyant particles have not yet been quantified at Station ALOHA, they are also considered to be negligible. That leaves particle sinking, the downward diffusion of DOM, and diel vertical migrations of mesozooplankton as the major pathways for C and N export.

Based on an analysis of data collected at Station ALOHA during the period 1990–1995, Emerson et al. (1997) concluded that sediment trap-collected particles represented ~50% of the total C export. Since that time, improvements in our understanding of the controls on the BCP and an increase in field observations have further reduced our uncertainty of the "multi-faceted" particle pumps (Dall'Olmo et al., 2016; Boyd et al., 2019; see Section 4.5).

Hannides et al. (2009) analyzed the impact of diel zooplankton vertical migration on material transfer from the surface to the mesopelagic zone at Station ALOHA for the period 1994–2005. Total diel migrant-mediated export (including respiration, as well as excretion of both inorganic and organic matter) averaged 19% and 38% of the contemporaneous PC and PN export, respectively, that was collected by the ALOHA sediment traps (Hannides et al., 2009). However, considerable temporal variation in the relative contributions of active versus passive fluxes was also observed. For example, during the 12-yr period, total active export of PC ranged from 0.23 to 63% of the sediment trap collected export, with no temporal trend for the active:passive flux ratio (Hannides et al., 2009).

Unfortunately, there is no reference material or standard that can be used to assess the accuracy of particle collection using PIT-style sediment traps. Benitez-Nelson et al. (2001) measured ^{234}Th:^{238}U disequilibria at Station ALOHA during 9 HOT cruises from Apr 1999 – Mar 2000. The ^{234}Th activity measurements were interpreted using models with either steady-state or non steady-state scavenging assumptions (SS and NSS, respectively; Buesseler et al., 1995) to constrain PC export. The ^{234}Th-based PC export varied considerably between the two models both in absolute magnitude of the estimated PC export and in the sign and percentage difference between the two independent models (NOTE: there is also an error in their Table 1, p. 2603 in the listing of average SS and NSS C fluxes; Benitez-Nelson et al., 2001). Although the average ^{234}Th export (ThE) was ~60% higher than the sediment trap measurements, most of that difference was due to two large export events in Oct and Dec 1999 when the traps under-collected for ^{234}Th by factors of 2–4 (Benitez-Nelson et al., 2001). Consequently, higher primary production may lead to underestimated export (and lower apparent e-ratios) due to PC under-collection. Inherent in many of these short-term (<10 yr) studies of primary production and export at Station ALOHA was the importance of interannual environmental variability that might lead to variations in the strength and efficiency of the BCP, as we document herein.

A comparison between surface-tethered PIT traps (so-called "Clap" Traps) and neutrally-buoyant sediment traps (NBSTs) was made at Station ALOHA during the period 22 Jun – 8 Jul 2004 (Lamborg et al., 2008). The Clap Trap array differed slightly from the standard HOT program PIT array as it included a drogue at the base of the mooring line to reduce hydrodynamic slip, and it had a mechanism to close the traps with a lid prior to recovery. The fluxes obtained using Clap Traps and NBSTs "agreed fairly well" (p. 1552, Lamborg et al., 2008), and conformed to the long-term average summertime PC and PN fluxes reported herein. For particle collections at 150 m, the NBSTs had a mean molar PC:PN ratio of 8.57, slightly higher than the 30-yr mean of 8.09 for summer export at Station ALOHA.

4.5. PC export efficiency: e-ratios

Cross-ecosystem analyses of contemporary primary production and PC export from a broad range of oceanic habitats suggest that the e-ratio is a positive, non-linear function of total euphotic zone primary production, with values ranging from less than 0.1 for oligotrophic regions to >0.5 in highly productive coastal regions (Suess, 1980; Pace et al., 1987; Baines et al., 1994). Buesseler and Boyd (2009) have recently suggested that the e-ratio reference point should be set at the compensation irradiance for photosynthesis (the depth where net primary production = 0), rather than at a fixed depth. However, the depth of the compensation irradiance at Station ALOHA is itself variable (Letelier et al., 2004; Laws et al., 2016), so in practice it may be difficult to achieve this otherwise sound recommendation.

At Station ALOHA, the e-ratios varied considerably during the 30-yr observation period from 0.020 to 0.149 (mean = 0.054, SD = 0.021, n = 248), with lowest values in fall (Figs. 14 and 15). Monthly estimates were considerably less variable (range = 0.046 for Sep to 0.063 for Feb), and had a nearly identical mean value of 0.053 (Figs. 14 and 15). However, annually-averaged values displayed a much broader range from ~0.09 in 1990 to ~0.03 in 2013 (Fig. 15).

Although primary production and particle export are inextricably linked at Station ALOHA, they may not always be synchronized. Based on initial observations at Station ALOHA, Karl et al. (1996) presented evidence for an unexpected 3-yr duration, negative relationship between primary production and PC export with e-ratios ranging from 0.10 in spring 1990 to <0.05 in late fall 1992. Three hypotheses were presented for this apparent production-export decoupling, including: (1) a primary production-dependent difference between dissolved and particulate organic matter fluxes, (2) variable C-specific energy fluxes with maximum values coinciding with highest rates of primary production, and (3) dominance of horizontal, rather than vertical, export processes. Implicit in the Karl et al. (1996) study was the conclusion that the observations must be incorrect and, hence, need to be "explained away." As we now know from the extensive 30-yr data sets from Station ALOHA, both primary production and PC export are temporally variable on scales ranging from months to decades. Furthermore, oligotrophic regions like Station ALOHA are remineralization-intensive ecosystems where N_2 fixation supports a major fraction of new production, so small differences in the supply of new nitrogen can lead to large changes in the e-ratio. We also know that there are substantial day-to-day variations in light both at the sea surface and throughout the water column. The former is caused mostly by variations in clouds, and the latter by turbulent mixing in surface waters and inertial motions at greater depths. Individual populations within the ecosystem will have distinct generation times integrating over different spatial and temporal scales. Although Jones et al. (1996) concluded that living microbial biomass in the upper 150 m at Station ALOHA has a mean growth rate of ~1 per day, the variability in export production may be driven by "cryptic" assemblages over multiple temporal scales (as discussed in Karl et al., 2012). In the final analysis, it is the magnitude of export, rather than the e-ratio, that matters for the BCP. Therefore, perhaps primary production and export in oligotrophic waters should be viewed as uncoupled processes at both short (<week) and long (>year) time scales, with a common link back to seasonal variations in solar irradiance and nutrient availability (i.e., the two processes are coupled at seasonal time scales; Figs. 14 and 15).

Laws and Maiti (2019) diagnosed the previously reported negative correlations between primary production and export at Station ALOHA and concluded that time lags confound the conventional estimation of e-

ratios. Using a biogeochemical model, Henson et al. (2015) reported a time lag of ~5 days between primary production and export for oligotrophic ecosystems like Station ALOHA. A recent series of mesocosm experiments evaluated the time lag between peaks in water column Chl *a* and carbon sedimentation. The 4 separate experiments returned a broad range of time lags in sedimentation following a phytoplankton bloom from 2 to 5 days in Gullmar Fjord, Sweden to >12 days in Gando Bay, Gran Canaria. It is unknown how representative these mesocosm studies are of the oligotrophic conditions of Station ALOHA where blooms seldom occur. Our results document a relatively large variability in the e-ratios calculated on a cruise-to-cruise basis that is greatly reduced when the data are presented as monthly climatologies (Fig. 14). This result is consistent with a variable time lag between primary production and export of greater than a few days and less than one month as suggested by Laws and Maiti (2019). However, at the annual time scale, uncoupling between primary production and export appears to become greater (Fig. 15). Over the 30-year time series, the observed increasing trend in primary production is not reflected in higher export, so the e-ratio time-series displays a significant decreasing trend ($p < 0.01$; Fig. 15 and Table 2).

The low e-ratios (~0.05; Figs. 14 and 15) reported for oligotrophic ocean regions like Station ALOHA suggest that most of the recently produced organic matter is locally recycled within the microbial food web, and this intensive remineralization process provides the recycled nutrients necessary to sustain primary production the following day in an otherwise "nutrient-free" euphotic zone. Higher efficiencies of remineralization will lead to higher "regenerated" primary production and lower particle export. In the extreme case where all nutrients are recycled – as in a materially closed energetically open ecosystem – primary production would be maximized and there would be no export. Indeed, under steady-state conditions, the input of macronutrients (nitrate and phosphate) must equal or exceed the nutrients that are exported by sinking particles and other means. The rate of delivery of the limiting nutrient at Station ALOHA (either iron or phosphate; Letelier et al., 2019), combined with the elemental stoichiometry of exported matter, sets an upper constraint on PC export via the N_2 fixation-powered BCP (Karl et al., 2003). Station ALOHA appears to be poised at a euphotic zone depth-averaged remineralization efficiency of >95%, which likely varies in time and depth of the water column (also see Section 4.6).

Emerson (2014) presented a comprehensive status report on annual NCP and the BCP in the world ocean, including Station ALOHA. Based on a combination of observations, model simulations, and large-scale geochemical constraints, his analysis revealed an annual NCP of 2.5 (SD = 0.7) mol C m^{-2} for Station ALOHA. Mean annual PC export at 150 m accounts for less than half of this estimate although, as we show here, there is significant interannual variability in PC export at Station ALOHA (Figs. 11, 14, and 15). Emerson (2014) hypothesized that the downward flux of DOC at Station ALOHA, coupled with upper mesopelagic zone respiration, may be a dominant mode of C export from the euphotic zone. He estimated that two thirds of the organic matter oxidized in the 110–210 m depth zone at Station ALOHA was supplied by DOC rather than by sinking particles. If true, this would represent a fundamentally different view of the major C and energy export pathway than one dominated by sinking particles (McCave, 1975; Martin et al., 1987). As noted previously, the photosynthetic compensation depth at Station ALOHA is ~175 m (Laws et al., 2014), so much of the region modeled by Emerson (2014) is within the euphotic zone, not beneath it. Because the HOT program routinely measures PC export at 150 m, rather than the 100 m reference depth used in Emerson's (2014) analysis, the PC fluxes should be extrapolated to the same reference depth (using the Martin curve; Martin et al., 1987) or, better yet, directly measured in the field. Recent particle flux profiles at Station ALOHA have shown a much larger PC export at the 100 m reference depth (e.g., 47.1 mg C m^{-2} d^{-1} at 100 m versus 32.3 mg C m^{-2} d^{-1} at 150 m; Grabowski et al., 2019), so Emerson's (2014) conclusion on the role of particles relative to dissolved matter as a vehicle for C export may need to be reassessed. Clearly, the gravitational settling of particulate matter is a more rapid and efficient means to fuel mesopelagic and abyssal biomes than the downward diffusive or advective flux of DOC (Karl et al., 2012; Grabowski et al., 2019). Furthermore, since the average molar C:N ratio of DOM in the upper 0–100 m at Station ALOHA is nearly twice as large as the observed 30-yr mean value of ~8 for the sediment trap-collected particles (Foreman et al., 2019), the downward diffusive or advective flux of DOM from the euphotic zone would export an excess of C relative to N, and there is no evidence for selective retention of dissolved, fixed N in the euphotic zone. Hence, there is an urgent need for additional field observations and improved modeling of the ocean's BCP.

Finally, with an acknowledgement that primary production and PC export are complex processes that exhibit substantial variability and at times may be locally decoupled, Cael et al. (2018) hypothesized that a relationship might emerge over broader spatio-temporal scales. Using an innovative theoretical framework to analyze and interpret the probability distributions of primary production and PC export for a given region, they demonstrated that both ecosystem processes were log normally distributed for a given biome. Furthermore, the log moments of the distributions were linearly related to each other such that the distribution of PC export is consistent with predictions made from the statistics of the primary production distribution (Cael et al., 2018). Only time (and more field observations) will tell if this theory of probability distributions will lead to an improved understanding of the BCP at Station ALOHA.

4.6. *Does the NPSG operate as a two-layered system?*

The NPSG has previously been termed as a "two-layered system" with primary production in the upper (0–75 m) portion of the euphotic zone controlled by nutrient availability and the lower portion (>75 m) by light availability. Knauer et al. (1984) hypothesized that new production (sensu Dugdale and Goering, 1967) was minimal in the upper layer and that most of the sinking particles probably originate from the lower portion of the euphotic zone. A possible exception to this two-layered structure would be N_2 fixation-favorable periods when near surface production and export are most likely coupled. Based on field measurements of ^{234}Th:^{238}U disequilibria in the dissolved and particulate matter pools, Coale and Bruland (1987) also concluded that for oligotrophic ecosystems like Station ALOHA, most of the new production and, hence, particle export (based on ^{234}Th scavenging) occurs in the lower portion of the euphotic zone. NCP in the remineralization-intensive, upper portion of the water column in this hypothesized two-layered ecosystem would approach zero and, under steady-state conditions, export would also approach zero. Consequently, the e-ratios reported herein for Station ALOHA (and elsewhere for other oligotrophic ecosystems worldwide) may underestimate the true export efficiencies for the lower euphotic zone. Since the lower euphotic zone (75–125 m) primary production has increased by 36.6% during the 30-yr observation period without a concomitant increase in PC export (Fig. 15; Table 2), the efficiency of PC export must have decreased since the fundamental layered structure of the water column has not changed.

Small et al. (1987) also reported a two-layered system for an oligotrophic station in the tropical North Pacific Ocean. The upper layer supported relatively high primary production, but did not export any measurable particulate organic matter. However, sediment traps positioned near the base of the euphotic zone collected 38 mg C m^{-2} d^{-1}, a value that is slightly greater than the mean 150 m PC export during summer at Station ALOHA (33.5 mg m^{-2} d^{-1}; Fig. 15). Notwithstanding the potential for hydrodynamical bias and under-trapping for free-drifting sediment traps deployed in near-surface waters, several independent lines of evidence support the two-layered model. Ferrón et al. (2015) reported diel O_2 dynamics for a 7-d period during Mar 2014 near Station ALOHA. Daily NCP in the mixed layer varied from a system that

was net heterotrophic (−0.28 mmol O_2 m^{-3} d^{-1}) to one that was demonstrably net autotrophic (+0.48 mmol O_2 m^{-3} d^{-1}). The mean value for the week-long study was + 0.11 mmol O_2 m^{-3} d^{-1}, a slightly autotrophic net metabolic balance. The large day-to-day variability observed for NCP might lead to a non steady-state, or pulsed pattern of export, depending on the residence times of particulate and dissolved organic matter in the euphotic zone. During a typical HOT cruise, the sediment traps are deployed for ~60–70 hr (with a typical start time of ~0000 hr local on day 1), so they may not capture the full range of variability observed by Ferrón et al. (2015).

White et al. (2017) reported mixed layer estimates of GPP and R based on diel cycles of optically derived PC. GPP was calculated from the daytime increases in PC and nighttime losses, using changes in particle beam attenuation as described previously (Siegel et al., 1989; Claustre et al., 2008). Clear diel cycles in particle abundances were observed with minima at dawn and maxima at dusk. The mixed layer amplitude of the nighttime decline (%Δ = 25 ± 10%) was nearly identical to the amplitude of the daily production (%Δ = 22 ± 8%), indicating that the net daily change (equivalent to NCP) was not significantly different from zero (White et al., 2017), thereby supporting the existence of a two-layer ecosystem at Station ALOHA. The remaining ~75% of the signal did not oscillate and was interpreted as a background particulate detrital signal (White et al., 2017). If this interpretation is correct, then there are at least two major pools of suspended PC, one actively turning over on a daily time scale, and the other with a longer residence time. Regardless of dynamics, the bulk suspended particulate matter pool stoichiometry in the upper euphotic zone appears to be nearly identical to that of newly synthesized organic matter (C:N = 6.5–7 on a molar basis; Hebel and Karl, 2001).

Nicholson et al. (2015) pioneered the use of autonomous Seagliders equipped with oxygen optodes to quantify the diel periodicity in O_2 concentrations at Station ALOHA. During a Seaglider mission in summer 2012, they fitted their field observations to an idealized diel cycle that was based on time-varying photosynthesis versus irradiance using the well-established model of Jassby and Platt (1976), corrected for air-sea O_2 flux. If R is assumed to be constant over the diel cycle, then GPP, R, and NCP could be estimated (Nicholson et al., 2015). For 110 daily measurements using two separate Seaglider missions near Station ALOHA, 73 days had a statistically significant fit to the model. Though not discussed in their paper, nearly one-third of their observations had a signal that was too low to resolve (diel cycles <±0.2 mmol O_2 m^{-3}), indicating that even during the productive summer months there must also be very low productivity periods or regions. Since the experimental design was not Lagrangian, we do not know whether there was an oscillation between low GPP, high R net heterotrophic periods (when remineralized nutrients might locally accumulate) followed by subsequent bursts of GPP leading to net autotrophy. Mixed layer GPP for the period Jun-Sep had a mean 1.8 (SD = 0.7) mmol O_2 m^{-3} d^{-1} and was 3.2 times greater than contemporaneous (but these independent measurements were not conducted at identical locations) ^{14}C-based primary production that was measured on 43 days (Jun through mid-Sep) of the much longer Seaglider mission (Nicholson et al., 2015). Several very high GPP values (up to 7–8 mmol O_2 m^{-3} d^{-1}) were detected, as well as many low GPP events, once again confirming significant spatial or temporal heterogeneity, or both. Despite the variable and, sometimes, exceptionally large GPP observed in this study, mixed layer NCP was always <5% of GPP, again emphasizing the intense daily remineralization that must occur in the mixed layer at Station ALOHA to sustain primary production. This leaves very little particulate matter (or potential energy) remaining for export from the upper euphotic zone.

More recently, Barone et al. (2019b) investigated diel variations in O_2 at Station ALOHA, and interpreted the field observations using an improved biological-physical model. Their data set included O_2 measurements during 4 separate Seaglider missions in both an anticyclonic eddy in summer 2015 and a cyclone-anticyclone eddy dipole in spring 2016 in the NPSG. Estimates of GPP and R were obtained from a total of 191 days of data during the Seaglider missions. Combining all field observations, GPP and R in surface waters were identical with a weighted mean and weighted SD of 1.0 ± 0.7 O_2 mmol m^{-3} d^{-1} (Barone et al., 2019b). This result is consistent with the two-layer model where NCP is negligible in the upper euphotic zone and cannot support PC export without an organic matter subsidy. However, because the signal-to-noise ratio in oligotrophic waters is very low, Barone et al. (2019b) presented rates that were averaged over multiple consecutive days. Using a time window of 7 d for data collected during a 3-month period in late summer-early fall 2015, they documented significant week-to-week changes (±100% of 3-month mean) in the magnitudes of both GPP and R, as well as in the estimated weekly autotroph-heterotroph metabolic balances (Barone et al., 2019b). Though not examined in this otherwise comprehensive study, the relatively large, short-term (~1 week) variations in GPP and R are likely to also impact PC export. The spatial and temporal mosaic of GPP and R, at least for conditions in the mixed layer of the euphotic zone, is probably a much more accurate representation of the oligotrophic NPSG than "once per month" ship-based observations, so it is very likely that Seagliders will continue to provide invaluable data at Station ALOHA.

4.7. *Primary production and export models*

One of the initial justifications for the establishment of Station ALOHA was to provide an accessible field site where observations and measurements would be representative of a much larger biome, the NPSG. A unique contribution of programs like HOT is their ability to reveal unexpected ecological and biogeochemical relationships that, in conjunction with the time-series data sets, can be used to refine existing models of the BCP, or to develop improved ones. Because seascapes like the NPSG are grossly undersampled, the use of models is the only means for basin-wide scaling of fundamental ecosystem processes and for predicting future states of the global ocean.

Euphotic zone depth-integrated primary production has been modeled using a variety of increasingly sophisticated approaches (Kyewalyanga et al., 1992; Behrenfeld and Falkowski, 1997; Ondrusek et al., 2001; Banse and Postel, 2003; Stock et al., 2014; Schulien et al., 2017). Carr et al. (2006) presented the results of the third algorithm intercomparison for 24 models of depth-integrated primary production from satellite measurements of ocean color, as well as 7 general circulation models (GCMs) coupled with ecosystem or biogeochemical models. Most models of phytoplankton production in the ocean employ surface PAR, the optical properties of the water column, and the response of the plankton assemblage to light (e.g., photosynthesis versus irradiance parameters; Kirk, 2011). This comprehensive analysis revealed that the pair-wise correlations among the various ocean color-based models always exceeded 0.5 (generally greater than 0.7), but that the GCM-based models were poorly correlated with the ocean color models (Carr et al., 2006).

Most primary production models use Chl as an implicit representation of phytoplankton biomass. This is mainly due to data density and ability to estimate Chl from satellite-based ocean color measurements. However, as mentioned previously, there are photoacclimation effects both in the surface waters (lower Chl *a* per phytoplankton cell biomass) in summer compared to winter, and with depth in the water column, especially at the DCM in the fall-winter period. Ocean color satellites can only detect Chl within the first optical depth which at Station ALOHA ranges from 18 to 27 m with a mean of 22.9 (SD = 1.7 m). During our 30-yr observation period, Chl *a* integrated over the first optical depth accounted for ~9% of the 0–200 m total, and ^{14}C-based primary production in the same region was ~28% of the total.

In order to accommodate the well known variability in phytoplankton C:Chl *a* ratios, Westberry et al. (2008) developed a C-based primary production model using satellite observations of particle backscatter coefficients (Behrenfeld et al., 2005), and empirical relationships between backscatter and phytoplankton C. Their vertical

model produced estimates of Chl *a*, PC, and primary production. The model, validated using data from Station ALOHA and from BATS in the North Atlantic Ocean, reproduced the observed seasonality in C:Chl *a* ratios measured at Station ALOHA (as indicated by the seasonality of *Prochlorococcus* Chl *a* fluorescence to cell ratios) with maximum values of ~200 in winter and minima of ~150 in summer. However, a major fraction of the total suspended PC in the surface waters at Station ALOHA is non-living detritus, so the true phytoplankton C: Chl *a* ratio is probably closer to 50–100 (Eppley et al., 1971; Christian and Karl, 1994). And, while the C-based primary production model performed better than the vertically generalized production model (VGPM) in reproducing the mean values for ^{14}C-based observations from Station ALOHA for the period 1998–2003, it failed to capture the seasonal cycle (Westberry et al., 2008).

More recently, Saba et al. (2010) evaluated the performance of 22 satellite-based ocean color models and 14 GCM coupled biogeochemical models for the estimation of euphotic zone depth-integrated primary production. They compared the model output to ^{14}C-based primary production from BATS and HOT. Performance of each model was judged on its ability to reproduce the observed mean value, the temporal variability, and the long-term trends from 1989 to 2007 (Saba et al., 2010). For Station ALOHA, the satellite-based models had a higher skill than the GCM-biogeochemical models, although there were exceptions. The use of the HOT program HPLC-Chl *a* dataset further improved the model skill compared to either fluorometric-Chl *a* or Chl derived from ocean color. Furthermore, the ocean color models using satellite-derived Chl, as is most commonly employed (see Carr et al., 2006), report decreasing trends in Chl (e.g., Behrenfeld et al., 2006; Polovina et al., 2008) and, hence, primary production, neither of which is observed over the 30-yr observation period at Station ALOHA. The central conclusion of this comprehensive intercomparison was that the majority of contemporary models underestimate the mean and variability of NPP at both oligotrophic ocean sites. This assumes, of course, that the 12-hr ^{14}C-based methods employed accurately reflect NPP. Unfortunately, there is no "certified reference material" for oceanic primary production, so the accuracy of currently employed field measurements is unknown.

Kovač et al. (2016) extrapolated photosynthesis versus irradiance functions through the water column to obtain an analytical solution for the vertical profiles of daily primary production. The solution was then fitted to the Station ALOHA ^{14}C-based field data, as previously reported by Letelier et al. (1996) for the first 4 years of HOT program data. Their analytical solution explained >97% of the variance in the measured Chl (biomass) normalized production at individual depths, and also recovered the seasonal cycle (Kovač et al., 2016). However, their analysis did not consider light-dependent ^{14}C-DOC production or the systematic depth changes in the ratio of ^{18}O-based GPP:^{14}C-based primary production, discussed previously. While their analytical model appeared to reproduce the mean state of primary production at Station ALOHA, it did not predict the outliers, nor did it explain the observed subdecadal variability or longer term trends in primary production reported herein for similar conditions of irradiance and water column transparency.

A number of empirical models have been devised to estimate PC export from euphotic zone depth-integrated primary production (Suess, 1980; Betzer et al., 1984; Berger et al., 1987; Pace et al., 1987; Lohrenz et al., 1992) or Chl *a* (Baines et al., 1994). The accuracy of these models was evaluated by Karl et al. (1996) using the first few years of HOT program data. None of the models accurately predicted the PC export at Station ALOHA or the observed interannual variability. Smith et al. (2005) developed a comprehensive one-dimensional multi-element (C, N, P, and Si) model similar to the NEMURO model (Fujii et al., 2002) to simulate primary production and export at Station ALOHA. Two versions of the model were tested against the field observations, one with and one without overflow DOC production and recycling that might be expected to occur under low nutrient / high light conditions. By including overflow production of DOC, the model was able to simulate the observed profile of DOC, but underestimated both primary production and PC export compared to field observations at Station ALOHA (Smith et al., 2005).

In a comprehensive synthesis of field data from the JGOFS program, Laws et al. (2000) formulated a quantitative model linking primary production to export in a broad range of marine ecosystems, including Station ALOHA. Their nitrogen-based food web model partitioned total primary production into two separate food chains, one supported by large phytoplankton that produced only particulate detritus and the other by small phytoplankton that produced only dissolved detritus. The model assumptions and input values led to a steady-state solution where the external loading of limiting nutrient (nitrate in their model) was equal to the loss of particulate detrital N (Laws et al., 2000). This solution was conceptually identical to the pioneering work of Eppley and Peterson (1979) who hypothesized that export should equate to new production (that fraction of total primary production that is supported by exogenous nutrients) under steady-state conditions. However, instead of the hyperbolic relationship proposed by Eppley and Peterson (1979), Laws et al. (2000) reported that temperature and NPP were the critical variables that control export production, and that the e-ratio varied considerably from minima of ~0.1–0.2 at temperatures >25 °C to a maximum of ~0.67 for ecosystems where the temperature is in the range of 0–10 °C. In their analysis of 11 field studies covering this full range of environmental conditions, temperature alone explained 86% of the variance in export when applied to observations at Station ALOHA.

For the analysis of Station ALOHA data in their model, Laws et al. (2000) used an input temperature of 25 °C which is a reasonable annual mean sea surface temperature (SST; Fig. 1). However, during the 30-yr observation period there were significant seasonal and interannual variations in SST of up to 5 °C (range 20.7–29.4), with extended periods of anomalously high SST in 1996 and 2015–2018 (Fig. 1). Neither of these extreme SST conditions impacted euphotic zone depth-integrated ^{14}C-based primary production or PC export based on our field observations (Fig. 15). Furthermore, the predictable seasonal variation in SST at Station ALOHA (Fig. 1) has no effect on the e-ratio which remains low (~0.05) throughout the year (Fig. 14). There is also a strong temperature gradient within the euphotic zone at Station ALOHA (Fig. 1), so the input temperature for the model should be a depth-production weighted value rather than SST. For example, during mid-summer periods when primary production is at its maximum, considerably less than half of the total primary production occurs in the isothermal mixed layer, and >20% of the production occurs at depths where the ambient temperature is 5–6 °C cooler than the SST. Furthermore, as mentioned above, it has been hypothesized that chronically oligotrophic ecosystems like Station ALOHA are essentially two-layered systems (Knauer et al., 1984; Coale and Bruland, 1987; Small et al., 1987), where most, if not all, of the exported particulate matter is produced in the lower, colder portion of the water column. If the BCP at Station ALOHA performs as a two-layered system, then the model input temperature should be ~20 °C, which would predict an e-ratio of >0.25 (Laws et al., 2000). Finally, the role of N_2 fixation as a significant source of new N, especially in surface waters during summer and fall periods, is well established at Station ALOHA. The periodic nature of nutrient delivery via N_2 fixation and the possibility for a bloom of larger phytoplankton, such as diatoms containing endosymbiotic diazotrophs (Karl et al., 2012), would require a significant change in the model input values and possibly require a revised food web model structure to accurately predict export during late summer periods at Station ALOHA.

Henson et al. (2011) challenged the model of Laws et al. (2000) on the grounds that traditional ^{15}N-labeled experiments do not account for euphotic zone nitrification and would, therefore, overestimate export. They introduced an alternative model that was based on estimation of PC export using field measurements of the disequilibrium between ^{238}U and its radiogenic daughter, ^{234}Th (ThE-ratio; Buesseler et al., 1998, 2006). To compare satellite-based primary production to the field measurements of ^{234}Th scavenging, they used ocean color data from 16 days prior to the field measurements to reflect the estimated residence

time of ^{234}Th in the euphotic zone. There were large discrepancies between the two models through the entire range of temperatures (0–30 °C). For warm (>25 °C), oligotrophic subtropical ecosystems like Station ALOHA, where the Laws et al. (2000) model predicted an e-ratio of 0.15, the Henson et al. (2011) model predicted a range of values from <0.01 to >0.25 (Henson et al., 2011; their Fig. 1) with an exponential relationship with temperature. For the ^{234}Th-based export model, temperature alone explained ~50% of the variance. Finally, Henson et al. (2015) subsequently used a high-resolution, global scale biogeochemical model to investigate export efficiency of the BCP. The model included slow- and fast-sinking detrital material, and considered flux attenuation as a function of temperature and ballast minerals. Also considered in their model was the potential time lag between primary production and export which could bias estimation of the contemporaneous e-ratio. As expected, they determined that this source of error was probably greatest in high latitude regions where errors in estimated export efficiency can be up to ± 60% (Henson et al., 2015).

5. Future prospectus

At the start of the HOT program, the research community was engaged in a lively debate regarding primary production in the NPSG. The nature of the dispute and the ecological implications of a resolution were succinctly summarized in a review article by Platt et al. (1989), subtitled "the case for consensus." In the end, the authors concluded that the answer to the rather straightforward question "What is the primary production in the open ocean?" had no simple answer because "photosynthetic rates in the pelagic ocean are ever-changing rather than steady-state, and at times can be surprisingly high" (Platt et al., 1989). The results of our long-term observations of primary production at Station ALOHA support the Platt et al. (1989) claim of intermittency, but also reveal an unexpected three-decades-long trend of increasing primary production.

Gregg et al. (2005) reported satellite-based Chl concentrations in the NPSG for a 6-yr period (1998–2003). They documented a significant decrease in Chl (-2.7% per annum) along with a corresponding increase in sea surface temperature (0.31 °C per annum). These observations were consistent with an earlier report that the most oligotrophic regions of the NPSG, where Chl *a* concentrations were ≤ 0.07 mg m^{-3}, were expanding (McClain et al., 2004), a trend that was later confirmed by Polovina et al. (2008). A more recent, comprehensive analysis of Chl estimates in the NPSG for the period 1998–2012 revised the magnitude of the decreasing trend to a value of −1.1% yr^{-1} (Gregg and Rousseaux, 2014). A major challenge was to blend the observations from different ocean color sensors, each with a decadal scale mission lifetime, into a consistent longer term data set.

Boyce et al. (2010) combined historical records of ocean transparency using the standardized Secchi disk, in situ Chl *a* measurements, and satellite-based ocean color observations since 1979 to produce a century-long record of phytoplankton biomass in key regions of the world's ocean. They reported significant declines in 8 out of the 10 ocean regions, including the North Pacific. While there were interannual-to-decadal fluctuations in phytoplankton biomass that were attributed to basin-scale climate variations, the global rate of decline averaged ~1% of the global median value per annum, and was correlated with long-term increases in sea-surface temperature (Boyce et al., 2010). The temperature effect was particularly pronounced for tropical and subtropical regions where enhanced thermal-induced stratification leads to a reduction in the supply of nutrients. This century-long data set supports the previous conclusions of Gregg et al. (2005) and others, based on shorter satellite ocean color observations. The satellite-based observations are also consistent with most current ocean ecosystem models that predict decreases in marine productivity during the 21st century (Steinacher et al., 2010; Bopp et al., 2013). The projected decrease derives from changes in sea surface temperature, pH, mixed layer depth, and nutrient delivery to the surface ocean.

Both Secchi disk and satellite observations are restricted to the near-surface ocean, generally the first optical depth of the upper euphotic zone at Station ALOHA (mean = 22.9, SD = 1.7 m). Our 30-yr time series demonstrates that both Chl *a* and primary production in the upper 0–25 m were relatively constant over the 30-yr observation period, with significant increases observed only at depths >45 m (Tables 2 and 3). In an attempt to reconcile the discrepancies between satellite-based observations and ecosystem model predictions with our extensive field observations, Kavanaugh et al. (2018) suggested that the location of Station ALOHA at the edge of the subtropics and other pivot points (Chavez et al., 2011), may lead to differential regional effects of variable climate indices and longer term climate change. It was suggested that Station ALOHA may serve as a key sentinel and, perhaps, a leading indicator for future changes throughout the NPSG (Kavanaugh et al., 2018). Nevertheless, improving our understanding of how the lower euphotic zone in this vast and well stratified environment will respond to these future changes remains a 21st century challenge.

Despite dire predictions about the future state of the ocean, two major groups of picocyanobacteria, *Prochlorococcus* and *Synechococcus*, are predicted to increase globally by 2100 and, hence, to continue to make a major contribution to primary production (Flombaum et al., 2013). The increase of picocyanobacteria in their quantitative niche model was most sensitive to temperature and, hence, to the predicted global expansion of tropical and subtropical seascapes. Although not explicitly included in their model, phototrophic microbial assemblages can be viewed as complex adaptive systems with enormous metabolic flexibility that renders them at least partially resilient to the otherwise deleterious impacts of climate change (Martiny et al., in preparation).

Finally, our observations at Station ALOHA, which document a sustained 30-yr long increase in Chl *a*, suspended PC and PN, and primary production, especially for the lower portion of the euphotic zone, is not predicted by current ecosystem models of the NPSG. We cannot yet reject the hypothesis that the observed increasing trend in primary production is actually part of an oscillation about a longer term (decades to century) mean state. And while at monthly-to-seasonal scales the export of particulate organic matter at the base of the euphotic zone appears to vary as a function of primary production, the lack of correlation between these two fluxes at annual-to-decadal scales suggests that small, yet unresolved, changes in the pelagic ecosystem structure or function may play a disproportionate role in these key biogeochemical processes. It is sobering to consider the possibility of other inconvenient sea truths: *"too fundamental to be ignored, too incomplete to be understood"* (Munk, 2009).

Declaration of Competing Interest

The authors declare that they have no known competing financial interests or personal relationships that could have appeared to influence the work reported in this paper.

Acknowledgements

We thank the many scientists, field and laboratory technicians, students, post-doctoral scholars, ships' officers and crew, and HOT program support staff who have contributed to the success of the Hawaii Ocean Time-series (HOT) program since 1988. While this list of colleagues is too long to name, several individuals stand out as superlative examples of dedication to excellence. L. Fujieki participated in more than 200 HOT program cruises and was responsible for creating and maintaining our data distribution system, HOT-DOGS. Fujieki and L. Lum also provided invaluable support to the preparation of this manuscript. D. Sadler, F. Santiago-Mandujano, and J. Snyder also participated in >200 HOT expeditions, and B. Watkins, S. Curless, and D. Hebel in >100 each. Professor Roger Lukas co-founded (with DMK) the HOT program in 1988, and designed and led the physical oceanography core component of HOT during the first three decades. His vision and efforts helped to establish the world-class program that we enjoy today. Professor Michael Landry designed and leads the mesozooplankton core

component of HOT. Finally, we acknowledge the continuous (since 1988), generous support from the National Science Foundation (current grant OCE-1756517; AEW, P.I.) and the Simons Foundation (#329108).

Appendix A. Supplementary material

Supplementary data to this article can be found online at https://doi.org/10.1016/j.pocean.2021.102563.

References

Albani, S., Mahowald, N.M., Perry, A.T., Scanza, R.A., Zender, C.S., Heaves, N.G., Maggi, V., Kok, J.F., Otto-Bliesner, B.L., 2014. Improved dust representation in the Community Atmosphere Model. J. Adv. Model. Earth Syst. 6 (3), 541–570. https://doi.org/10.1002/2013MS000279.

Alexander, H., Rouco, M., Haley, S.T., Wilson, S.T., Karl, D.M., Dyhrman, S.T., 2015. Functional group-specific traits drive phytoplankton dynamics in the oligotrophic ocean. Proc. Natl. Acad. Sci. USA 112 (44), E5972–E5979. https://doi.org/10.1073/pnas.1518165112.

Al-Mutairi, H., Landry, M.R., 2001. Active export of carbon and nitrogen at Station ALOHA by diel migrant zooplankton. Deep-Sea Res. Pt. II 48 (8), 2083–2103. https://doi.org/10.1016/S0967-0645(00)00174-0.

Ascani, F., Richards, K.J., Firing, E., Grant, S., Johnson, K.S., Jia, Y., Lukas, R., Karl, D. M., 2013. Physical and biological controls of nitrate concentrations in the upper subtropical North Pacific Ocean. Deep-Sea Res. Pt. II 93, 119–134. https://doi.org/10.1016/j.dsr2.2013.01.034.

Baines, S.B., Pace, M.L., Karl, D.M., 1994. Why does the relationship between sinking flux and planktonic primary production differ between lakes and oceans? Limnol. Oceanogr. 39 (2), 213–226. https://doi.org/10.4319/lo.1994.39.2.0213.

Banse, K., Postel, J.R., 2003. On using pigment-normalized, light-saturated carbon uptake with satellite-derived pigment for estimating column photosynthesis. Global Biogeochem. Cy. 17 (3), 1079. https://doi.org/10.1029/2002GB002021.

Barone, B., Coenen, A.R., Beckett, S.J., McGillicuddy Jr., D.J., Weitz, J.S., Karl, D.M., 2019a. The ecological and biogeochemical state of the North Pacific Subtropical Gyre is linked to sea surface height. J. Mar. Res. 77 (Suppl.), 215–245. https://doi.org/10.1357/002224019828474241.

Barone, B., Nicholson, D.P., Ferrón, S., Firing, E., Karl, D.M., 2019b. The estimation of gross oxygen production and community respiration from autonomous time-series measurements in the oligotrophic ocean. Limnol. Oceanogr.: Meth. 17 (12), 650–664. https://doi.org/10.1002/lom3.10340.

Behrenfeld, M.J., Falkowski, P., 1997. Photosynthetic rates derived from satellite-based chlorophyll concentrations. Limnol. Oceanogr. 42 (1), 1–20. https://doi.org/10.4319/lo.1997.42.1.0001.

Behrenfeld, M.J., Boss, E., Siegel, D.A., Shea, D.M., 2005. Carbon-based ocean productivity and phytoplankton physiology from space. Global Biogeochem. Cy. 19 (1), GB1006. https://doi.org/10.1029/2004GB002299.

Behrenfeld, M.J., O'Malley, R.T., Siegel, D.A., McClain, C.R., Sarmiento, J.L., Feldman, G.C., Milligan, A.J., Falkowski, P.G., Letelier, R.M., Boss, E.S., 2006. Climate-driven trends in contemporary ocean productivity. Nature 444 (7120), 752–755. https://doi.org/10.1038/nature05317.

Benitez-Nelson, C., Buesseler, K.O., Karl, D.M., Andrews, J., 2001. A time-series study of particulate matter export in the North Pacific Subtropical Gyre based on ^{234}Th: ^{238}U disequilibrium. Deep-Sea Res. Pt. I 48 (12), 2595–2611. https://doi.org/10.1016/S0967-0637(01)00032-2.

Berger, W.H., Fischer, K., Lai, C., Wu, G., 1987. Ocean Productivity and Organic Carbon Flux. I. Overview and Maps of Primary Production and Export Production. University of California, San Diego.

Betzer, P.R., Showers, W.J., Laws, E.A., Winn, C.D., DiTullio, G.R., Kroopnick, P.M., 1984. Primary productivity and particle fluxes on a transect of the equator at 153°W in the Pacific Ocean. Deep-Sea Res. Pt. A 31, 1–11. https://doi.org/10.1016/0198-0149(84)90068-2.

Bidigare, R.R., Schofield, O., Prézelin, B.B., 1989. Influence of zeaxanthin on quantum yield of photosynthesis of *Synechococcus* clone WH7803 (DC2). Mar. Ecol. Prog. Ser. 56, 177–188.

Bidigare, R.R., Van Heukelem, L., Trees, C.C., 2005. Analysis of algal pigments by high-performance liquid chromatography. In: Andersen, R.A. (Ed.), Algal Culturing Techniques. Academic Press, New York, pp. 327–345.

Bidigare, R.R., Chai, F., Landry, M.R., Lukas, R., Hannides, C.C.S., Christensen, S., Karl, D.M., Shi, L., Chao, Y., 2009. Subtropical ocean ecosystem structure changes forced by North Pacific climate variations. J. Plankton Res. 31 (10), 1131–1139. https://doi.org/10.1093/plankt/fbp064.

Bidigare, R.R., Buttler, F.R., Christensen, S.J., Barone, B., Karl, D.M., Wilson, S.T., 2014. Evaluation of the utility of xanthophyll cycle pigment dynamics for assessing upper ocean mixing processes at Station ALOHA. J. Plankton Res. 36 (6), 1423–1433. https://doi.org/10.1093/plankt/fbu069.

Bond, N.A., Overland, J.E., Spillane, M., Stabeno, P., 2003. Recent shifts in the state of the North Pacific. Geophys. Res. Lett. 30 (23) https://doi.org/10.1029/2003GL018597.

Bopp, L., Resplandy, L., Orr, J.C., Doney, S.C., Dunne, J.P., Gehlen, M., Halloran, P., Heinze, C., Hyina, T., Séférian, R., Tjiputra, J., Vichi, M., 2013. Multiple stressors of ocean ecosystems in the 21st century: projections with CMIP5 models. Biogeosciences 10 (10), 6225–6245. https://doi.org/10.5194/bg-10-6225-2013.

Böttjer, D., Dore, J.E., Karl, D.M., Letelier, R.M., Mahaffey, C., Wilson, S.T., Zehr, J., Church, M.J., 2017. Temporal variability of dinitrogen fixation and particulate nitrogen export at Station ALOHA. Limnol. Oceanogr. 62 (1), 200–216. https://doi.org/10.1002/lno.10386.

Boyce, D.G., Lewis, M.R., Worm, B., 2010. Global phytoplankton decline over the past century. Nature 466 (7306), 591–596. https://doi.org/10.1038/nature09268.

Boyd, P.W., Claustre, H., Levy, M., Siegel, D.A., Weber, T., 2019. Multi-faceted particle pumps drive carbon sequestration in the ocean. Nature 568 (7752), 327–335. https://doi.org/10.1038/s41586-019-1098-2.

Brewer, P.G., Bruland, K.W., Eppley, R.W., McCarthy, J.J., 1986. The Global Ocean Flux Study (GOFS): Status of the U.S. GOFS program. Eos. Trans. Am. Geophys. Union 67 (44), 827–832. https://doi.org/10.1029/EO067i044p00827.

Briggs, N., Dall'Olmo, G., Claustre, H., 2020. Major role of particle fragmentation in regulating biological sequestration of CO_2 by the oceans. Science 367 (6479), 791–793. https://doi.org/10.1126/science.aay1790.

Brix, H., Gruber, N., Karl, D.M., Bates, N.R., 2006. On the relationships between primary, net community, and export production in subtropical gyres. Deep-Sea Res. Pt. II 53 (5), 698–717. https://doi.org/10.1016/j.dsr2.2006.01.024.

Brzezinski, M.A., Krause, J.W., Church, M.J., Karl, D.M., Li, B., Jones, J.L., Updyke, B., 2011. The annual silica cycle of the North Pacific subtropical gyre. Deep-Sea Res. Pt. I 58 (10), 988–1001. https://doi.org/10.1016/j.dsr.2011.08.001.

Buesseler, K.O., Boyd, P.W., 2009. Shedding light on processes that control particle export and flux attenuation in the twilight zone of the open ocean. Limnol. Oceanogr. 54 (4), 1210–1232. https://doi.org/10.4319/lo.2009.54.4.1210.

Buesseler, K.O., Andrews, J.E., Hartman, M.C., Belastock, R., Chai, F., 1995. Regional estimates of the export flux of particulate organic carbon derived from thorium-234 during the JGOFS EQPAC program. Deep-Sea Res. Pt. II 42 (2), 777–804. https://doi.org/10.1016/0967-0645(95)00043-P.

Buesseler, K., Ball, L., Andrews, J., Benitez-Nelson, C., Belastock, R., Chai, F., Chao, Y., 1998. Upper ocean export of particulate organic carbon in the Arabian Sea derived from thorium-234. Deep-Sea Res. Pt. II 45, 2461–2488. https://doi.org/10.1016/S0967-0645(98)80022-2.

Buesseler, K.L., Benitez-Nelson, C.R., Moran, S.B., Burd, A., Charette, M., Cochran, J.K., Coppola, L., Fisher, N.S., Fowler, S.W., Gardner, W.D., Guo, L.D., Gustafsson, Ö., Lamborg, C., Masque, P., Miquel, J.C., Passow, U., Santschi, P.H., Savoye, N., Stewart, G., Trull, T., 2006. An assessment of particulate organic carbon to thorium-234 ratios in the ocean and their impact on the application of Th-234 as a POC flux proxy. Mar. Chem. 100 (3), 213–233. https://doi.org/10.1016/j.marchem.2005.10.013.

Cael, B.B., Bisson, K., Follett, C.L., 2018. Can rates of ocean primary production and biological carbon export be related through their probability distributions? Global Biogeochem. Cy. 32 (6), 954–970. https://doi.org/10.1029/2017GB005797.

Calvin, M., Benson, A.A., 1948. The path of carbon in photosynthesis. Science 107 (2784), 476–480.

Campbell, L., Nolla, H.A., Vaulot, D., 1994. The importance of *Prochlorococcus* to community structure in the central North Pacific Ocean. Limnol. Oceanogr. 39 (4), 954–961. https://doi.org/10.4319/lo.1994.39.4.0954.

Campbell, L., Liu, H., Nolla, H.A., Vaulot, D., 1997. Annual variability of phytoplankton and bacteria in the subtropical North Pacific Ocean at Station ALOHA during the 1991–1994 ENSO event. Deep-Sea Res. Pt. I 44 (2), 167–192. https://doi.org/10.1016/S0967-0637(96)00102-1.

Carr, M.-E., Friedrichs, M.A.M., Schmeltz, M., Aita, M.N., Antoine, D., Arrigo, K.R., Asanuma, I., Aumont, O., Barber, R., Behrenfeld, M., Bidigare, R., Buitenhuis, E.T., Campbell, J., Ciotti, A., Dierssen, H., Dowell, M., Dunne, J., Esaias, W., Gentili, B., Gregg, W., Groom, S., Hoepffner, N., Ishizaka, J., Kameda, T., Le Quéré, C., Lohrenz, S., Marra, J., Mélin, F., Moore, K., Morel, A., Reddy, T.E., Ryan, J., Scardi, M., Smyth, T., Turpie, K., Tilstone, G., Waters, K., Yamanaka, Y., 2006. A comparison of global estimates of marine primary production from ocean color. Deep-Sea Res. Pt. II 53 (5), 741–770. https://doi.org/10.1016/j.dsr2.2006.01.028.

Chai, F., Dugdale, R.C., Peng, T.-H., Wilkerson, F.P., Barber, R.T., 2002. One dimensional ecosystem model of the equatorial Pacific upwelling system, Part I: model development and silicon and nitrogen cycle. Deep-Sea Res. Pt. II 49 (13), 2713–2745. https://doi.org/10.1016/S0967-0645(02)00055-3.

Chave, K.E., 1965. Carbonates: Association with organic matter in surface seawater. Science 148 (3678), 1723–1724. https://doi.org/10.1126/science.148.3678.1723.

Chavez, F.P., Messié, M., Pennington, J.T., 2011. Marine primary production in relation to climate variability and change. Ann. Rev. Mar. Sci. 3, 227–260. https://doi.org/10.1146/annurev.marine.010908.163917.

Chen, S., Qiu, B., 2010. Mesoscale eddies northeast of the Hawaiian archipelago from satellite altimeter observations. J. Geophys. Res. Oceans 115 (C3). https://doi.org/10.1029/2009JC005698.

Chisholm, S.W., Olson, R.J., Zettler, E.R., Goericke, R., Waterbury, J.B., Welschmeyer, N. A., 1988. A novel free-living prochlorophyte abundant in the oceanic euphotic zone. Nature 334 (6180), 340–343. https://doi.org/10.1038/334340a0.

Christian, J.R., Karl, D.M., 1994. Microbial community structure at the U.S.-Joint Global Ocean Flux Study Station ALOHA: Inverse methods for estimating biochemical indicator ratios. J. Geophys Res. Oceans 99 (C7), 14269–14276. https://doi.org/10.1029/94JC00681.

Church, M.J., Jenkins, B.D., Karl, D.M., Zehr, J.P., 2005. Vertical distributions of nitrogen-fixing phylotypes at Stn ALOHA in the oligotrophic North Pacific Ocean. Aquat. Microb. Ecol. 38 (1), 3–14. https://doi.org/10.3354/ame038003.

Church, M.J., Mahaffey, C., Letelier, R.M., Lukas, R., Zehr, J.P., Karl, D.M., 2009. Physical forcing of nitrogen fixation and diazotroph community structure in the North Pacific subtropical gyre. Global Biogeochem. Cy. 23 (2), GB2020. https://doi.org/10.1029/2008GB003418.

Church, M.J., Lomas, M.W., Muller-Karger, F., 2013. Sea change: Charting the course for biogeochemical ocean time-series research in a new millennium. Deep-Sea Res. Pt. II 93, 2–15. https://doi.org/10.1016/j.dsr2.2013.01.035.

Ciais, P., Sabine, C., Bala, G., Bopp, L., Brovkin, V., Canadell, J., Chhabra, A., DeFries, R., Galloway, J., Heimann, M., Jones, C., Le Quéré, C., Myneni, R.B., Piao, S.,Thornton, P., 2013. Chapter 6: Carbon and other biogeochemical cycles. In: Stocker, T.F., Qin, D., Plattner, G.-K., Tignor, M., Allen, S.K., Boschung, J., Nauels, A., Xia, Y., Bex, V., Midgley, P.M. (Eds.), Climate Change 2013: The Physical Science Basis. Contribution of Working Group I to the Fifth Assessment Report of the Intergovernmental Panel on Climate Change. Cambridge University Press, Cambridge, United Kingdom and New York, NY, USA, pp. 465-570.

Claustre, H., Huot, Y., Obernosterer, I., Gentili, B., Tailliez, D., Lewis, M., 2008. Gross community production and metabolic balance in the South Pacific Gyre, using a non intrusive bio-optical method. Biogeosciences 5 (2), 463–474. https://doi.org/10.5194/bg-5-463-2008.

Close, H.G., Shah, S.R., Ingalls, A.E., Diefendorf, A.F., Brodie, E.L., Hansman, R.L., Freeman, K.H., Aluwihare, L.I., Pearson, A., 2013. Export of submicron particulate organic matter to mesopelagic depth in an oligotrophic gyre. Proc. Natl. Acad. Sci. USA 110 (31), 12565–12570. https://doi.org/10.1073/pnas.1217514110.

Coale, K.H., Bruland, K.W., 1987. Oceanic stratified euphotic zone as elucidated by ^{234}Th:^{238}U disequilibria. Limnol. Oceanogr. 32 (1), 189–200. https://doi.org/10.4319/lo.1987.32.1.0189.

Cook, J.R., 1963. Adaptations in growth and division in *Euglena* effected by energy supply. J. Protozool. 10 (4), 436–444. https://doi.org/10.1111/j.1550-7408.1963.tb01703.x.

Corno, G., Letelier, R.M., Abbott, M.R., Karl, D.M., 2005. Assessing primary production variability in the North Pacific Subtropical Gyre: A comparison of Fast Repetition Rate Fluorometry and ^{14}C measurements. J. Phycol. 42 (1), 51–60. https://doi.org/10.1111/j.1529-8817.2006.00163.x.

Corno, G., Karl, D.M., Church, M.J., Letelier, R.M., Lukas, R., Bidigare, R.R., Abbott, M. R., 2007. Impact of climate forcing on ecosystem processes in the North Pacific Subtropical Gyre. J. Geophys. Res. Oceans 112 (C4), C04021. https://doi.org/10.1029/2006JC00370.

Corno, G., Letelier, R.M., Abbott, M.R., Karl, D.M., 2008. Temporal and vertical variability in photosynthesis in the North Pacific Subtropical Gyre. Limnol. Oceanogr. 53 (4), 1252–1265. https://doi.org/10.4319/lo.2008.53.4.1252.

Dabundo, R., Lehmann, M.F., Treibergs, L., Tobias, C.R., Altabet, M.A., Moisander, P.H., Granger, J., 2014. The contamination of commercial $^{15}N_2$ gas stocks with ^{15}N-labeled nitrate and ammonium and consequences for nitrogen fixation measurements. PLoS ONE 9 (10), e110335. https://doi.org/10.1371/journal.pone.0110335.

Dall'Olmo, G., Dingle, J., Polimene, L., Brewin, R.J.W., Claustre, H., 2016. Substantial energy input to the mesopelagic ecosystem from the seasonal mixed layer pump. Nature Geosci. 9, 820–823. https://doi.org/10.1038/ngeo2818.

Dave, A.C., Lozier, M.S., 2010. Local stratification control of marine productivity in the subtropical North Pacific. J. Geophys. Res. 115, C12032. https://doi.org/10.1029/2010JC006507.

de Boyer Montégut, C., Madec, G., Fischer, A.S., Lazar, A., Iudicone, D., 2004. Mixed layer depth over the global ocean: An examination of profile data and a profile-based climatology. J. Geophys. Res.-Oceans 109 (C12), C12003. https://doi.org/10.1029/2004JC002378.

Devassy, V.P., Bhattathiri, P.M.A., Quasim, S.Z., 1979. Succession of organisms following *Trichodesmium* phenomenon. Indian J. Mar. Sci. 8, 89–93. http://nopr.niscair.res.in/handle/123456789/39188.

Dore, J.E., Brum, J.R., Tupas, L.M., Karl, D.M., 2002. Seasonal and interannual variability in sources of nitrogen supporting export in the oligotrophic subtropical North Pacific Ocean. Limnol. Oceanogr. 47 (6), 1595–1607. https://doi.org/10.4319/lo.2002.47.6.1595.

Dore, J.E., Letelier, R.M., Church, M.J., Lukas, R., Karl, D.M., 2008. Summer phytoplankton blooms in the oligotrophic North Pacific Subtropical Gyre: Historical perspective and recent observations. Prog. Oceanogr. 76 (1), 2–38. https://doi.org/10.1016/j.pocean.2007.10.002.

Dore, J.E., Church, M.J., Karl, D.M., Sadler, D.W., Letelier, R.M., 2014. Paired windward and leeward biogeochemical time series reveal consistent surface ocean CO_2 trends across the Hawaiian Ridge. Geophys. Res. Lett. 41, 6459–6467. https://doi.org/10.1002/2014GL060725.

Duce, R.A., LaRoche, J., Altieri, K., Arrigo, K.R., Baker, A.R., Capone, D.G., Cornell, S., Dentener, F., Galloway, J., Ganeshram, R.S., Geider, R.J., Jickells, T., Kuypers, M.M., Langlois, R., Liss, P.S., Liu, S., Middelburg, J.J., Moore, C.M., Nickovic, S., Oschlies, A., Pedersen, T., Prospero, J., Schlitzer, R., Seitzinger, S., Sorensen, L.L., Uematsu, M., Ulloa, O., Voss, M., Ward, B., Zamora, L., 2008. Impacts of atmospheric anthropogenic nitrogen on the open ocean. Science 320 (5878), 893–897. https://doi.org/10.1126/science.1150369.

Dugdale, R.C., Goering, J.J., 1967. Uptake of new and regenerated forms of nitrogen in primary productivity. Limnol. Oceanogr. 12 (2), 196–206. https://doi.org/10.4319/lo.1967.12.2.0196.

Emerson, S., 2014. Annual net community production and the biological carbon flux in the ocean. Global Biogeochem. Cy. 28 (10), 14–28. https://doi.org/10.1002/2013GB004680.

Emerson, S., Quay, P., Karl, D., Winn, C., Tupas, L., Landry, M., 1997. Experimental determination of the organic carbon flux from open-ocean surface waters. Nature 389 (6654), 951–954. https://doi.org/10.1038/40111.

Eppley, R.W., Peterson, B.J., 1979. Particulate organic matter flux and planktonic new production in the deep ocean. Nature 282 (5740), 677–680. https://doi.org/10.1038/282677a0.

Eppley, R.W., Carlucci, A.F., Holm-Hansen, O., Kiefer, D., McCarthy, J.J., Venrick, E., Williams, P.M., 1971. Phytoplankton growth and composition in shipboard cultures supplied with nitrate, ammonium, or urea as the nitrogen source. Limnol. Oceanogr. 16 (5), 741–751. https://doi.org/10.4319/lo.1971.16.5.0741.

Ferrón, S., Wilson, S.T., Martínez-García, S., Quay, P.D., Karl, D.M., 2015. Metabolic balance in the mixed layer of the oligotrophic North Pacific Ocean from diel changes in O_2/Ar saturation ratios. Geophys. Res. Lett. 42 (9), 3421–3430. https://doi.org/10.1002/2015GL063555.

Fitzwater, S.E., Knauer, G.A., Martin, J.H., 1982. Metal contamination and its effect on primary production measurements. Limnol. Oceanogr. 27 (3), 544–551. https://doi.org/10.4319/lo.1982.27.3.0544.

Flombaum, P., Gallegos, J.L., Gordillo, R.A., Rincón, J., Zabala, L.L., Jiao, N., Karl, D.M., Li, W.K.W., Lomas, M.W., Veneziano, D., Vera, C.S., Vrugt, J.A., Martiny, A.C., 2013. Present and future global distributions of the marine cyanobacteria *Prochlorococcus* and *Synechococcus*. Proc. Natl. Acad. Sci. USA 110 (24), 9824–9829. https://doi.org/10.1073/pnas.1307701110.

Flynn, K.J., 1988. The concept of "primary production" in aquatic ecology. Limnol. Oceanogr. 33 (5), 1215–1216. https://doi.org/10.4319/lo.1988.33.5.1215.

Foreman, R.K., Björkman, K.M., Carlson, C.A., Opalk, K., Karl, D.M., 2019. Improved ultraviolet photo-oxidation system yields estimates for deep-sea dissolved organic nitrogen and phosphorus. Limnol. Oceanogr.: Meth. 17 (4), 277–291. https://doi.org/10.1002/lom3.10312.

Fujii, M., Murashige, S., Ohnishi, Y., Yuzawa, A., Miyasaka, H., Suzuki, Y., Komiyama, H., 2002. Decomposition of phytoplankton in seawater. Part 1: Kinetic analysis of the effect of organic matter concentration. J. Oceanogr. 58 (3), 433–438. https://doi.org/10.1023/A:1021296713132.

Garside, C., 1982. A chemiluminescent technique for the determination of nanomolar concentrations of nitrate and nitrite in seawater. Mar. Chem. 11 (2), 159–167. https://doi.org/10.1016/0304-4203(82)90039-1.

Grabowski, M.N.W., Church, M.J., Karl, D.M., 2008. Nitrogen fixation rates and controls at Stn ALOHA. Aquat. Microb. Ecol. 52 (2), 175–183. https://doi.org/10.3354/ame01209.

Grabowski, E., Letelier, R.M., Laws, E.A., Karl, D.M., 2019. Coupling carbon and energy fluxes in the North Pacific Subtropical Gyre. Nature Commun. 10 (1), 1–9. https://doi.org/10.1038/s41467-019-09772-z.

Gregg, W.W., Rousseaux, C.S., 2014. Decadal trends in global pelagic ocean chlorophyll: A new assessment integrating multiple satellites, in situ data, and models. J. Geophys. Res. – Oceans 119 (9), 5921–5933. https://doi.org/10.1002/2014JC010158.

Gregg, W.W., Casey, N.W., McClain, C.R., 2005. Recent trends in global ocean chlorophyll. Geophys. Res. Lett. 32 (3), L03606. https://doi.org/10.1029/2004GL021808.

Großkopf, T., Mohr, W., Baustian, T., Schunck, H., Gill, D., Kuypers, M.M.M., Lavik, G., Schmitz, R.A., Wallace, D.W.R., Laroche, J., 2012. Doubling of marine dinitrogen-fixation rates based on direct measurements. Nature 488 (7411), 361–364. https://doi.org/10.1038/nature11338.

Gundersen, K.R., Corbin, J.S., Hanson, C.L., Hanson, M.L., Hanson, R.B., Russell, D.J., Stollar, A., Yamada, O., 1976. Structure and biological dynamics of the oligotrophic ocean photic zone off the Hawaiian islands. Pac. Sci. 30, 45–68.

Halsey, K.H., Milligan, A.J., Behrenfeld, M.J., 2011. Linking time-dependent carbon-fixation efficiencies in *Dunaliella tertiolecta* (Chlorphyceae) to underlying metabolic pathways. J. Phycol. 47 (1), 66–76. https://doi.org/10.1111/j.1529-8817.2010.00945.x.

Halsey, K.H., O'Malley, R.T., Graff, J.R., Milligan, A.J., Behrenfeld, M.J., 2013. A common partitioning strategy for photosynthetic products in evolutionarily distinct phytoplankton species. New Phytol. 198 (4), 1030–1038. https://doi.org/10.1111/nph.12209.

Hannides, C.C.S., Landry, M.R., Benitez-Nelson, C.R., Styles, R.M., Montoya, J.P., Karl, D. M., 2009. Export stoichiometry and migrant-mediated flux of phosphorus in the North Pacific Subtropical Gyre. Deep-Sea Res. Pt. I 56, 73–88. https://doi.org/10.1016/j.dsr.2008.08.003.

Hayward, T.L., 1987. The nutrient distribution and primary production in the central North Pacific. Deep-Sea Res. Pt. A 34, 1593–1627. https://doi.org/10.1016/0198-0149(87)90111-7.

Hayward, T.L., 1991. Primary production in the North Pacific Central Gyre: A controversy with important implications. Trends Ecol. Evol. 6 (9), 281–284. https://doi.org/10.1016/0169-5347(91)90005-I.

Hayward, T.L., Venrick, E.L., McGowan, J.A., 1983. Environmental heterogeneity and plankton community structure in the central North Pacific. J. Mar. Res. 41 (4), 711–729. https://doi.org/10.1357/002224083788520441.

Hebel, D.V., Karl, D.M., 2001. Seasonal, interannual and decadal variations in particulate matter concentrations and composition in the subtropical North Pacific Ocean. Deep-Sea Res. Pt. II 48 (8), 1669–1695. https://doi.org/10.1016/S0967-0645(00)00155-7.

Henson, S.A., Sanders, R., Madsen, E., Morris, P.J., Le Moigne, F., Quartly, G.D., 2011. A reduced estimate of the strength of the ocean's biological carbon pump. Geophys. Res. Lett. 38 (4), L04606. https://doi.org/10.1029/2011GL046735.

Henson, S.A., Yool, A., Sanders, R., 2015. Variability in efficiency of particulate organic carbon export: A model study. Geophys. Res. Lett. 29, 33–45. https://doi.org/10.1002/2014GB004965.

Jassby, A.D., Platt, T., 1976. Mathematical formulation of the relationship between photosynthesis and light for phytoplankton. Limnol. Oceanogr. 21 (4), 540–547. https://doi.org/10.4319/lo.1976.21.4.0540.

Jenkins, W., Goldman, J., 1985. Seasonal oxygen cycling and primary production in the Sargasso Sea. J. Mar. Res. 43 (2), 465–491. https://doi.org/10.1357/002224085788438702.

Johnson, K.S., Riser, S.C., Karl, D.M., 2010. Nitrate supply from deep to near-surface waters of the North Pacific subtropical gyre. Nature 465 (7301), 1062–1065. https://doi.org/10.1038/nature09170.

Jones, D.R., Karl, D.M., Laws, E.A., 1996. Growth rates and production of heterotrophic bacteria and phytoplankton in the North Pacific subtropical gyre. Deep-Sea Res. Pt. I 43 (10), 1567–1580. https://doi.org/10.1016/S0967-0637(96)00079-9.

Juranek, L.W., Quay, P.D., 2005. *In vitro* and *in situ* gross primary and net community production in the North Pacific Subtropical Gyre using labeled and natural abundance isotopes of dissolved O_2. Global Biogeochem. Cy. 19 (3), GB3009. https://doi.org/10.1012/2004GB002384.

Juranek, L.W., White, A.E., Dugenne, M., Henderikx Freitas, F., Dutkiewicz, S., Ribalet, F., Ferrón, S., Armbrust, E.V., Karl, D.M., 2020. The importance of the phytoplankton "middle class" to ocean net community production. Global Biogeochem. Cy. 34 https://doi.org/10.1029/2020GB006702.

Kara, A.B., Rochford, P.A., Hurlburt, H.E., 2000. An optimal definition for ocean mixed layer depth. J. Geophys. Res. 105 (C7), 16803–16821. https://doi.org/10.1029/2000JC900072.

Karl, D.M., 2002. Nutrient dynamics in the deep blue sea. Trends Microbiol. 10 (9), 410–418. https://doi.org/10.1016/S0966-842X(02)02430-7.

Karl, D.M., Church, M.J., 2017. Ecosystem structure and dynamics in the North Pacific Subtropical Gyre: New views of an old ocean. Ecosystems 20 (3), 433–457. https://doi.org/10.1007/s10021-017-0117-0.

Karl, D.M., Knauer, G.A., 1984a. Detritus-microbe interactions in the marine pelagic environment: Selected results from the VERTEX experiment. Bull. Mar. Sci. 35 (3), 550–565.

Karl, D.M., Knauer, G.A., 1984b. Vertical distribution, transport, and exchange of carbon in the northeast Pacific Ocean: Evidence for multiple zones of biological activity. Deep-Sea Res. Pt. A 31 (3), 221–243. https://doi.org/10.1016/0198-0149(84)90103-1.

Karl, D.M., Lukas, R., 1996. The Hawaii Ocean Time-series (HOT) program: Background, rationale and field implementation. Deep-Sea Res. Pt. II 43 (2), 129–156. https://doi.org/10.1016/0967-0645(96)00005-7.

Karl, D.M., Tien, G., 1992. MAGIC: A sensitive and precise method for measuring dissolved phosphorus in aquatic environments. Limnol. Oceanogr. 37 (1), 105–116. https://doi.org/10.4319/lo.1992.37.1.0105.

Karl, D.M., Tien, G., 1997. Temporal variability in dissolved phosphorus concentrations in the subtropical North Pacific Ocean. Mar. Chem. 56 (1), 77–96. https://doi.org/10.1016/S0304-4203(96)00081-3.

Karl, D.M., Letelier, R., Hebel, D., Tupas, L., Dore, J., Christian, J., Winn, C., 1995. Ecosystem changes in the North Pacific subtropical gyre attributed to the 1991–92 El Niño. Nature 373 (6511), 230–234. https://doi.org/10.1038/373230a0.

Karl, D.M., Christian, J., Dore, J.E., Hebel, D.V., Letelier, R.M., Tupas, L.M., Winn, C.D., 1996. Seasonal and interannual variability in primary production and particle flux at Station ALOHA. Deep-Sea Res. Pt. II 43 (2), 539–568. https://doi.org/10.1016/0967-0645(96)00002-1.

Karl, D.M., Hebel, D.V., Björkman, K., Letelier, R.M., 1998. The role of dissolved organic matter release in the productivity of the oligotrophic North Pacific Ocean. Limnol. Oceanogr. 43 (6), 1270–1286. https://doi.org/10.4319/lo.1998.43.6.1270.

Karl, D.M., Bidigare, R.R., Letelier, R.M., 2001a. Long-term changes in plankton community structure and productivity in the North Pacific Subtropical Gyre: The domain shift hypothesis. Deep-Sea Res. Pt. II 48 (8), 1449–1470. https://doi.org/10.1016/S0967-0645(00)00149-1.

Karl, D.M., Björkman, K.M., Dore, J.E., Fujieki, L., Hebel, D.V., Houlihan, T., Letelier, R.M., Tupas, L.M., 2001b. Ecological nitrogen-to-phosphorus stoichiometry at Station ALOHA. Deep-Sea Res. Pt. II 48 (8), 1529–1566. https://doi.org/10.1016/S0967-0645(00)00152-1.

Karl, D.M., Bidigare, R.R., Letelier, R.M., 2002. Sustained and aperiodic variability in organic matter production and phototrophic microbial community structure in the North Pacific Subtropical Gyre. In: Williams, P.J. le B., Thomas, D.R., Reynolds, C.S. (Eds.), Phytoplankton Productivity and Carbon Assimilation in Marine and Freshwater Ecosystems. Blackwell Publishers, Oxford, UK, pp. 222–264. https://doi.org/10.1002/9780470995204.ch9.

Karl, D., Bates, N.R., Emerson, S., Harrison, P.J., Jeandel, C., Llinas, O., Liu, K.-K., Marty, J.-C., Michaels, A.F., Miquel, J.C., Neuer, S., Nojiri, Y., Wong, C.S., 2003. Temporal studies of biogeochemical processes determined from ocean time-series observations during the JGOFS era. In: Fasham, M.J.R. (Ed.), Ocean Biogeochemistry: The Role of the Ocean Carbon Cycle in Global Change. Springer, New York, pp. 239–267.

Karl, D.M., Bidigare, R.R., Church, M.J., Dore, J.E., Letelier, R.M., Mahaffey, C., Zehr, J., 2008. The nitrogen cycle in the North Pacific trades biome: An evolving paradigm. In: Capone, D.G., Bronk, D.A., Mulholland, M.R., Carpenter, E.J. (Eds.), Nitrogen in the Marine Environment. Academic Press, Burlington, MA, pp. 705–769. https://doi.org/10.1016/B978-0-12-372522-6.00016-5.

Karl, D.M., Church, M.J., Dore, J.E., Letelier, R.M., Mahaffey, C., 2012. Predictable and efficient carbon sequestration in the North Pacific Ocean supported by symbiotic nitrogen fixation. Proc. Natl. Acad. Sci. USA 109 (6), 1842–1849. https://doi.org/10.1073/pnas.1120312109.

Katsura, S., Oka, E., Qiu, B., Schneider, N., 2013. Formation and subduction of North Pacific Tropical Water and their interannual variability. J. Phys. Oceanogr. 43 (11), 2400–2415. https://doi.org/10.1175/JPO-D-13-031.1.

Kavanaugh, M.T., Emerson, S.R., Hales, B., Lockwood, D.M., Quay, P.D., Letelier, R.M., 2014. Physicochemical and biological controls on primary and net community production across northeast Pacific seascapes. Limnol. Oceanogr. 59 (6), 2013–2027. https://doi.org/10.4319/lo.2014.59.6.2013.

Kavanaugh, M.T., Church, M.J., Davis, C.O., Karl, D.M., Letelier, R.M., Doney, S.C., 2018. ALOHA from the edge: Reconciling three decades of *in situ* Eulerian observations and geographic variability in the North Pacific Subtropical Gyre. Front. Mar. Sci. 5, 130. https://doi.org/10.3389/fmars.2018.00130.

Keeling, C.D., Brix, H., Gruber, N., 2004. Seasonal and long-term dynamics of upper ocean carbon cycle at Station ALOHA near Hawaii. Global Biogeochem. Cy. 18 (4), GB4006. https://doi.org/10.1029/2004GB002227.

Kim, I.-N., Lee, K., Gruber, N., Karl, D.M., Bullister, J.L., Yang, S., Kim, T.-W., 2014. Increasing anthropogenic nitrogen in the North Pacific Ocean. Science 346 (6213), 1102–1106. https://doi.org/10.1126/science.1258396.

Kirk, J.T.O., 2011. Light and Photosynthesis in Aquatic Ecosystems, 3rd ed. Cambridge University Press, New York.

Knauer, G.A., Martin, J.H., Bruland, K.W., 1979. Fluxes of particulate carbon, nitrogen, and phosphorous in the upper water column of the northeast Pacific. Deep-Sea Res. Pt. A 26 (8), 97–108. https://doi.org/10.1016/0198-0149(79)90089-X.

Knauer, G.A., Martin, J.H., Karl, D.M., 1984. The flux of particulate organic matter out of the euphotic zone. In: Global Ocean Flux Study: Proceedings of a Workshop, September 10-14, 1984. National Academy of Sciences Woods Hole Study Center, Woods Hole, Massachusetts, National Academy Press, Washington, D.C., p. 136.

Ko, Y.H., Lee, K., Takahashi, T., Karl, D.M., Kang, S.-H., Lee, E., 2018. Carbon-based estimate of nitrogen fixation-derived net community production in N-depleted ocean gyres. Global Biogeochem. Cy. 32 (8), 1241–1252. https://doi.org/10.1029/2017GB005634.

Kovač, Z., Platt, T., Sathyendranath, S., Morovič, M., 2016. Analytical solution for the vertical profile of daily production in the ocean. J. Geophys. Res. Oceans 121 (5), 3532–3548. https://doi.org/10.1002/2015JC011293.

Kyewalyanga, M., Platt, T., Sathyendranath, S., 1992. Ocean primary production calculated by spectral and broad-band models. Mar. Ecol. Prog. Ser. 85, 171–185. https://doi.org/10.3354/meps085171.

Lal, D., 1977. The oceanic microcosm of particles. Science 198 (4321), 997–1009. https://doi.org/10.1126/science.198.4321.997.

Lamborg, C.H., Buesseler, K.O., Valdes, J., Bertrand, C.H., Bidigare, R., Manganini, S., Pike, S., Steinberg, D., Trull, T., Wilson, S., 2008. The flux of bio- and lithogenic material associated with sinking particles in the mesopelagic "twilight zone" of the northwest and North Central Pacific Ocean. Deep-Sea Res. Pt. II 55 (14), 1540–1563. https://doi.org/10.1016/j.dsr2.2008.04.011.

Landry, M.R., Al-Mutairi, H., Selph, K.E., Christensen, S., Nunnery, S., 2001. Seasonal patterns of mesozooplankton abundance and biomass at Station ALOHA. Deep-Sea Res. Pt. II 48 (8), 2037–2061. https://doi.org/10.1016/S0967-0645(00)00172-7.

Laws, E.A., 2013. Evaluation of in situ phytoplankton growth rates: A synthesis of data from varied approaches. Annu. Rev. Mar. Sci. 5, 247–268. https://doi.org/10.1146/annurev-marine-121211-172258.

Laws, E.A., Maiti, K., 2019. The relationship between primary production and export production in the ocean: Effects of time lags and temporal variability. Deep-Sea Res. Pt. I 148, 100–107. https://doi.org/10.1016/j.dsr.2019.05.006.

Laws, E.A., Falkowski, P.G., Smith Jr., W.O., Ducklow, H., McCarthy, J.J., 2000. Temperature effects on export production in the open ocean. Global Biogeochem. Cy. 14 (4), 1231–1246. https://doi.org/10.1029/1999GB001229.

Laws, E.A., Letelier, R.M., Karl, D.M., 2014. Estimating the compensation irradiance in the ocean: The importance of accounting for non-photosynthetic uptake of inorganic carbon. Deep-Sea Res. Pt. I 93, 35–40. https://doi.org/10.1016/j.dsr.2014.07.011.

Laws, E.A., Bidigare, R.R., Karl, D.M., 2016. Enigmatic relationship between chlorophyll *a* concentrations and photosynthetic rates at Station ALOHA. Heliyon 2 (9), e00156. https://doi.org/10.1016/j.heliyon.2016.e00156.

Lee, K., Karl, D.M., Wanninkhof, R., Zhang, J.-Z., 2002. Global estimates of net carbon production in the nitrate-depleted tropical and subtropical oceans. Geophys. Res. Lett. 29 (19), 1907. https://doi.org/10.1029/2001GL014198.

Legendre, L., LeFèvre, I., 1989. Hydrodynamical singularities as controls of recycled versus export production in oceans. In: Berger, W.H., Smetacek, V.S., Wefer, G. (Eds.), Productivity of the Ocean: Present and Past. John Wiley & Sons, New York, pp. 49–63.

Letelier, R.M., Karl, D.M., 1996. Role of *Trichodesmium* spp. in the productivity of the subtropical North Pacific Ocean. Mar. Ecol. Prog. Ser. 133, 263–273. https://doi.org/10.3354/meps133263.

Letelier, R.M., Karl, D.M., 1998. *Trichodesmium* spp. physiology and nutrient fluxes in the North Pacific subtropical gyre. Aquat. Microb. Ecol. 15 (3), 265–276. https://doi.org/10.3354/ame015265.

Letelier, R.M., Bidigare, R.R., Hebel, D.V., Ondrusek, M., Winn, C.D., Karl, D.M., 1993. Temporal variability of phytoplankton community structure based on pigment analysis. Limnol. Oceanogr. 38 (7), 1420–1437. https://doi.org/10.4319/lo.1993.38.7.1420.

Letelier, R.M., Dore, J.E., Winn, C.D., Karl, D.M., 1996. Seasonal and interannual variations in photosynthetic carbon assimilation at Station ALOHA. Deep-Sea Res. Pt. II 43 (2), 467–490. https://doi.org/10.1016/0967-0645(96)00002-1.

Letelier, R.M., Karl, D.M., Abbott, M.R., Flament, P., Freilich, M., Lukas, R., Strub, T., 2000. Role of late winter mesoscale events in the biogeochemical variability of the upper water column of the North Pacific Subtropical Gyre. J. Geophys. Res. – Oceans 105 (C12), 28723–28739. https://doi.org/10.1029/1999JC000306.

Letelier, R.M., Karl, D.M., Abbott, M.R., Bidigare, R.R., 2004. Light driven seasonal patterns of chlorophyll and nitrate in the lower euphotic zone of the North Pacific Subtropical Gyre. Limnol. Oceanogr. 49 (2), 508–519. https://doi.org/10.4319/lo.2004.49.2.0508.

Letelier, R.M., White, A.E., Bidigare, R.R., Barone, B., Church, M.J., Karl, D.M., 2017. Light absorption by phytoplankton in the North Pacific subtropical gyre. Limnol. Oceanogr. 62 (4), 1526–1540. https://doi.org/10.1002/lno.10515.

Letelier, R.M., Björkman, K.M., Church, M.J., Hamilton, D.S., Mahowald, N.M., Scanza, R.A., Schneider, N., White, A.E., Karl, D.M., 2019. Climate-driven oscillation

of phosphorus and iron limitation in the North Pacific Subtropical Gyre. Proc. Natl. Acad. Sci. USA 116 (26), 12720–12728. https://doi.org/10.1073/pnas.1900789116.
Letscher, R.T., Primeau, F., Moore, J.K., 2016. Nutrient budgets in the subtropical ocean gyre dominated by lateral transport. Nat. Geosci. 9 (11), 815–819. https://doi.org/10.1038/NGEO2812.
Levitus, S., 1982. Climatological Atlas of the World Ocean, NOAA Professional Paper 13. National Oceanic and Atmospheric Administration, Rockville, Maryland, p. 173.
Li, B., Karl, D.M., Letelier, R.M., Church, M.J., 2011. Size-dependent photosynthetic variability in the North Pacific Subtropical Gyre. Mar. Ecol. Prog. Ser. 440, 27–40. https://doi.org/10.3354/meps09345.
Li, B., Karl, D.M., Letelier, R.M., Bidigare, R.R., Church, M.J., 2013. Variability of chromophytic phytoplankton in the North Pacific Subtropical Gyre. Deep-Sea Res. Pt. II 93, 84–95. https://doi.org/10.1016/j.dsr2.2013.03.007.
Li, W.K.W., Harrison, W.G., 1982. Carbon flow into the end-products of photosynthesis in short and long incubations of a natural phytoplankton population. Mar. Biol. 72 (2), 175–182. https://doi.org/10.1007/BF00396918.
Lohrenz, S.E., Wiesenburg, D.A., Rein, C.R., Arnone, R.A., Taylor, C.D., Knauer, G.A., Knap, A.H., 1992. A comparison of *in situ* and simulated *in situ* methods for estimating oceanic primary production. J. Plankton Res. 14 (2), 201–221. https://doi.org/10.1093/plankt/14.2.201.
Longhurst, A.R., Harrison, W.G., 1989. The biological pump: Profiles of plankton production and consumption in the upper ocean. Prog. Oceanogr. 22, 47–123. https://doi.org/10.1016/0079-6611(89)90010-4.
Longhurst, A., Sathyendranath, S., Platt, T., Caverhill, C., 1995. An estimate of global primary production in the ocean from satellite radiometer data. J. Plankton Res. 17 (6), 1245–1271. https://doi.org/10.1093/plankt/17.6.1245.
Lukas, R., 2001. Freshening of the upper thermocline in the North Pacific subtropical gyre associated with decadal changes of rainfall. Geophys. Res. Lett. 28 (18), 3485–3488. https://doi.org/10.1029/2001GL013116.
Lukas, R., Santiago-Mandujano, F., 2008. Interannual to interdecadal salinity variations observed near Hawaii. Oceanogr. 21 (1), 46–55. https://doi.org/10.5670/oceanog.2008.66.
Luo, Y.-W., Ducklow, H.W., Friedrichs, M.A.M., Church, M.J., Karl, D.M., Doney, S.C., 2012. Interannual variability of primary production and dissolved organic nitrogen storage in the North Pacific Subtropical Gyre. J. Geophys. Res.: Biogeosci. 117 (G3), G03019. https://doi.org/10.1029/2011JG001830.
Mague, T.H., Weare, N.M., Holm-Hansen, O., 1974. Nitrogen fixation in the North Pacific Ocean. Mar. Biol. 24 (2), 109–119. https://doi.org/10.1007/BF00389344.
Mahaffey, C., Björkman, K.M., Karl, D.M., 2012. Phytoplankton response to deep seawater nutrient addition in the North Pacific Subtropical Gyre. Mar. Ecol. Prog. Ser. 460, 13–34. https://doi.org/10.3354/meps09699.
Mantua, N.J., Hare, S.R., Zhang, Y., Wallace, J.M., Francis, R.C., 1997. A Pacific interdecadal climate oscillation with impacts on salmon production. Bull. Am. Meteorol. Soc. 78 (6), 1069–1079. https://doi.org/10.1175/1520-0477(1997)078<1069:APICOW>2.0.CO;2.
Marra, J., 2009. Net and gross productivity: weighing in with ^{14}C. Aquat. Microb. Ecol. 56 (2–3), 123–131. https://doi.org/10.3354/ame01306.
Marra, J., Heinemann, K.R., 1987. Primary production in the North Pacific Central Gyre: some new measurements based on ^{14}C. Deep-Sea Res. Pt. A 34 (11), 1821–1829. https://doi.org/10.1016/0198-0149(87)90056-2.
Martin, J.H., Knauer, G.A., Karl, D.M., Broenkow, W.W., 1987. VERTEX: Carbon cycling in the Northeast Pacific. Deep-Sea Res. Pt. A 34 (2), 267–285. https://doi.org/10.1016/0198-0149(87)90086-0.
Martiny, A., Hagstrom, G., DeVries, T., Letscher, R., Britten, G., Garcia, C., Galbraith, E., Karl, D., Levin, S., Lomas, M., Moreno, A., Talmy, D., Wang, W.-L., Matsumoto, K. Marine phytoplankton resilience may moderate oligotrophic ecosystem responses and biogeochemical feedbacks to climate change. Limnol. Oceanogr., in preparation.
McAndrew, P.M., Björkman, K.M., Church, M.J., Morris, P.J., Jachowski, N., Williams, P. J.leB., Karl, D.M., 2007. Metabolic response of oligotrophic plankton communities to deep water nutrient enrichment. Mar. Ecol. Prog. Ser. 332, 63–75. https://doi.org/10.3354/meps332063.
McCave, I.N., 1975. Vertical flux of particles in the ocean. Deep-Sea Res. 22 (7), 491–502. https://doi.org/10.1016/0011-7471(75)90022-4.
McClain, C.R., Signorini, S.R., Christian, J.R., 2004. Subtropical gyre variability observed by ocean-color satellites. Deep-Sea Res. Pt. II 51, 281–301. https://doi.org/10.1016/j.dsr2.2003.08.002.
Michaels, A.F., Bates, N.R., Buesseler, K.O., Carlson, C.A., Knap, A.H., 1994. Carbon-cycle imbalances in the Sargasso Sea. Nature 372 (6506), 537–540. https://doi.org/10.1038/372537a0.
Milligan, A.J., Halsey, K.H., Behrenfeld, M.J., 2015. Advancing interpretations of ^{14}C-uptake measurements in the context of phytoplankton physiology and ecology. J. Plankton Res. 37 (4), 692–698. https://doi.org/10.1093/plankt/fbv051.
Mohr, W., Großkopf, T., Wallace, D.W.R., LaRoche, J., 2010. Methodological underestimation of oceanic nitrogen fixation rates. PLoS ONE 5 (9), e12583. https://doi.org/10.1371/journal.pone.0012583.
Montoya, J.P., Voss, M., Kahler, P., Capone, D.G., 1996. A simple, high-precision, high-sensitivity tracer assay for N_2 fixation. Appl. Environ. Microbiol. 62 (3), 986–993.
Moore, C.M., Mills, M.M., Arrigo, K.R., Berman-Frank, I., Bopp, L., Boyd, P.W., Galbraith, E.D., Geider, R.J., Guieu, C., Jaccard, S.L., Jickells, T.D., La Roche, J., Lenton, T.M., Mahowald, N.M., Marañón, E., Marinov, I., Moore, J.K., Nakatsuka, T., Oschlies, A., Saito, M.A., Thingstad, T.F., Tsuda, A., Ulloa, O., 2013. Processes and patterns of oceanic nutrient limitation. Nature Geosci. 6 (9), 701–710. https://doi.org/10.1038/NGEO1765.
Morris, I., 1981. Photosynthetic products, physiological state and phytoplankton growth. Can. Bull. Fish. Aquat. Sci. 210, 83–102.
Morris, I., Glover, H.E., Yentsch, C.S., 1974. Products of photosynthesis by marine phytoplankton: the effect of environmental factors on the relative rates of protein synthesis. Mar. Biol. 27 (1), 1–9. https://doi.org/10.1007/BF00394754.
Munk, W., 2009. An inconvenient sea truth: Spread, steepness, and skewness of surface slopes. Annu. Rev. Mar. Sci. 1, 377–415. https://doi.org/10.1146/annurev.marine.010908.163940.
Neuer, S., Davenport, R., Freudenthal, T., Wefer, G., Llinás, O., Rueda, M.-J., Steinberg, D.K., Karl, D.M., 2002. Differences in the biological carbon pump at three subtropical ocean sites. Geophys. Res. Lett. 29 (18), 1885. https://doi.org/10.1029/2002GL015393.
Nicholson, D.P., Wilson, S.T., Doney, S.C., Karl, D.M., 2015. Quantifying subtropical North Pacific gyre mixed layer primary productivity from Seaglider observations of diel oxygen cycles. Geophys. Res. Lett. 42 (10), 4032–4039. https://doi.org/10.1002/2015GL063065.
Nie, X., Gao, S., Wang, F., Qu, T., 2016. Subduction of North Pacific Tropical Water and its equatorward pathways as shown by a simulated passive tracer. J. Geophys. Res. – Oceans 121 (12), 8770–8786. https://doi.org/10.1002/2016JC012305.
Olive, J.H., Benton, D.M., Kishler, J., 1969. Distribution of C-14 in products of photosynthesis and its relationship to phytoplankton composition and rate of photosynthesis. Ecology 50 (3), 380–386. https://doi.org/10.2307/1933886.
Ondrusek, M.E., Bidigare, R.R., Waters, K., Karl, D.M., 2001. A predictive model for estimating rates of primary production in the subtropical North Pacific Ocean. Deep-Sea Res. Pt. II 48 (8), 1837–1863. https://doi.org/10.1016/S0967-0645(00)00163-6.
Pace, M.L., Knauer, G.A., Karl, D.M., Martin, J.H., 1987. Primary production, new production and vertical flux in the eastern Pacific Ocean. Nature 325 (6107), 803–804. https://doi.org/10.1038/325803a0.
Pace, M.L., Cole, J.J., Carpenter, S.R., Kitchell, J.F., 1999. Trophic cascades revealed in diverse ecosystems. Trends Ecol. Evol. 14 (12), 483–488. https://doi.org/10.1016/S0169-5347(99)01723-1.
Pasulka, A.L., Landry, M.R., Taniguchi, D.A.A., Taylor, A.G., Church, M.J., 2013. Temporal dynamics of phytoplankton and heterotrophic protists at station ALOHA. Deep-Sea Res. Pt. II 93, 44–57. https://doi.org/10.1016/j.dsr2.2013.01.007.
Pei, S., Laws, E.A., 2014. Does the ^{14}C method estimate net photosynthesis? II. Implications from cyclostat studies of marine phytoplankton. Deep-Sea Res. Pt. I 91, 94–100. https://doi.org/10.1016/j.dsr.2014.05.015.
Perin, S., Lean, D.R.S., Pick, F.R., Mazumder, A., 2002. Photosynthetic carbon allocation: Effects of planktivorous fish and nutrient enrichment. Aquat. Sci. 64 (3), 217–238. https://doi.org/10.1007/s00027-002-8069-6.
Pinedo-Gonzalez, P., Hawco, N.J., Bundy, R.M., Armbrust, E.V., Follows, M.J., Cael, B.B., White, A.E., Ferrón, S., Karl, D.M., John, S.G., 2020. Anthropogenic Asian aerosols provide Fe to the North Pacific. Proc. Natl. Acad. Sci. USA 117 (45), 27862–27868. https://doi.org/10.1073/pnas.2010315117.
Platt, T., Harrison, W.G., 1986. Reconciliation of carbon and oxygen fluxes in the upper ocean. Deep-Sea Res. Pt. A 33 (2), 273–276. https://doi.org/10.1016/0198-0149(86)90123-8.
Platt, T., Harrison, W.G., Lewis, M.R., Li, W.K.W., Sathyendranath, S., Smith, R.E., Vezina, A.F., 1989. Biological production of the oceans: the case for consensus. Mar. Ecol. Prog. Ser. 52, 77–88.
Polovina, J.J., Howell, E.A., Abecassis, M., 2008. Ocean's least productive waters are expanding. Geophys. Res. Lett. 35 (3), L03618. https://doi.org/10.1029/2007GL031745.
Qu, T., Chen, J., 2009. A North Pacific decadal variability in subduction rate. Geophys. Res. Lett. 36 (22), L22602. https://doi.org/10.1029/2009GL040914.
Quay, P.D., Peacock, C., Björkman, K., Karl, D.M., 2010. Measuring primary production rates in the ocean: Enigmatic results between incubation and non-incubation methods at Station ALOHA. Global Biogeochem. Cy. 24 (3), GB3014. https://doi.org/10.1029/2009GB003665.
Richardson, T.L., Jackson, G.A., 2007. Small phytoplankton and carbon export from the surface ocean. Science 315 (5813), 838–840. https://doi.org/10.1126/science.1133471.
Rii, Y.M., Karl, D.M., Church, M.J., 2016. Temporal and vertical variability in picophytoplankton primary productivity in the North Pacific Subtropical Gyre. Mar. Ecol. Prog. Ser. 562, 1–18. https://doi.org/10.3354/meps11954.
Rii, Y.M., Bidigare, R.R., Church, M.J., 2018. Differential responses of eukaryotic phytoplankton to nitrogenous nutrients in the North Pacific Subtropical Gyre. Front. Mar. Sci. 5, 92. https://doi.org/10.3389/fmars.2018.00092.
Ripple, W.J., Estes, J.A., Schmitz, O.J., Constant, V., Kaylor, M.J., Lenz, A., Motley, J.L., Self, K.E., Taylor, D.S., Wolf, C., 2016. What is a trophic cascade? Trends Ecol. Evol. 31 (11), 842–849. https://doi.org/10.1016/j.tree.2016.08.010.
Rivkin, R.B., 1985. Carbon-14 labelling patterns of individual marine phytoplankton from natural populations. Mar. Biol. 89 (2), 135–142. https://doi.org/10.1007/BF00392884.
Ruben, S., Kamen, M.D., 1940. Photosynthesis with radioactive carbon. IV. Molecular weight of the intermediate products and a tentative theory of photosynthesis. J. Amer. Chem. Soc. 62 (12), 3451–3455. https://doi.org/10.1021/ja01869a044.
Saba, V.S., Friedrichs, M.A.M., Carr, M.-E., Antoine, D., Armstrong, R.A., Asanuma, I., Aumont, O., Bates, N.R., Behrenfeld, M.J., Bennington, V., Bopp, L., Bruggeman, J., Buitenhuis, E.T., Church, M.J., Ciotti, A.M., Doney, S.C., Dowell, M., Dunne, J., Dutkiewicz, S., Gregg, W., Hoepffner, N., Hyde, K.J.W., Ishizaka, J., Kameda, T., Karl, D.M., Lima, I., Lomas, M.W., Marra, J., Mckinley, G.A., Mélin, F., Moore, J.K., Morel, A., O' Reilly, J., Salihoglu, B., Scardi, M., Smyth, T.J., Tang, S., Tjiputra, J., Uitz, J., Vichi, M., Waters, K., Westberry, T.K., Yool, A., 2010. Challenges of modeling depth-integrated marine primary productivity over multiple decades: A case study at BATS and HOT. Global Biogeochem. Cy. 24 (3), GB3020. https://doi.org/10.1029/2009GB003655.

Scharek, R., Latasa, M., Karl, D.M., Bidigare, R.R., 1999. Temporal variations in diatom abundance and downward vertical flux in the oligotrophic North Pacific gyre. Deep-Sea Res. Pt. I 46 (6), 1051–1075. https://doi.org/10.1016/S0967-0637(98)00102-2.

Schulien, J.A., Behrenfeld, M.J., Hair, J.W., Hostetler, C.A., Twardowski, M.S., 2017. Vertically-resolved phytoplankton carbon and net primary production from a high spectral resolution lidar. Opt. Express 25 (12), 13577–13587. https://doi.org/10.1364/OE.25.013577.

Sharp, J.H., 1974. Improved analysis for "particulate" organic carbon and nitrogen from seawater. Limnol. Oceanogr. 19 (6), 984–989. https://doi.org/10.4319/lo.1974.19.6.0984.

Sheridan, C.C., Landry, M.R., 2004. A 9-year increasing trend in mesozooplankton biomass at the Hawaii Ocean Time-series Station ALOHA. ICES J. Mar. Sci. 61 (4), 457–463. https://doi.org/10.1016/j.icesjms.2004.03.023.

Siegel, D.A., Dickey, T.D., Washburn, L., Hamilton, M.K., Mitchell, B.G., 1989. Optical determination of particulate abundance and production variations in the oligotrophic ocean. Deep-Sea Res. Pt. A 36 (2), 211–222. https://doi.org/10.1016/0198-0149(89)90134-9.

Simoneit, B.R.T., Grimalt, J.O., Fischer, K., Dymond, J., 1986. Upward and downward flux of particulate organic material in abyssal waters of the Pacific Ocean. Naturwissenschaften 73 (6), 322–325. https://doi.org/10.1007/BF00451479.

Small, L.F., Knauer, G.A., Tuel, M.D., 1987. The role of sinking fecal pellets in stratified euphotic zones. Deep-Sea Res. 34 (10), 1705–1712. https://doi.org/10.1016/0198-0149(87)90019-7.

Smith, S.L., Yamanaka, Y., Kishi, M.J., 2005. Attempting consistent simulations of Stn. ALOHA with a multi-element ecosystem model. J. Oceanogr. 61 (1), 1–23. https://doi.org/10.1007/s10872-005-0016-4.

Steemann Nielsen, E., 1951. Measurement of the production of organic matter in the sea by means of carbon-14. Nature 167 (4252), 684–685. https://doi.org/10.1038/167684b0.

Steemann Nielsen, E., 1952. The use of radio-active carbon (C^{14}) for measuring organic production in the sea. J. Cons. Perm. Int. Explor. Mer. 18, 117–140.

Steinacher, M., Joos, F., Frölicher, T.L., Bopp, L., Cadule, P., Cocco, V., Doney, S.C., Gehlen, M., Lindsay, K., Moore, J.K., Schneider, B., Segschneider, J., 2010. Projected 21st century decrease in marine productivity: a multi-model analysis. Biogeosciences 7 (3), 979–1005. https://doi.org/10.5194/bg-7-979-2010.

Stock, C.A., Dunne, J.P., John, J.G., 2014. Global-scale carbon and energy flows through the marine planktonic food web: An analysis with a coupled physical-biological model. Prog. Oceanogr. 120, 1–28. https://doi.org/10.1016/j.pocean.2013.07.001.

Suárez, I., Marañón, E., 2003. Photosynthate in a temperate sea over an annual cycle: the relationship between protein synthesis and phytoplankton physiological state. J. Sea Res. 50 (4), 285–299. https://doi.org/10.1016/j.seares.2003.04.002.

Suess, E., 1980. Particulate organic carbon flux in the oceans-surface productivity and oxygen utilization. Nature 288 (5788), 260–263. https://doi.org/10.1038/288260a0.

Venrick, E.L., 1982. Phytoplankton in an oligotrophic ocean: Observations and questions. Ecol. Monogr. 52 (2), 129–154. https://doi.org/10.2307/1942608.

Venrick, E.L., 1988. The vertical distributions of chlorophyll and phytoplankton species in the North Pacific central environment. J. Plankton Res. 10 (5), 987–998. https://doi.org/10.1093/plankt/10.5.987.

Venrick, E.L., 1990. Phytoplankton in an oligotrophic ocean: Species structure and interannual variability. Ecology 71 (4), 1547–1563. https://doi.org/10.2307/1938291.

Venrick, E.L., 1993. Phytoplankton seasonality in the central North Pacific: The endless summer reconsidered. Limnol. Oceanogr. 38 (6), 1135–1149. https://doi.org/10.4319/lo.1993.38.6.1135.

Venrick, E.L., 1997. Comparison of the phytoplankton species composition and structure in the Climax area (1973–1985) with that of Station ALOHA (1994). Limnol. Oceanogr. 42 (7), 1643–1648. https://doi.org/10.4319/lo.1997.42.7.1643.

Venrick, E.L., McGowan, J.A., Cayan, D.R., Hayward, T.L., 1987. Climate and chlorophyll a: Long-term trends in the central North Pacific Ocean. Science 238 (4823), 70–72. https://doi.org/10.1126/science.238.4823.70.

Villareal, T.A., Altabet, M.A., Culver-Rymsza, K., 1993. Nitrogen transport by vertically migrating diatom mats in the North Pacific Ocean. Nature 363 (6431), 709–712. https://doi.org/10.1038/363709a0.

Viviani, D.A., Karl, D.M., Church, M.J., 2015. Variability in photosynthetic production of dissolved and particulate organic carbon in the North Pacific Subtropical Gyre. Front. Mar. Sci. 2, article 73. https://doi.org/10.3389/fmars.2015.00073.

Volk, T., Hoffert, M.I., 1985. Ocean carbon pumps: Analysis of relative strengths and efficiencies in ocean-driven atmospheric CO_2 changes. In: Sundquist, E.T., Broecker, W.S. (Eds.), The Carbon Cycle and Atmospheric CO_2: Natural Variations Archaean to Present. American Geophysical Union, Washington, D.C., pp. 99–110

Westberry, T., Behrenfeld, M.J., Siegel, D.A., Boss, E., 2008. Carbon-based primary productivity modeling with vertically resolved photoacclimation. Global Biogeochem. Cy. 22 (2), GB2024. https://doi.org/10.1029/2007GB003078.

White, A.E., Letelier, R.M., Whitmire, A.L., Barone, B., Bidigare, R.R., Church, M.J., Karl, D.M., 2015. Phenology of particle size distributions and primary productivity in the North Pacific subtropical gyre (Station ALOHA). J. Geophys. Res. - Oceans 120 (11), 7381–7399. https://doi.org/10.1002/2015JC010897.

White, A.E., Barone, B., Letelier, R.M., Karl, D.M., 2017. Productivity diagnosed from the diel cycle of particulate carbon in the North Pacific Subtropical Gyre. Geophys. Res. Lett. 44 (8), 3752–3760. https://doi.org/10.1002/2016GL071607.

White, A.E., Watkins-Brandt, K.S., Church, M.J., 2018. Temporal variability of *Trichodesmium* spp. and diatom-diazotroph assemblages in the North Pacific Subtropical Gyre. Front. Mar. Sci. 5, 27. https://doi.org/10.3389/fmars.2018.00027.

White, A.E., Granger, J., Selden, C., Gradoville, M.R., Potts, L., Bourbonnais, A., Fulweiler, R.W., Knapp, A.N., Mohr, W., Moisander, P., Tobias, C.R., Wilson, S.T., Benavides, M., Bonnet, S., Chang, B., Mulholland, M., 2020. A review of the $^{15}N_2$ tracer method to measure diazotroph production in pelagic ecosystems. Limnol. Oceanogr.: Meth. 18, 129–147. https://doi.org/10.1002/lom3.10353.

Williams, P.J.le.B., 1993. On the definition of plankton production terms. ICES Mar. Sci. Symp. 197, 9–19.

Williams, P.J.le.B., 2014. Plankton respiration, net community production and the organic carbon cycle in the oceanic water column. In: Karl, D.M., Schlesinger, W.H. (Eds.), Treatise on Geochemistry, 2nd edition. Elsevier, Waltham, MA, pp. 593–612. https://doi.org/10.1016/B978-0-08-095975-7.00815-9.

Williams, P.J.le.B., Robertson, J.I., 1989. A serious inhibition problem from a Niskin sampler during plankton productivity studies. Limnol. Oceanogr. 34 (7), 1300–1305. https://doi.org/10.4319/lo.1989.34.7.1300.

Wilson, S.T., Böttjer, D., Church, M.J., Karl, D.M., 2012. Comparative assessment of nitrogen fixation methodologies conducted in the oligotrophic North Pacific Ocean. Appl. Environ. Microbiol. 78 (18), 6516–6523. https://doi.org/10.1128/AEM.01146-12.

Wilson, S.T., Barone, B., Ascani, F., Bidigare, R.R., Church, M.J., del Valle, D.A., Dyhrman, S.T., Ferrón, S., Fitzsimmons, J.N., Juranek, L.W., Kolber, Z.S., Letelier, R. M., Martínez-García, S., Nicholson, D.P., Richards, K.J., Rii, Y.M., Rouco, M., Viviani, D.A., White, A.E., Zehr, J.P., Karl, D.M., 2015. Short-term variability in euphotic zone biogeochemistry and primary productivity at Station ALOHA: A case study of summer 2012. Global Biogeochem. Cy. 29 (8), 1145–1164. https://doi.org/10.1002/2015GB005141.

Wilson, S.T., Aylward, F.O., Ribalet, F., Barone, B., Casey, J.R., Connell, P.E., Eppley, J. M., Ferrón, S., Fitzsimmons, J.N., Hayes, C.T., Romano, A.E., Turk-Kubo, K.A., Vislova, A., Armbrust, E.V., Caron, D.A., Church, M.J., Zehr, J.P., Karl, D.M., DeLong, E.F., 2017. Coordinated regulation of growth, activity and transcription in natural populations of the unicellular nitrogen-fixing cyanobacterium *Crocosphaera*. Nature Microbiol. 2, 17118. https://doi.org/10.1038/nmicrobiol.2017.118.

Winn, C.D., Mackenzie, F.T., Carrillo, C.J., Sabine, C.L., Karl, D.M., 1994. Air-sea carbon dioxide exchange in the North Pacific subtropical gyre: Implications for the global carbon budget. Global Biogeochem. Cy. 8 (2), 157–163. https://doi.org/10.1029/94GB00387.

Winn, C.D., Campbell, L., Christian, J.R., Letelier, R.M., Hebel, D.V., Dore, J.E., Fujieki, L., Karl, D.M., 1995. Seasonal variability in the phytoplankton community of the North Pacific Subtropical Gyre. Global Biogeochem. Cy. 9 (4), 605–620. https://doi.org/10.1029/95GB02149.

Zehr, J.P., Capone, D.G., 2020. Changing perspectives in marine nitrogen fixation. Science 368 (6492), eaay9514. https://doi.org/10.1126/science.aay9514.

Zehr, J.P., Mellon, M.T., Zani, S., 1998. New nitrogen fixing microorganisms detected in oligotrophic oceans by the amplification of nitrogenase (*nifH*) genes. Appl. Environ. Microbiol. 64 (9), 3444–3450. https://doi.org/10.1128/AEM.64.9.3444-3450.1998.

Zehr, J.P., Carpenter, E.J., Villareal, T.A., 2000. New perspectives on nitrogen-fixing microorganisms in tropical and subtropical oceans. Trends Microbiol. 8 (2), 68–73. https://doi.org/10.1016/S0966-842X(99)01670-4.

Zehr, J.P., Waterbury, J.B., Turner, P.J., Montoya, J.P., Omoregie, E., Steward, G.F., Hansen, A., Karl, D.M., 2001. Unicellular cyanobacteria fix N_2 in the subtropical North Pacific Ocean. Nature 412 (6847), 635–638. https://doi.org/10.1038/35088063.

Zehr, J.P., Bench, S.R., Carter, B.J., Hewson, I., Niazi, F., Shi, T., Tripp, H.J., Affourtit, J. P., 2008. Globally distributed uncultivated oceanic N_2-fixing cyanobacteria lack oxygen photosystem II. Science 322 (5904), 1110–1112. https://doi.org/10.1126/science.1165340.